
**Pacific Northwest
National Laboratory**

Operated by Battelle for the
U.S. Department of Energy

Plutonium Speciation in Support of Oxidative-Leaching Demonstration Test

SI Sinkov

October 2007



Prepared for the U.S. Department of Energy
under Contract DE-AC05-76RL01830

DISCLAIMER

This report was prepared as an account of work sponsored by an agency of the United States Government. Neither the United States Government nor any agency thereof, nor Battelle Memorial Institute, nor any of their employees, makes **any warranty, express or implied, or assumes any legal liability or responsibility for the accuracy, completeness, or usefulness of any information, apparatus, product, or process disclosed, or represents that its use would not infringe privately owned rights.** Reference herein to any specific commercial product, process, or service by trade name, trademark, manufacturer, or otherwise does not necessarily constitute or imply its endorsement, recommendation, or favoring by the United States Government or any agency thereof, or Battelle Memorial Institute. The views and opinions of authors expressed herein do not necessarily state or reflect those of the United States Government or any agency thereof.

PACIFIC NORTHWEST NATIONAL LABORATORY

operated by

BATTELLE

for the

UNITED STATES DEPARTMENT OF ENERGY

under Contract DE-AC05-76RL01830

Plutonium Speciation in Support of Oxidative-Leaching Demonstration Test

S. I. Sinkov

October 2007

Test specification: 24590-PTF-TSP-RT-06-002, Rev 0.

Test plan: TP-RPP-WTP-445

Test exceptions: none

R&T focus area: Pretreatment

Test scoping statements(s): None

Pacific Northwest National Laboratory
Richland, Washington 99352


Completeness of Testing

This report describes the results of work and testing specified by test plan TP-RPP-WTP-445. The work and any associated testing followed the quality assurance requirements outlined in the test specification/plan. The descriptions provided in this test report are an accurate account of both the conduct of the work and the data collected. Test plan results are reported. Also reported are any unusual or anomalous occurrences that are different from expected results. The test results and this report have been reviewed and verified.

Approved:



Gordon H. Beeman, Manager
WTP R&T Support Project



Date

Contents

Abbreviation/Acronym List	xiii
References	xv
Testing Summary	xix
Objectives	xix
Test Exceptions	xxiii
Results and Performance Against Success Criteria	xxiii
Quality Requirements	xxiv
R&T Test Conditions	xxv
Simulant Use	xxv
Discrepancies and Follow-on Tests	xxv
1.0 Introduction	1.1
1.1 Oxidation States and Redox Stability of Pu(IV, V, and V) in an Alkaline Medium	1.2
1.2 Solubility of Pu(IV, V, and VI) in an Alkaline Medium	1.3
1.3 Controversy in Determination of Stability Fields of Pu(IV), Pu(V), and Pu(VI) Soluble Species on Eh-pH Diagrams in Alkaline Solutions	1.5
1.4 Direct Speciation of Pu at Low Micromolar Concentrations by Spectroscopic Techniques	1.8
1.5 Pu Solubilization and Speciation in the Process of Oxidative Alkaline Leaching of Hanford Tank Sludges	1.10
1.6 The Project Goals	1.10
1.7 Quality Assurance and Quality Control	1.11
1.7.1 Application of RPP-WTP Quality Assurance Requirements	1.11
1.7.2 Conduct of Experimental and Analytical Work	1.12
1.7.3 Internal Data Verification and Validation	1.12
2.0 Experimental and Data Processing	2.1
2.1 Reagents and Solvents Used in Calibration, Sludge Preparation, and Oxidative-Leaching Experiments	2.1
2.2 The Preparation, Purification, and Valence-State Adjustment of Pu Stock Solutions	2.1
2.3 Spectrophotometric Equipment	2.2
2.4 Calibration and Speciation Experiments with LWCC (cold testing and Pu calibrations)	2.3
2.5 Determination of Pu Concentration in Calibration Solutions and Leachates	2.3
2.6 Preparation of the Fe(OH) ₃ /Cr(OH) ₃ /Pu(OH) ₄ Sludge Simulant and Oxidative-Leaching Procedure	2.4

2.7	Measurements of Eh and pH	2.5
2.8	Determination of Cr(VI), Mn(VII), and Mn(VI) Concentrations in the Course of Oxidative-Leaching Experiments.....	2.6
2.9	Baseline Subtraction and Net Peak Intensity Determination in Nd and Pu Calibration Experiments.....	2.6
2.10	Simulation and Elimination of Waveform-Shaped Spectral Interference in LWCC Spectra Burdened with Low-Frequency Noise	2.6
3.0	Results and Discussion.....	3.1
3.1	Light-Transmission Efficiency of LWCC	3.1
3.2	Demonstration of Identity of Spectral Features of Nd(III) in H ₂ O and D ₂ O.....	3.4
3.3	Cold Testing of LWCC Using Nd(III) Complex with EDTA in 0.1 M NaOH and 0.1 M NaOD	3.5
3.4	Pu(VI) Calibration and Speciation Experiments in DNO ₃ and NaOD	3.8
3.4.1	Pu(VI) Calibration Experiment in DNO ₃	3.8
3.4.2	Pu(VI) Calibration Experiments in NaOD.....	3.10
3.4.3	Pu(VI) Spectra in the Presence of Carbonate at Constant Concentration of Hydroxide	3.15
3.5	Pu(V) Calibration and Speciation Experiments in NaOD.....	3.17
3.5.1	Preparation and Characterization of Pu(V) Solution in 14 M of NaOD	3.17
3.5.2	Pu(V) Calibration and Speciation Experiments in NaOD	3.20
3.5.3	Pu(V) Spectra in the Presence of Carbonate at Constant Concentration of Hydroxide	3.24
3.5.4	Pu(V) Redox Speciation After Acidification of Initially Alkaline Pu(V) Solution by DNO ₃ at a Low Micromolar Concentration of Pu(V).....	3.29
3.5.5	Determination of Formal Electrochemical Potential of Pu(VI)/Pu(V) Couple in 0.25 M to 1.0 M NaOD Using Direct Potentiometric Measurement with an ORP Electrode	3.31
3.6	Pu(IV) Spectral Measurements in DNO ₃ and NaOD	3.32
3.6.1	Verification of Identity of Spectral Features of Pu(IV) in 4 M of HNO ₃ and 4 M of DNO ₃	3.32
3.6.2	Pu(IV) Calibration Experiment in 0.75 M of DNO ₃	3.34
3.6.3	Pu(IV) Speciation and Solubility in 0.25 M NaOD	3.35
3.6.4	Pu(IV) Speciation and Solubility in 0.25 M NaOD in the Presence of Carbonate	3.37
3.7	Oxidative Dissolution of Pu(IV) Hydroxide Suspension by Permanganate and Manganate in 0.25 M NaOD.....	3.41
3.7.1	Oxidative Dissolution of Pu ^{IV} (OH) ₄ Suspension by NaMnO ₄ in 0.25 M NaOD	3.41
3.7.2	Oxidative Dissolution of Pu ^{IV} (OH) ₄ Suspension by Sodium Manganate in 0.25 M NaOD	3.46
3.8	Oxidation of Pu(IV) by Permanganate in Acidic Solution.....	3.48
3.8.1	Oxidative Dissolution of Pu(IV) Hydroxide Suspension by Permanganate in 1 M DNO ₃	3.48

3.8.2	Oxidation of Ionic Pu(IV) by Permanganate in 1 M DNO ₃ and the Effect of Dichromate on the Kinetics of this Process	3.50
3.9	Interaction of Pu(V) with Low Levels of Manganate in 0.25 M NaOD	3.51
3.9.1	ORP Measurements in Manganate-Containing Solutions and Manganate-Permanganate Mixtures in NaOD Solutions.....	3.51
3.9.2	Instability of Permanganate and Manganate in 0.25 M NaOD at Low Micromolar Concentration of Initially Added Mn(VII) by Spectral Measurements with LWCC.....	3.52
3.9.3	Oxidation of Pu(V) by Manganate in 0.25 M NaOD Monitored by LWCC Spectroscopy	3.54
3.10	Oxidative Leaching of Fe(OH) ₃ /Cr(OH) ₃ /Pu(OH) ₄ Sludge Simulant with Permanganate	3.55
3.10.1	Leaching in 0.25 M NaOD Solution	3.56
3.10.2	Leaching in 3 M NaOD Solution	3.59
3.10.3	Quenching of Excessive Manganate in the Leachates with Weakly Acidic Solution of Cr(III)	3.61
3.10.4	Comparison of Oxidative Alkaline Leaching of Pu from Sludge Simulant with Other Studies.....	3.63
4.0	Conclusions.....	4.1
4.1	Summary of Dissolution of Pu(OH) ₄ (solid) in Alkaline Permanganate and Manganate Solutions.....	4.2
4.2	Summary of Oxidative Leaching of Fe(OH) ₃ +Cr(OH) ₃ +Pu(OH) ₄ Sludge Simulant	4.2

Figures

1.1. Formal Potentials of Various Pu Couples as a Function of NaOH Concentrations.....	1.3
1.2. Solubility Curves of Pu(IV), Pu(V) and Pu(VI) as a Function of NaOH Concentration.....	1.4
1.3. Eh-pH Diagram for Plutonium Based on Standard Redox Potentials and Hydrolysis Reactions of Pu(III, IV, V, and VI) Ions in Aqueous Solution	1.6
1.4. Eh-pH Diagram for Plutonium in Groundwater Containing Hydroxide, Carbonate, and Fluoride Ions	1.7
1.5. Eh-pH Diagram for Plutonium in Groundwater at 25°C Under Conditions Representative of J-13 Water Found Near the Proposed Yucca Mountain Nuclear Waste Repository	1.8
2.1. Net Peaks' Intensity Determination in Pu(V) Spectra	2.7
2.2. Manganate Reduction After Adding Pu(V). Initial Mn(VI) and Pu(V) concentrations are 15 μ M and 12.5 μ M, respectively	2.8
3.1. Light Intensity Spectra After Exiting a 5-m LWCC Filled with 99.8% D ₂ O	3.2
3.2. Light-Intensity Spectra After Passing Through a 1-cm Quartz Cell Filled with 99.8% D ₂ O	3.2
3.3. Light-Intensity Spectra with Direct Light Coupling to the Spectrophotometer.....	3.3
3.4. Spectra of 0.2 mM Nd(NO ₃) ₃ Solution in D ₂ O and H ₂ O in 0.015% HNO ₃ and DNO ₃ , Respectively, Using LWCC Detection	3.5
3.5. Spectra of Na ₂ CrO ₄ Solution in D ₂ O at 4 mM and 40 mM of Cr(VI)	3.6
3.6. Calibration of LWCC Using Nd(III) Solution in the Presence of 0.25 M of Na ₄ EDTA in 0.1 M of Sodium Hydroxide: a) NaOH/H ₂ O no chromate b) NaOD/D ₂ O no chromate c) NaOH/H ₂ O + 50 mM of Na ₂ CrO ₄ d) NaOD/D ₂ O + 50 mM of Na ₂ CrO ₄	3.7
3.7. Pu(VI) Acidic Stock Solution Spectra in 0.5 M of HNO ₃ [a) and b)] and 0.5 M of DNO ₃ [c) and d)]......	3.9
3.8. Calibration Experiment with Pu(VI) in 0.1 M of DNO ₃ Using 500 cm LWCC	3.10
3.9. Calibration Experiments with Pu(VI) in 0.1 M of NaOD.....	3.12
3.10. Calibration Experiments with Pu(VI) in 1 M NaOD	3.13
3.11. Spectral Evidence of Partial Reduction of Pu(VI) to Pu(V) in 1 M NaOD with Time.....	3.14
3.12. Pu(VI) Spectra in 0.1 M NaOD a), 0.25 M NaOD b), and 1 M NaOD c) in the Presence of Carbonate.	3.16

3.13. Literature Data on Pu(V) Spectra in Concentrated Sodium Hydroxide.....	3.18
3.14. Pu Spectra in 14 M NaOD 20 Days After Adding Acidic Pu(IV) (red trace) and Pu(VI) (black trace) to an Excess of 14.9 M NaOD	3.20
3.15. Comparison of the Stock Solution of 0.811 mM Pu(V) in 14 M NaOD Measured with 1-cm cell (red trace) with 23.6- μ M Pu(V) Solution Spectrum in 1 M NaOD Measured by LWCC (blue trace).....	3.21
3.16. Calibration Experiments with Pu(V) in 1 M NaOD	3.22
3.17. Calibration Experiment with Pu(V) in 0.25 M NaOD	3.23
3.18. Calibration Experiments with Pu(V) in 1 M NaOD in the Presence of 50 mM Chromate.....	3.25
3.19. Calibration Experiments with Pu(V) in 0.25 M NaOD in the Presence of 50 mM Chromate.....	3.26
3.20. Pu(V) Spectra in 0.25 M NaOD a), and 1 M NaOD b) in the Presence of Carbonate.....	3.28
3.21. Spectra of Pu(V) After Acidic Strike of Small Amount of Pu(V) Stock in 14 M NaOD with a Slight Molar Excess of 0.4 M DNO ₃ Solution.....	3.30
3.22. Spectra of Pu(V) After Acidic Strike of Tiny Amount of Pu(V) Stock in 14 M NaOD into a Slight Molar Excess of 0.4 M DNO ₃ Containing 5 mM of Chromate (physically present as 2.5 mM dichromate)	3.31
3.23. Spectra of Pu(VI)+Pu(V) Solutions in NaOD Solutions at Total Concentration of Pu at 20 μ M.....	3.33
3.24. Optical Absorbance Spectra of 18 mM Pu(IV) in 4.0 M HNO ₃ (black trace) and 4.0 M DNO ₃ (red trace)	3.34
3.25. Calibration Experiment with Pu(IV) in 0.75 M of DNO ₃ Using a 500-cm LWCC	3.35
3.26. Pu(IV) Spectra in 0.25 M NaOD for Freshly Spiked (bold black trace, 0.027 μ M of total Pu) and 3-Day-Old Solution (bold red trace; 0.016 μ M of total Pu)	3.36
3.27. Pu(IV) Spectra in 0.25 M NaOD in the Presence of Carbonate	3.38
3.28. Effect of Carbonate on the Solubility of Pu(IV) in 0.25 M NaOD	3.39
3.29. Spectral Monitoring over Mn(VII) Conversion to Mn(VI) in the Presence of Added Pu(OH) ₄	3.42
3.30. Spectral Monitoring over Mn(VII) Conversion to Mn(VI) in the Presence of <i>in situ</i> Generated Pu(OH) ₄ in Alkaline Solution of Mn(VII).....	3.44
3.31. The Kinetics of Oxidative Dissolution of Pu ^{IV} (OH) ₄ Suspension in a Series of NaMnO ₄ Solutions in 0.25 M of NaOD/D ₂ O at Three Levels of Permanganate	3.45

3.32. The Effect of Carbonate Concentration on the Kinetics of Oxidative Dissolution of $\text{Pu}^{\text{IV}}(\text{OH})_4$ Suspension in a Series of NaMnO_4 Solutions in 0.25 M $\text{NaOD}/\text{D}_2\text{O}$ at 0.75 mM of Permanganate	3.47
3.33. Spectral Monitoring over $\text{Mn}(\text{VI})$ Consumption in the Presence of Oxidative Alkaline Leaching of $\text{Pu}(\text{OH})_4$ in 0.25 M NaOD	3.48
3.34. The Kinetics of Dissolution of $\text{Pu}(\text{OH})_4$ by $\text{Mn}(\text{VII})$ in 1 M DNO_3	3.49
3.35. The Kinetics of the Oxidation of Monomeric $\text{Pu}(\text{IV})$ by $\text{Mn}(\text{VII})$, $\text{Cr}(\text{VI})$, and Their Mixture in 1 M HNO_3	3.51
3.36. Evidence of $\text{Mn}(\text{VII})$ and $\text{Mn}(\text{VI})$ Reduction in 0.25 M NaOD Using LWCC Detection	3.53
3.37. Red Trace Spectrum from 2.2 After Application of the Waveform Suppression Treatment and Spectral Smoothing	3.56
3.38. Oxidative Leaching of $\text{Fe}(\text{OH})_3/\text{Cr}(\text{OH})_3/\text{Pu}(\text{OH})_4$ Sludge Simulant with a Substoichiometric to Stoichiometric Amount of Permanganate in 0.25 M NaOH	3.57
3.39. Oxidative Leaching of $\text{Fe}(\text{OH})_3/\text{Cr}(\text{OH})_3/\text{Pu}(\text{OH})_4$ Sludge Simulant with Excessive Amount of Permanganate	3.58
3.40. The Kinetics of Oxidative Leaching of $\text{Fe}(\text{OH})_3/\text{Cr}(\text{OH})_3/\text{Pu}(\text{OH})_4$ Sludge Simulant with Excessive Amount of Permanganate	3.60
3.41. Cold Experiment on Stepwise Reduction of Manganate by $\text{Cr}(\text{OH})_4^-$ in 2.5 M NaOD	3.62
3.42. Quenching of Excessive $\text{Mn}(\text{VI})$ with Soluble $\text{Cr}(\text{III})$ Nitrate in 3 M NaOD Leachate 6 Days After Oxidative Treatment of $\text{Fe}(\text{OH})_3/\text{Cr}(\text{OH})_3/\text{Pu}(\text{OH})_4$ Sludge Simulant with 15% Molar Excess of $\text{Mn}(\text{VI})$: a) $\text{Mn}(\text{VI})$ peak intensity decrease with increasing amount of $\text{Cr}(\text{III})$ added; b) concentration profile of soluble plutonium at various stages of elimination of $\text{Mn}(\text{VI})$ from solution.....	3.64

Tables

S.1. Discussion of Objectives.....	xix
S.2. Discussion of Success Criteria	xxiii
S.3. Discussion of R&T Test Conditions	xxv
1.1. Standard Potentials for Plutonium for the Hypothetical Condition of Zero Ionic Strength.....	1.2
3.1. Summary of Calibration Experiments with 5-m LWCC Using Nd-EDTA Complex in NaOH and NaOD	3.8
3.2. Summary of Calibration Experiments with Pu(VI) in 0.1 M of DNO ₃ , 0.1 M and 1 M of NaOD.....	3.10
3.3. Summary of Calibration Experiments with Pu(V) in 0.25 M and 1 M NaOD	3.27
3.4. Calculation of Formal Potentials of the Pu(VI)/Pu(V) Couple in NaOD Solution.....	3.33
3.5. Comparison of Experimentally Determined Solubilities of Pu in Mixed Hydroxy-Carbonate Medium at Constant Level of 0.25 M NaOD/D ₂ O with Predictions of the SRNL Pu Solubility Model	3.41
3.6. Oxidation Reduction Potentials of Manganate Solutions and Permanganate-Manganate Mixtures in NaOD	3.52
3.7. Concentrations of Cr(VI) and Soluble Pu in the 3 M NaOD Leachates with Substoichiometric to Stoichiometric Addition of Mn(VII).....	3.61

Abbreviation/Acronym List

ASO	Analytical Service Organization
BNI	Bechtel National, Incorporated
D ₂ O	Deuterated (heavy) Water
DOE	U.S. Department of Energy
EDTA	EthyleneDiamineTetraacetic Acid
Eh	Oxidation Potential
FWHM	Full Width at Half Maximum. Characteristic of absorbance peak sharpness and resolution in Optical Absorbance Spectroscopy. Typically expressed in nm.
IR	Infrared (region of optical spectrum)
LIPAS	Laser-Induced Photoacoustic Spectroscopy
LSC	Liquid Scintillation Counting
LWCC	Liquid Waveguide Capillary Cell
M	Molar; concentration in moles per liter
M&TE	Measuring and Test Equipment
NaOD	Deuterated Sodium Hydroxide
OAS	Optical Absorbance Spectroscopy (synonym: Spectrophotometry)
Orion	Combination Redox/ORP Electrode
ORP	Oxidation-Reduction Potential
pH	Solution Acidity
PNNL	Pacific Northwest National Laboratory
PNWD	Battelle—Pacific Northwest Division
PUREX	Plutonium-URanium EXtraction (solvent extraction process)
QAP	Quality Assurance Program
QAPjP	Quality Assurance Project Plan
QARD	Quality Assurance Requirements and Descriptions
redox	reduction-oxidation (pertaining to oxidation-reduction reactions or oxidation-reduction electrical potentials)
REDOX	REDuction-OXidation (solvent extraction process)
RPL	Radiochemical Processing Laboratory
SBMS	Standards-Based Management System
SOW	Statement of Work

SP	Support Program
SRNL	Savannah River National laboratory
TRU	Transuranic
UV	Ultraviolet (region of optical spectrum)
VIS	VISible (region of optical spectrum)
WTPSP	Waste Treatment Plant Support Project
WTP	Waste Treatment Plant
WPI	World Precision Instruments
ϵ	Molar Absorptivity (or molar extinction) of a light absorbing species in solution. Normally ϵ is expressed in $\text{M}^{-1} \text{cm}^{-1}$ units. Its physical meaning is the optical absorbance created by a 1 M solution of a light-absorbing species in a 1-cm-thick layer of solution

References

- Allard B, H Kipatsi, and JO Liljenzin. 1980. "Expected Species of Uranium, Neptunium and Plutonium in Neutral Aqueous Solutions." *J. Inorg. Nucl. Chem.* 42:1015-1027.
- Altmaier M, V Neck, R Muller, Th Fanghänel. 2005. "Solubility of $\text{ThO}_2 \cdot x\text{H}_2\text{O}(\text{am})$ in Carbonate Solution and the Formation of Ternary Th(IV) Hydroxide-Carbonate Complexes." *Radiochimica Acta* 93:83-92.
- Barney GS, and CH Delegard. 1999. "Chemical Species of Plutonium in Hanford Site Radioactive Tank Wastes." In: *Actinide Speciation in High Ionic Strength Media*. DT Reed, SB Clark, and L Rao (Eds.). Kluwer Academic/Plenum Publishers.
- Beitz JV, MM Boxtader, VA Maroni, S Okajima, and DT Reed. 1990. "High Sensitivity Photoacoustic Spectrometer for Variable Temperature Solution Studies." *Rev. Sci. Instrum.* 61(5):1395-1403.
- Bourges J. 1972. "Préparation et Identification du Plutonium à l'Etat d'Oxydation-V en Milieu Basique." *Radiochem. Radioanal. Lett.* 12:111.
- Budantseva NA, IG Tananaev, AM Fedoseev, AA Bessonov, and CH Delegard. 1997. *Investigation of the Behavior of Pu(V) in Alkaline Media*. PNNL-11624, Richland, WA.
- Byrne RH, X Liu, EA Kaltenbacher, K Sell. 2002. "Spectrophotometric Measurement of Total Inorganic Carbon in Aqueous Solutions Using A Liquid Core Waveguide" *Anal. Chim. Acta.* 451(2):221-229.
- Carnall WT. 1979. "The Absorption and Fluorescence Spectra of Rare Earth Ions in Solution." Chapter 24 in *Handbook on the Physics and Chemistry of Rare Earths* (KA Gschneider, Jr and L Eyring, Eds.). Published by the *Journal of Applied Crystallography*.
- Clark DL, DE Hobart, and MP Neu. 1995. "Actinide Carboante Complexes and Their Importance in Actinide Environmental Chemistry." *Chemical Reviews* 95(1):25-48.
- Cohen D. 1961. The Absorption Spectra of Plutonium Ions in Perchloric Acid Solutions. *J. Inorg. Nucl. Chem.* **18**, 211-218.
- Delegard CH. 1987. "Solubility of $\text{PuO}_2 \cdot x\text{H}_2\text{O}$ in Alkaline Hanford High-Level Waste Solution." *Radiochimica Acta* 41:11-21.
- Gelis AV, P Vanishek, MP Jensen, and KL Nash. 2001. "Electrochemical and Spectrophotometric Investigations of Neptunium in Alkaline Media." *Radiochimica Acta.* 89:565-571.
- Gmelin Handbuch der Anorganischen Chemie*. 1975. Manganese and references therein, Springer-Verlag, Berlin-Heidelberg-New York, Vol. 56, Part C2.
- Koltunov VS. 1974. *Kinetics of Actinide Reactions* [in Russian]. Atomizdat, Moscow.

- Krot NN, AA Bessonov, AV Gelis, VP Shilov, VP Perminov, and LN Astafurova. 1998. "Coprecipitation of Transuranium Elements from Alkaline Solutions by the Method of Appearing Reagents. I. Coprecipitation of Pu(VI,V) with Manganese Dioxide." *Radiochemistry* 40(4):347-352.
- Lierse Ch, and JI Kim. 1986. *Chemical Behavior of Plutonium in Natural Aquatic Systems: Hydrolysis, Carbonate Complexation and Redox Reactions*. RCM 02286, Institut für Radiochemie der Technischen Universität München, Garching, Germany.
- Nash KL, M Borkowski, M Hancock, and I Laszak. 2005. "Oxidative Leaching of Plutonium from Simulated Hanford Tank-Waste Sludges." *Separation Science and Technology* 40:1497-1512.
- Neck V, JI Kim, BS Seidel, CM Marquardt, K Dardenne, MP Jensen, and W Hauser. 2001. "A Spectroscopic Study of the Hydrolysis, Colloid Formation and Solubility of Np." *Radiochimica Acta* 89:439-446.
- Neck V, M Altmaier, A Seibert, JI Kim, JI Jun, CM Marquardt, and Th Fanghänel. 2007. "Solubility and Redox Reactions of Pu(IV) Hydrated Oxide: Evidence for the Formation of PuO_{2+x} (s, hyd)." *Radiochimica Acta* 93:193-207.
- Neu MP, DC Hoffman, KE Roberts, H Nitsche, and RJ Silva. 1994. "Comparison of Chemical extractions and Laser Photoacoustic Spectroscopy for Determination of Plutonium Species in Carbonate Solution." *Radiochimica Acta* 66/67:251.
- Peretrukhin VF, and VI Spitsyn. 1982. "Electrochemical Determination of the Oxidation Potentials and the Thermodynamic Stability of the Valence States of the Transuranium Elements in Aqueous Alkaline Media". *Izv. Akad. Nauk SSSR, Ser. Khim*, **4**, 826-831.
- Peretrukhin VF, SV Kryuchkov, VI Silin, and IG Tananaev. 1996. *Determination of the Solubility of Np(IV)-(VI), Pu(III)-(VI), Am(III)-(VI) and Tc(IV), (V) Hydroxo Compounds in 0.5 – 14 M NaOH solutions*. WHC-EP-0987, Westinghouse Hanford Company. Richland, WA.
- Perez-Bustamante JA. 1965. "Solubility Product of Tetravalent Plutonium Hydroxide and Study of the Amphoteric Character of Hexavalent Plutonium Hydroxide." *Radiochimica Acta* 4(1):67-75.
- Rai D, NJ Hess, AR Felmy, DA Moore, M Yui, and P Vitorge. 1999. "A Thermodynamic Model for the Solubility of PuO₂ (am) in the Aqueous K⁺ - HCO₃⁻ - CO₃²⁻ - OH⁻ - H₂O System." *Radiochimica Acta* 86:89-99.
- Rapko BM, JGH Geeting, SI Sinkov, and JD Vienna. 2004. *Oxidative-Alkaline Leaching of Washed 241-SY-102 and 241-SX-101 Tank Sludges*. WTP-RPT-117, Rev 0, Battelle—Pacific Northwest Division, Richland, WA.
- Ray M, IC Pius, MM Charyvlu, and CK Sivaramakrishnan. 1988. "Spectrophotometric Studies on the Behaviour of Plutonium in Basic Media. Preprint # CT-36." In: *Radiochemistry and Radiation Chemistry Symposium*. Bombay, India, February 22-26, 1988.
- Reilly SD, WK Myers, SA Stout, DM Smith, MA Ginder-Vogel, and MP Neu. 2003. "Plutonium(VI) Sorption to Manganese Dioxide." In: *AIP Conference Proceedings*, Vol. 673 (Plutonium Futures—The Science), pp. 375-376.

- Reilly SD, W Runde, and MP Neu. 2007. "Solubility of Pu(VI) Carbonate in Saline Solutions." *Geochimica et Cosmochimica Acta* 71:2672-2679.
- Rudisill TS, DT Hobbs, and TB Edwards. 2004. *Preliminary Results from Plutonium/Americium Solubility Studies Using Simulated Savannah River Site Waste Solutions*. WSRC-TR-2004-00349, Westinghouse Savannah River Company, Aiken, SC.
- Runde W. 2000. "The Chemical Interactions of Actinides in the Environment." In: *Los Alamos Science*. Number 26, Challenges in Plutonium Science, Volume II: pp. 392-411.
- Spitsyn VI, AD Gelman, NN Krot, MP Mefodiyeva, FA Zakharova, Yu A Komkov, VP Shilov, and IV Smirnova. 1969. "Heptavalent State of Neptunium and Plutonium." *J. Inorg. Nucl. Chem.* 31:2733-2745.
- Varlashkin PG, GM Begun, and JR Peterson. 1984a. "Electrochemical and Spectroscopic Studies of Neptunium in Concentrated Aqueous Carbonate and Carbonate-Hydroxide Solutions." *Radiochimica Acta* 35:91-96.
- Varlashkin PG, GM Begun, and JR Peterson. 1984b. "Electrochemical and Spectroscopic Studies of Plutonium in Concentrated Aqueous Carbonate and Carbonate-Hydroxide Solutions." *Radiochimica Acta* 35:211-218.
- Waterbury RD, W Yao, and RH Byrne. 1997. "Long Pathlength Absorbance Spectroscopy: Trace Analysis of Fe(II) using a 4.5 m Liquid Core Waveguide." *Anal. Chim. Acta.* 357(1-2):99-102.
- Weigel F, JJ Katz, and GT Seaborg. 1986. "Plutonium." Chapter 7 in: *The Chemistry of Actinide Elements*. JJ Katz, GT Seaborg, LR Morse (Eds.). Volume I. Chapman and Hall.
- Wilson RE, Y-J Hu, and H Nitsche. 2005. "Detection and Quantification of Pu(III, IV, V, and VI) using a 1.0-meter Liquid Core Waveguide." *Radiochimica Acta* 93:203-206.
- Yamaguchi T, Y Sakamoto, and T Ohnuki. 1994. "Effect of the Complexation on Solubility of Pu(IV) in Aqueous Carbonate System." *Radiochimica Acta* 66/67:9-14.

Testing Summary

Objectives

Bechtel National, Inc. (BNI) is evaluating the plutonium speciation in caustic solutions that reasonably represent the process streams from the oxidative-leaching demonstration test. Battelle—Pacific Northwest Division (PNWD) was contracted to develop a spectrophotometric method to measure plutonium speciation at submicromolar ($< 10^{-6}$ M) concentrations in alkaline solutions in the presence of chromate and carbonate. Data obtained from the testing will be used to identify the oxidation state of Pu(IV), Pu(V), and Pu(VI) species, which potentially could exist in caustic leachates. Work was initially conducted under contract number 24590-101-TSA-W000-00004 satisfying the needs defined in Appendix C of the *Research and Technology Plan* TSS A-219 to evaluate the speciation of chromium, plutonium, and manganese before and after oxidative leaching. In February 2007, the contract mechanism was switched to Pacific Northwest National Laboratory (PNNL) Operating Contract MOA: 24590-QL-HC9-WA49-00001.

Table S.1 discusses the specific objectives of the work described in this report:

Table S.1. Discussion of Objectives

Test Objective	Objective Met (Y/N)	Discussion
1. Develop a spectrophotometric method to measure plutonium speciation at submicromolar ($< 10^{-6}$ M) concentrations of this element in alkaline solutions (0.1 to 1.0 M of NaOH) in the presence of chromate (0 to 0.05 M) and carbonate (0 to 0.1 M).	Yes	The applicability of a 500-cm Liquid Waveguide Capillary Cell (LWCC) for spectral measurements in alkaline aqueous solution using cold simulants was verified. Detection ranges in H ₂ O and in D ₂ O media were found to be 560 to 700 nm and 560 to 960 nm, respectively. A significant extension of a useable spectral range of LWCC-based detection in deuterated aqueous medium to the previously unexplored region was demonstrated. The presence of chromate up to 0.05 M concentration did not deteriorate spectral measurements and did not narrow these spectral ranges. The validity of the Beer law (linear relationship between concentration of a light absorbing species and magnitude of optical absorbance) was demonstrated for all eight absorbance bands of neodymium-ethylenediaminetetraacetic acid (Nd-EDTA) complex in 0.1 M NaOD/D ₂ O medium in a wide range of concentrations of this species. Detection limits achieved were less than 1×10^{-6} M for a number of Nd-EDTA peaks with molar absorptivities greater than $6 \text{ M}^{-1} \text{ cm}^{-1}$. Successful demonstration of the LWCC performance with cold simulants allowed experiments to be performed with Pu(VI) and Pu(V) in deuterated alkaline media from 0.1 M

Test Objective	Objective Met (Y/N)	Discussion
		to 1.0 M of NaOD in pure hydroxide solutions and in hydroxide-carbonate mixtures.
<p>2. Measure optical absorbance spectra and molar absorptivities of Pu(IV), Pu(V), and Pu(VI) complexes with hydroxide and mixed complexes with hydroxide and carbonate in the presence of chromate to identify the oxidation state(s) of plutonium in caustic solution and determine concentrations of these oxidation states.</p>	<p>Objective is partially met (two of the three oxidation states of plutonium in alkaline solution are spectrally characterized; Pu(IV) spectra could not be measured due to solubility problems).</p>	<p>Simple and straightforward procedures to prepare stable stock solutions of Pu(V) and Pu(VI) in deuterated alkaline medium were developed. Optical absorbance spectra and molar absorptivities of Pu(V) and Pu(VI) complexes in alkaline solutions in the absence and in the presence of carbonate were measured. These measurements were performed in a previously inaccessible range of submicromolar to low micromolar concentrations of Pu to establish the linearity of calibration curves and examine reduction-oxidation (redox) stability of Pu(V) from the viewpoint of its possible disproportionation to Pu(IV) and Pu(VI). All calibration series for the given oxidation state of Pu and the alkalinity level were prepared in duplicates with the first series of solutions measured within 1 to 3 hr after adding Pu to the alkaline medium, and the second series was measured 3 days after Pu addition. This was done to examine the possible redox perturbation of initially added oxidation states of Pu. In the case of Pu(V), experiments levels of soluble Pu in freshly prepared and aged solutions were determined and compared to monitor the possible formation of insoluble compounds of Pu. The effect of chromate on spectral features, redox speciation, and the solubility of initially added Pu(V) was determined.</p> <p>Attempts to measure optical absorbance spectra of Pu(IV) in alkaline medium were not successful because of the extremely low solubility of this oxidation state of Pu under the tested conditions of 0.25 M of NaOD. The presence of carbonate in the 0.05- to 0.25-M concentration range (at constant level 0.25 M of NaOD) was found to increase the solubility of the freshly prepared Pu(IV) 5.2 times with no spectral features attributable to Pu(IV). The effect of carbonate on the solubility of Pu(IV) was found to be more pronounced for more aged solutions (3-day-old series) starting from 0.20 M of carbonate. Very weak spectral features detected for these solutions indicated the presence of a mixed hydroxy-carbonate complex of Pu(V) in the solution. This observation provided evidence for the slow oxidation of poorly soluble Pu(IV) to more soluble Pu(V), most likely by the action of dissolved</p>

Test Objective	Objective Met (Y/N)	Discussion
		<p>oxygen under these conditions.</p> <p>An extensive series of experiments on the interaction of <i>in situ</i> prepared and aged Pu(OH)₄(solid) with permanganate in an alkaline medium was conducted to examine the possibility of Pu(IV) oxidation to higher and more soluble oxidation state(s) of Pu. A Significant increase of Pu(IV) solubility (up to 30 μM) in the presence of permanganate was observed. This effect was accompanied by the consumption of 3 molar equivalents of Mn(VII) per 1 molar equivalent of Pu(IV). Strong evidence that the final oxidation state of Pu in this reaction is Pu(VI) rather than Pu(V) was obtained in a separate experiment on very fast and quantitative oxidation of Pu(V) by manganate with direct spectral observation of Pu(VI) in the final solution using LWCC detection.</p> <p>More sensitive detection of plutonium in an alkaline medium can be achieved by applying even longer LWCCs than the 500-cm cell used in this project. This should improve the detection limits for Pu(VI) and Pu(V) and, more importantly, potentially allowing the spectral signature of an elusive hydroxocomplex of Pu(IV) in a caustic solution to be identified. Unfortunately, the range of commercially available LWCCs is limited to the longest optical pathlength of 500 cm that was already tested in this project. The technical feasibility of developing a LWCC with a much longer pathlength on a custom basis needs to be discussed with the technical experts from the LWCC manufacturing company (World Precision Instruments).</p> <p>A number of problems to be overcome on the way to the creation of the ultra-long LWCC include, but are not limited to</p> <ul style="list-style-type: none"> • significantly increased fluidic resistance of the liquid waveguide if its internal diameter is to be kept that same as in the 500-cm cell • more stringent requirements for the purity of the solvent (D₂O) and the solutes (NaOD, Na₂CrO₄, Pu(IV) stock in DNO₃, etc.) with respect to an allowable admixture of H₂O • possible narrowing of the useable spectral range due to a more significant light attenuation in the process of its propagation through longer optical distances.

Test Objective	Objective Met (Y/N)	Discussion
		<p>Additionally, the possibility should be considered of acquiring and using a better quality spectrophotometer than the one used in the course of this project. Instruments with a better resolution and with a higher signal-to-noise ratio have appeared on the market since 2003, when the spectrophotometer employed in this project was manufactured.</p>
<p>3. Determine detection limits for each oxidation state of Pu in alkaline solution.</p>	<p>Objective is partially met (detection limits for two of the three oxidation states of plutonium in alkaline solution are determined).</p>	<p>Detection limits of Pu(VI) in alkaline solutions determined using a major peak of Pu(VI) at 625 nm were found to be 0.47 μM and 0.55 μM for 0.1 M and 1.0 M NaOD concentrations, respectively. Pu(VI) was found to undergo a minor reduction to Pu(V) at higher alkalinity (1.0 M of NaOD).</p> <p>Detection limits of Pu(V) were determined in alkaline solutions at 1.0 M levels of sodium hydroxide concentration using the major absorbance peaks of Pu(V) at 653 nm and 809 nm. The former peak offers a better detection limit (0.24 μM vs 0.38 μM) despite ~ 4 times lower molar absorptivity compared with the 809 nm absorbance band. The presence of 50 mM of chromate in a 1.0 M NaOD solution does not affect the valence state of Pu(V) and does not change its spectral features.</p> <p>The detection of Pu(V) in 0.25 M of NaOD is more complicated because of the increased tendency of Pu(V) to disproportionation followed by precipitation of Pu(IV) from solution. Nevertheless, in a lower range of Pu(V) concentrations (0.8 to 1.6 μM), the detection of pentavalent Pu is possible with submicromolar detection limits. The presence of chromate at this alkalinity results in precipitation of a greater fraction of Pu from solution compared with chromate-free testing for aged series of solutions (3 days between Pu(V) spike and measurement).</p> <p>No detection limit for Pu(IV) in alkaline solution could be determined because of insufficient sensitivity of LWCC to identify its spectral features.</p> <p>The presence of carbonate (at a 0.1-M level) increases the solubility of Pu(IV) by approximately 4 times, but even this level of soluble plutonium (8×10^{-8} M) is still below the detection limits achieved in this project.</p> <p>A successful realization of the second objective in full should make it possible to determine the detection limit of</p>

Test Objective	Objective Met (Y/N)	Discussion
		Pu(IV) in an alkaline medium.

Test Exceptions

No test exceptions were generated during testing

Results and Performance Against Success Criteria

This task involved the development of a method to identify Pu speciation in caustic solutions that reasonably represent the process streams from anticipated plant flowsheet conditions. Specifically, the methods will identify the oxidation state of the Pu(IV), Pu(V), and Pu(VI) species that potentially could exist in caustic media (0.1 to 1.0 M of NaOH, 0 to 0.05 M of Na₂CrO₄, and 0.01 to 0.1 M of Na₂CO₃). The detection limit target is the greater of 5×10^{-8} M or a minimum Pu(IV) solubility in a given matrix (see Table S.2).

Table S.2. Discussion of Success Criteria

List Success Criteria	Explain How the Tests Did or Did Not Meet the Success Criteria
1. Development of a method to identify the oxidation state of the Pu(IV), Pu(V), and Pu(VI) species in caustic solutions that reasonably represent the process streams from anticipated plant flowsheet conditions.	Enhanced optical absorbance spectroscopy based on application a 500-cm pathlength LWCC is demonstrated to be capable of identifying the oxidation states of Pu(V) and Pu(VI) in 0.1-M to 1.0-M NaOH solutions in the presence and absence of chromate and carbonate with much greater sensitivity than was possible before with conventional spectrophotometry. Pu(IV) detection with the current configuration of LWCC is not possible due to low solubility of this oxidation state of Pu ($\sim 2 \times 10^{-8}$ M in 0.25 M sodium hydroxide). Detecting such low levels of Pu(IV) would require LWCC with 20 to 50 times longer optical pathlengths compared with the 500-cm pathlength employed in this project.
2. The detection limit target is the greater of 5×10^{-8} M or a minimum Pu(IV) solubility in a given matrix (0.1 to 1.0 M of NaOH, 0 to 0.05 M of Na ₂ CrO ₄ , and 0.01 to 0.1 M of Na ₂ CO ₃).	The detection limits for Pu species determined in this project are as follows: <ul style="list-style-type: none"> Pu(VI): $5.1 \pm 0.4 \times 10^{-7}$ M in 0.1 to 1.0 M NaOD based on major absorbance band of Pu(VI) at 625 nm Pu(V): $0.22 \pm 0.03 \times 10^{-7}$ M (653 nm peak) and $0.36 \pm 0.03 \times 10^{-7}$ M (809 nm peak) in

List Success Criteria	Explain How the Tests Did or Did Not Meet the Success Criteria
	<p>1 M NaOD</p> <ul style="list-style-type: none"> • Pu(V) $0.60 \pm 0.10 \times 10^{-7}$ M (653 nm peak) and $0.35 \pm 0.05 \times 10^{-7}$ M (809 nm peak) in 0.25 M NaOD • Pu(IV): no detection limit was determined due to very low solubility (2×10^{-8} M) of this oxidation state in 0.25 M NaOD and insufficiently intense molar absorptivities of absorbance bands of Pu(IV). <p>The reason for these higher-than-targeted detection limits is insufficiently intense absorbance peaks of Pu(VI) and Pu(V) suitable for their detection. Acidification of initially alkaline Pu-containing solutions with conversion of soluble Pu(V) and Pu(VI) to their unhydrolyzed forms (PuO_2^+ and PuO_2^{2+} respectively) is demonstrated as a possible solution of this problem. This technique allows the detection limit to be improved for Pu(V) by ~3 times (estimated) and by 100 times for Pu(VI). In the latter case, the experimentally measured detection limit is found to be 5.6×10^{-9} M of Pu(VI). The detection limit for Pu(IV) under acidic conditions was found to be 2.7×10^{-8} M, which is still not sufficient to detect this species after acidification of Pu(IV) containing alkaline solutions with initial soluble levels of Pu(IV) below 2×10^{-8} M.</p>

Quality Requirements

The data represented in this report will refer to PNWD (in support of *Bechtel National, Inc. Support Project* [BNI-SP] before February 12, 2007) or PNNL (in support of *Waste Treatment Plant Support Program* [RPP-WTP] following February 12, 2007). Work was performed for both of these projects to the same QA program.

PNNL implemented the RPP-WTP quality requirements by performing work in accordance with the River Protection Project-Waste Treatment Plant Support Program (RPP-WTP) Quality Assurance Plan (RPP-WTP-QA-001, QAP). Work was performed to the quality requirements of NQA-1-1989 Part I, *Basic and Supplementary Requirements*, NQA-2a-1990, Part 2.7, and DOE/RW-0333P, Rev 13, *Quality Assurance Requirements and Descriptions (QARD)*. These quality requirements were implemented through the River Protection Project-Waste Treatment Plant Support Program (RPP-WTP) Quality Assurance Manual (RPP-WTP-QA-003, QAM).

PNNL addressed internal verification and validation activities by conducting an Independent Technical Review of the final data report in accordance with PNNL's procedure QA-RPP-WTP-604. This review verifies that the reported results were traceable, inferences and conclusions were soundly based, and the reported work satisfied the Test Plan objectives.

R&T Test Conditions

Table S.3 discusses R&T test conditions implemented in a pertinent portion of the test specification.

Table S.3. Discussion of R&T Test Conditions

List R&T Test Conditions	Were Test Conditions Followed
Battelle shall prepare a test plan containing detailed information needed to implement this test specification.	Yes, Test Plan TP-RPP-WTP-445 was prepared to implement the plutonium speciation before and after oxidative-leaching bench scale test portion of the test specification. The client approved the test plan on 06/28/2006

Simulant Use

The tests described in Section 3.10 of this report used a simplified Hanford tank sludge simulant comprised of homogeneously co-precipitated iron(III) hydroxide, chromium(III) hydroxide, and trace amounts of Pu(IV) hydroxide. Section 2.6 of the report provides a detailed description of the simulant composition and conditions used in its preparation. The simulant was used to generate oxidative alkaline leachates as result of its treatment with permanganate to convert insoluble chromium(III) to soluble chromium(VI). These leachates were selected at the final stage of the project to simulate feed materials for speciation analysis of plutonium.

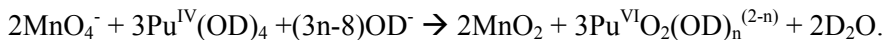
Discrepancies and Follow-on Tests

Most experiments specified in the Test Plan were performed in accordance with the proposed procedures. A number of changes were introduced into the procedures that were initially suggested for preparing alkaline stock solutions of Pu(V) and Pu(IV). In the case of Pu(V), a simpler and safer way was found to prepare a stable solution of purely pentavalent Pu in concentrated alkali (see Section 2.2 for more details). The original procedure for preparing the relatively concentrated Pu(IV) solution in 10 M sodium hydroxide was abandoned because of the impossibility of verifying its final oxidation state using liquid waveguide capillary cell spectroscopy in such a viscous medium. Instead, the working solutions of Pu(IV) in alkaline medium were generated by spiking small volumes of acidic Pu(IV) into a large excess of sodium hydroxide.

The results from this testing lead to the following recommendations for further study:

- 1) To obtain a direct proof of Pu(VI) being the only oxidation state in the oxidative-leaching simulants, the Pu(OD)₄ oxidative-dissolution experiments need to be performed with

substoichiometric additions of permanganate with respect to an amount of freshly generated Pu(OD)_4 , assuming 2:3 stoichiometry for the following reaction:



This reaction should be studied first in a carbonate free medium with detection of Pu(VI) in solution using its major peak at 625 nm.

- 2) It is desirable to repeat these experiments in a mixed deuterated hydroxy-carbonate medium to maximize the formation of the mixed $\text{Pu}^{\text{VI}}\text{O}_2(\text{OD})_n(\text{CO}_3)_m^{-(n+2m-2)}$ complex with a more-intense and better-defined absorbance peak of Pu(VI) with a maximum at 870 nm. Detecting this peak and verifying its molar absorptivity should serve as an additional proof of existence of dissolved plutonium solely in the hexavalent form.
- 3) A series of the $\text{Fe(OH)}_3/\text{Cr(OH)}_3/\text{Pu(OH)}_4$ sludge simulants with a variety of Fe(III) to Cr(III) to Pu(IV) molar ratios should be prepared and tested in alkaline oxidative-leaching experiments to understand better Pu leachability and post-leaching behavior as a function of the simulant composition and Mn(VII)-to-Cr(III) molar ratio.
- 4) This variation should include two simplified cases of only one macrocomponent present with homogeneous incorporation of Pu(IV) traces:
 - Fe(III) + Pu(IV) (with no Cr(III) present)
 - Cr(III) + Pu(IV) (with no Fe(III) present).

These simplified matrices are expected to elucidate the behavior of plutonium associated with the individual phases of Fe(OH)_3 and Cr(OH)_3 in the process of oxidative leaching.

- 5) Selective dissolution of the MnO_2 phase generated in the oxidant-treated sludge simulant as a product of permanganate reduction by Cr(OH)_3 should be tested (with determination of Pu leachability from MnO_2) to understand the distribution of insoluble plutonium between the remaining Fe(OH)_3 and the newly formed MnO_2 in the metathesized sludge simulant.

1.0 Introduction

Oxidative alkaline leaching of Hanford tank sludges using permanganate was shown to not only solubilize Cr(III) phases in the sludge, but to also increase the concentration of plutonium in the leachates. The extent of Pu solubilization is a sensitive function of the level of sodium hydroxide in the leachant, with a much higher percentage of Pu dissolution found in leachates at higher alkalinity (3 M NaOH). All previous tests with real Hanford tank sludges did not provide any information regarding the oxidation state and the chemical form of the dissolved Pu in alkaline leachates containing chromate (and occasionally permanganate as excessive or not fully reacted oxidant). Knowledge of Pu speciation in the leachates is of crucial importance for understanding and predicting the behavior of this fissionable material at subsequent stages of treating process streams. This treatment includes removing ^{137}Cs and other fission products using an ion-exchange process based on the application of a resin with a significant reduction potential. This property of the resin is related to the abundance of organic moieties of a reductive nature in its polymeric framework. The interaction of Pu in its higher and more soluble oxidation states (penta- and/or hexavalent plutonium) with an excess of the ion-exchange resin may induce the reduction of Pu to its much less soluble tetravalent form. This process may be followed by the precipitation of poorly soluble $\text{PuO}_2 \cdot x\text{H}_2\text{O}$ and its retention on the surface of the resin beads, or by its uncontrolled accumulation in pipelines and solution storage vessels at the subsequent stages of the leachate treatment process.

On the other hand, the effect of the solubilization of Pu by the oxidative treatment of the sludge might be related to the formation of the more soluble Pu(IV) species [without their oxidation to Pu(V) or Pu(VI)] due to increased temperature at the leaching stage or transformation of the hydrolyzed forms of Pu(IV) to its mixed hydroxy complexes with carbonate and, to a lesser extent, with chromate. The former agent is always present in the stock solutions of NaOH as a contaminant. Unlike Pu(V) or Pu(VI), these transformed species of Pu(IV) may interact with the resin beads in a completely different way.

The potential accumulation of significant amounts of the insoluble phase of Pu(IV) within the process equipment raises criticality safety concerns and calls for the development of a direct speciation analysis of Pu in the oxidative alkaline leachates before their treatment to remove fission products and other components from the post-leaching process streams.

Bechtel National, Inc. (BNI) is evaluating the plutonium speciation in caustic solutions that reasonably represent the process streams from oxidative-leaching demonstration test. Battelle—Pacific Northwest Division (PNWD) was contracted to develop a spectrophotometric method to measure plutonium speciation at submicromolar ($< 10^{-6}$ M) concentrations in alkaline solutions in the presence of chromate and carbonate. Data obtained from the testing will be used to identify the oxidation state of Pu(IV), Pu(V), and Pu(VI) species that potentially could exist in caustic leachates. Work was initially conducted under contract number 24590-101-TSA-W000-00004 satisfying the needs defined in Appendix C of the *Research and Technology Plan* TSS A-219 to evaluate the speciation of chromium, plutonium, and manganese before and after oxidative leaching. In February 2007, the contract mechanism was switched to Pacific Northwest National Laboratory (PNNL) Operating Contract DE-AC05-76RL01830.

This section provides background information for the following areas: the oxidation states and reduction-oxidation (redox) stability of Pu as well as the solubility of Pu in an alkaline medium; the controversy in determining the stability fields of Pu-soluble species on Eh-pH diagrams in alkaline solutions; the direct speciation of Pu at low micromolar concentrations; and Pu solubilization and speciation in the process of oxidative alkaline leaching. The goals of the project are also discussed.

1.1 Oxidation States and Redox Stability of Pu(IV, V, and VI) in an Alkaline Medium

Plutonium has a very diverse redox and complexation chemistry in aqueous solution, depending on the pH and redox potential. While the oxidation states of Pu and the redox equilibria between them have been well established in acidic medium (Weigel et al. 1986), the alkaline chemistry of Pu has not been investigated as thoroughly. Among a number of difficulties associated with studies of Pu redox and complexation chemistry in alkaline solutions, the low solubility of Pu(IV, V) and to a lesser extent of Pu(VI) should be mentioned as the major problem that makes it impossible in most cases to apply direct noninvasive techniques (such as Optical Absorbance Spectroscopy) for reliable identification of the oxidation states of Pu and possible interconversions between them.

The plutonium-reduction potentials for 1 M hydroxide were projected based on the respective potentials in acid and the corresponding hydrolysis reactions (Allard et al. 1980). Table 1.1 shows the results of this calculation.

Table 1.1. Standard Potentials for Plutonium for the Hypothetical Condition of Zero Ionic Strength. Values at pH 14 were calculated using hydrolysis data and solubility products for respective oxidation states of Pu.

Valence Change	pH	Dominating Reaction	E°, V
VI-V	0	$\text{PuO}_2^{2+} + \text{e}^- = \text{PuO}_2^+$	0.933
	14	$\text{PuO}_2(\text{OH})_3^- + \text{H}^+ + \text{e}^- = \text{PuO}_2(\text{OH})_2^- + \text{H}_2\text{O}$	0.16 ± 0.24
VI-IV	0	$\text{PuO}_2^{2+} + 4\text{H}^+ + 2\text{e}^- = \text{Pu}^{4+} + 2\text{H}_2\text{O}$	1.024
	14	$\text{PuO}_2(\text{OH})_3^- + 2\text{H}^+ + 2\text{e}^- = \text{Pu}(\text{OH})_5^-$	0.34 ± 0.12
V-IV	0	$\text{PuO}_2^+ + 4\text{H}^+ + \text{e}^- = \text{Pu}^{4+} + 2\text{H}_2\text{O}$	1.115
	14	$\text{PuO}_2(\text{OH})_2^- + \text{H}^+ + \text{H}_2\text{O} + \text{e}^- = \text{Pu}(\text{OH})_5^-$	0.52 ± 0.24
IV-III	0	$\text{Pu}^{4+} + \text{e}^- = \text{Pu}^{3+}$	1.017
	14	$\text{Pu}(\text{OH})_5^- + \text{H}^+ + \text{e}^- = \text{Pu}(\text{OH})_4^- + \text{H}_2\text{O}$	-1.04 ± 0.24

The authors pointed out that the formation of polynuclear species and the probable dehydration of $\text{Pu}(\text{OH})_4$ to PuO_2 with a decrease in solubility were not considered in their calculation. Therefore, they considered their description of aqueous plutonium chemistry in alkaline aqueous solution as partly qualitative with an emphasis on the need for accurate chemical data in this field.

Plutonium oxidation states in alkaline solution have been recently reviewed by Barney and Delegard (1999). Pu(III) and Pu(VII) were reported to be unstable in alkaline solutions at NaOH concentrations from 0.1 M to 15 M. The Pu(VI)/Pu(V) couple was found to be reversible, which implies that the respective plutonium species have similar structures. On the other hand, the Pu(V)/Pu(IV) was found to be irreversible, indicating structural differences between these two oxidation states of plutonium.

Dependence of the formal potentials of the Pu(VI)/Pu(V) and Pu(V)/Pu(IV) couples on the concentration of NaOH shows that the both dependences are linear functions of NaOH concentration over the ranges from 1 M to 14 M and 5 M to 14 M of NaOH, respectively, with a much more significant downward slope for the V/IV line than for the VI/V one. The two plots (Figure 1.1) cross each other at approximately 9 M of NaOH. This indicates that Pu(V) is unstable to disproportionation at NaOH concentrations lower than the crossing point.

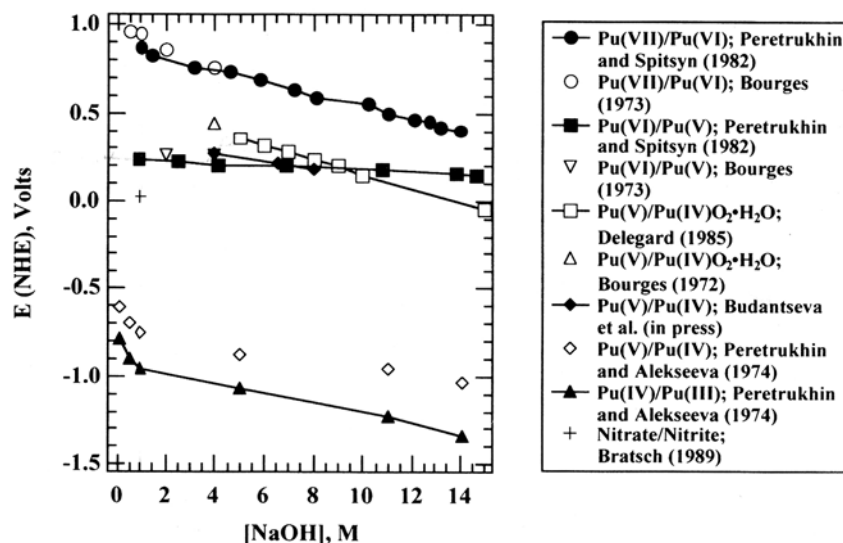


Figure 1.1. Formal Potentials of Various Pu Couples as a Function of NaOH Concentrations. Taken from (Barney and Delegard 1999).

Optical absorbance spectra of Pu(IV), Pu(V), and Pu(VI) in acidic aqueous solution are well established (see, for example, Table 7.96 [page 787] in [Weigel et al. 1986]). Their spectral features are sufficiently resolved both in the visible and near IR ranges of the spectrum to allow quantification of Pu speciation when two or more oxidation states coexist in the same solution. However, the alkaline chemistry of these oxidation states of plutonium is much less explored, and very few measurements of absorbance band positions and intensities are reported in the literature for Pu(V) and Pu(VI) (Budantseva et al. 1997) at NaOH concentrations from 2 M to 8 M. Essentially, no data on optical absorbance spectra of Pu(VI) and Pu(V) at low-to-moderate concentrations of NaOH (0.1 to 1 M) are reported. This lack of spectral measurements in the case of Pu(V) is attributed to a strong tendency of Pu(V) to disproportionation at low alkalinity (Budantseva et al. 1997). A spectrum of freshly prepared Pu(VI) in alkaline solution with a major peak position at 875 ± 3 nm is reported to be unstable at an NaOH concentration of < 2 M and at $Pu(VI) > 5 \times 10^{-4}$ M. No spectrum of Pu(IV) was reported at any concentration of NaOH, presumably because of the very low solubility of this oxidation state of Pu in an alkaline medium and especially at a lower concentration of NaOH.

1.2 Solubility of Pu(IV, V, and VI) in an Alkaline Medium

Plutonium-solution chemistry under alkaline conditions is dominated by the low solubility of amorphous hydroxide, $Pu(OH)_4$ (am), or hydrous oxide, $PuO_2 \cdot xH_2O$ (s), where designation “s” may stand for fresh, X-

ray amorphous precipitates (“am”) or for aged precipitates including both amorphous and microcrystalline fractions (Neck et al. 2007 and references therein). The stabilization of higher oxidation states and an increasing solubility of plutonium compounds are observed with increasing hydroxide concentrations. Figure 1.2, which is based on a recent review of Pu chemistry in alkaline media (Barney and Delegard 1999) shows solubilities of Pu(IV), Pu(V), and Pu(VI) compounds as a function NaOH concentrations.

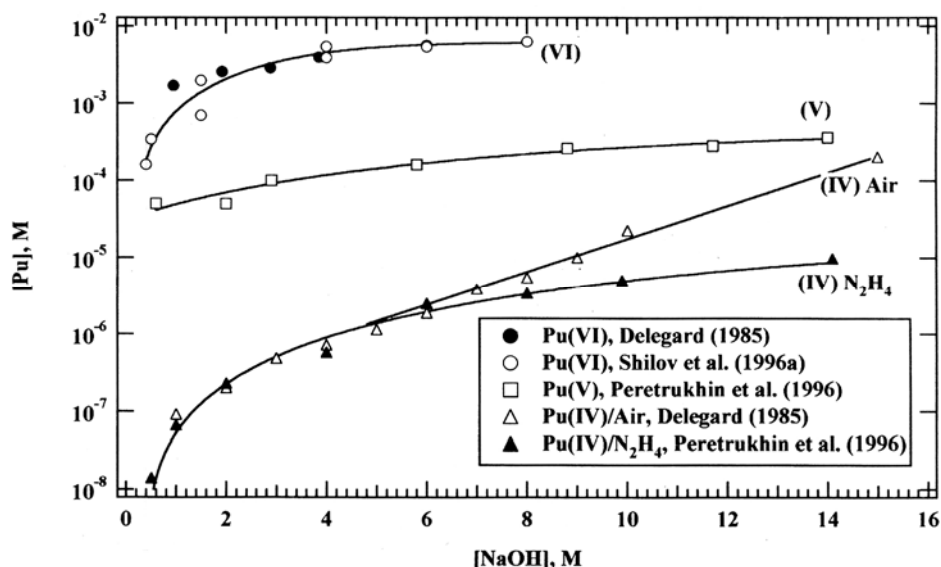


Figure 1.2. Solubility Curves of Pu(IV), Pu(V) and Pu(VI) as a Function of NaOH Concentration. Taken from Barney and Delegard’s review (Barney et al. 1999).

It should be noted that at lower hydroxide concentration (<1 M of NaOH), solubility data for Pu(V) and Pu(IV) cannot be considered reliable because the soluble species of Pu in equilibrium with respective salts or hydroxides of Pu(IV) and Pu(V) were never characterized by optical absorbance spectroscopy (OAS) to confirm that the final oxidation state of Pu corresponded to the initially added oxidation state. The perturbation of the initial oxidation state of Pu may occur through a number of Redox reactions (such as oxidation by dissolved oxygen or disproportionation reaction for intermediate oxidation states of Pu). Pu(VI) solubility remains relatively high and constant in a broad range of NaOH concentrations from 1 to 15 M, but rapidly goes down by several orders of magnitude in the 1 M to 0.4 M NaOH range. It appears that Pu(VI) solubility was not systematically measured in the 0.4 M to 0.1 M range of NaOH concentrations, and only one experimental point is available for Pu(VI) solubility at 0.11 M of NaOH where 10.5 μ M of Pu(VI) was found in equilibrium with the solid phase of plutonyl hydroxide (Perez-Bustamante 1965).

Pu chemistry in alkaline solution becomes even more complex in the presence of a high concentration of multicharged anions capable of competing with hydroxide for coordination sites around a plutonium metal center. The effect of a number of inorganic and organic complexing agents on the solubility of Pu(OH)₄ was studied in 1 M NaOH and 4 M NaOH solutions representing the conditions under which Hanford high level wastes are stored (Peretrukhin et al. 1996). In the absence of complexing agents, the solubility of Pu(IV) was found to be 0.067 μ M and 0.58 μ M in 1 M and 4 M NaOH solutions,

respectively. Among inorganic complexants tested (carbonate, phosphate, and fluoride), carbonate showed the most significant effect of solubility enhancement of Pu(IV) (from 5.2 to 16 times in 1 M of NaOH in the carbonate concentration range of 0.05 to 0.5 M), illustrating the effect of a mixed complex formation with this ligand. In regard to organic chelators tested (glycolate, citrate, ethylenediaminetetraacetate [EDTA], and oxalate), the first three agents showed practically the same level of solubility increase (25 to 28 times in the ligands' concentration range from 0.03 to 0.5 M). At higher alkalinity (4 M of NaOH), the effect of all complex-forming reagents on the solubility of Pu(IV) hydroxide becomes ~ 10 to 15 times less significant for organic chelators and 2 to 3 times less in the case of carbonate.

In a recent series of tests at Savannah River National laboratory (SRNL), Pu(IV) in nitric acid was mixed with a large number of different simulated waste compositions (Rudisill et al. 2004). These simulants contained sodium salts of NO_3^- , NO_2^- , OH^- , CO_3^{2-} , and $\text{Al}(\text{OH})_4^-$ anions. These solutions were mixed for 1 to 3 months, then sampled, filtered, and analyzed for total Pu concentration. It was determined that only CO_3^{2-} and OH^- were statistically significant factors in increasing Pu solubility. The analyses produced the following empirical model of Pu(IV) solubility (see Equation 1.1 below). The data also show that temperatures in the range 25 to 85°C do not have a statistically significant impact on Pu(IV) solubility.

$$[Pu] = -7.48 \times 10^{-8} + 1.2 \times 10^{-6} [\text{OH}^-] + 4.9 \times 10^{-6} [\text{CO}_3^{2-}] \quad (1.1)$$

(The derived coefficients are valid for OH^- and CO_3^{2-} concentrations expressed in molar scale.)

Since the reference process for oxidative leaching involves leaching between 0.1 M and 1.0 M of NaOH (with minimal carbonate), a reasonable lower limit on the Pu(IV) solubility under expected Waste Treatment Plant (WTP) conditions is 5×10^{-8} M. It is important to note that the calculated value of Pu(IV) solubility of 5×10^{-8} M is obtained by extrapolating the derived equation onto an unexplored range of alkalinity because the lowest hydroxide concentration tested in the SRNL study was 0.45 M of NaOH, and that solution also contained 0.073 M of Na_2CO_3 .

1.3 Controversy in Determination of Stability Fields of Pu(IV), Pu(V), and Pu(VI) Soluble Species on Eh-pH Diagrams in Alkaline Solutions

The Redox speciation of Pu as a function of solution acidity (pH) and oxidation potential (Eh) can be conveniently expressed in the form of Eh-pH diagrams. In a carbonate-free medium, hydrolysis constants of Pu(III), (IV), (V), and (VI) should be taken into account to derive functional expressions describing the Redox potentials of Pu(IV)/Pu(III), Pu(V)/Pu(IV), and Pu(VI)/Pu(V) Redox couples as a function of acidity. One of the first attempts to construct Eh-pH diagrams for Pu in carbonate-free aqueous solution was undertaken by Lierse and Kim (1986). Their diagram is reproduced here as Figure 1.3. According to their calculations, the region of stability of Pu(V) is limited not only by increasing acidity ($\text{pH} > 1.5$), but also by relatively low hydroxide concentration ($\text{pH} < 10.2$). At higher alkalinity, Pu(IV) exists in equilibrium with Pu(VI). This disappearance of Pu(V) from equilibrium with lower and higher oxidation states of Pu, to our understanding, is based of the fact that calculated potential of the Pu(V)/Pu(IV) couple exceeds the oxidation potential of the Pu(VI)/Pu(V), which makes Pu(V) unstable at $\text{pH} > 10.2$ due to its disproportionation to Pu(VI) and Pu(IV).

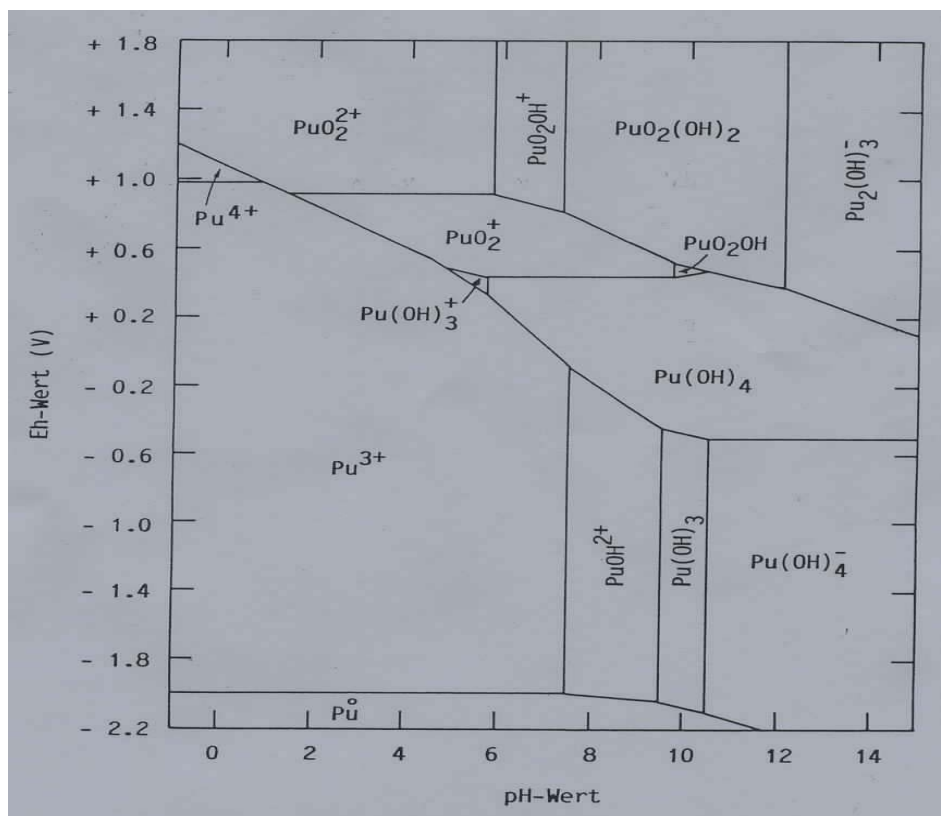


Figure 1.3. Eh-pH Diagram for Plutonium Based on Standard Redox Potentials and Hydrolysis Reactions of Pu(III, IV, V, and VI) Ions in Aqueous Solution. These are carbonate-free conditions (Lierse and Kim 1986).

More recently, Runde constructed the Eh-pH diagram for Pu in water containing hydroxide, carbonate, and fluoride with the ligands' concentrations comparable to those found in groundwater from well J-13 (Yucca Mountain, Nevada) (Runde 2000). This diagram is shown in Figure 1.4. In striking contrast with the previous figure, the alkaline side of this diagram shows a much larger stability field of Pu(V), extending all the way to a 1 M NaOH concentration (pH = 14). In the pH range from 8 to 12.3 Pu(V) is represented by a monocarbonate complex in equilibrium with bis- and tris-carbonate complexes of Pu(VI) at higher potentials. Complexation with carbonate and its effect on Redox potentials might be responsible for such prominent changes in the stability field of Pu(V) due to suppression of its disproportionation. However, starting from pH 12.3 and higher, the carbonate complexation of both Pu(V) and Pu(VI) yields to a formation of hydroxy complexes, the most predominant of which, according to the previous diagram, should result in eliminating Pu(V) from the equilibrium. Yet, a stability field Pu(V) is present in Figure 1.4 all the way to pH 14. This discrepancy between the Lierse's and Runde's calculations [both based on the similar values of hydrolysis constants of Pu(IV), Pu(V), and Pu(VI)] is difficult to understand.

Another attempt of Pu Redox speciation modeling in terms of the Eh-pH diagram was undertaken just a few months ago at Los Alamos National Laboratory by the same group of authors who did the calculation 7 years ago (Reilly et al. 2007). The new diagram is reproduced in Figure 1.5. Apparently, the same concentrations of fluoride and carbonate representative for the J-13 groundwater were used in both the calculations. It is amazing to see to what extent the alkaline portion of the diagram has been transformed

for the same matrix composition. It appears now that carbonate complexes of both Pu(V) and Pu(VI) do not yield to hydrolysis and, instead, dominate the speciation of these higher oxidation states of Pu up to 1 M NaOH concentration. The Redox potentials of Pu(V)/Pu(IV) and Pu(VI)/Pu(V) couples at pH = 14 dropped down from +0.21 and +0.36 V (old diagram) to -0.04 and 0.22 V (new diagram), respectively. The respective numbers for pH 13.5 (~0.31 M of NaOH) changed from +0.23 and +0.38 V to +0.02 and +0.24 V. To the best of our knowledge, the stability constants of hydroxide and carbonate complexes of Pu(IV), Pu(V), and Pu(VI) have not been remeasured or critically revised to any significant extent in the last 7 years, which would explain such significant changes in the positions of the stability fields of Pu(IV), Pu(V), and Pu(VI) as well as the drastic change between relative magnitudes of hydroxide and carbonate competition for the metal center.

Regardless of the controversy in the Redox field positions of soluble forms of Pu, one valuable feature of the Eh-pH diagram shown in Figure 1.5 never presented before should be mentioned here. This diagram shows areas of stability fields of the solubility controlling phases of Pu(III) [Pu(OH)CO₃(s)], Pu(IV) [Pu(OH)₄(s)], and Pu(VI) [PuO₂(OH)₂(s)] in equilibrium with soluble species of Pu. It is interesting to see that Pu(OH)₄(s) controls the soluble levels of Pu at much higher potentials than those that define the stability field of Pu(OH)₄(aq). This feature helps to better understand Pu speciation and solubility in heterogeneous systems.

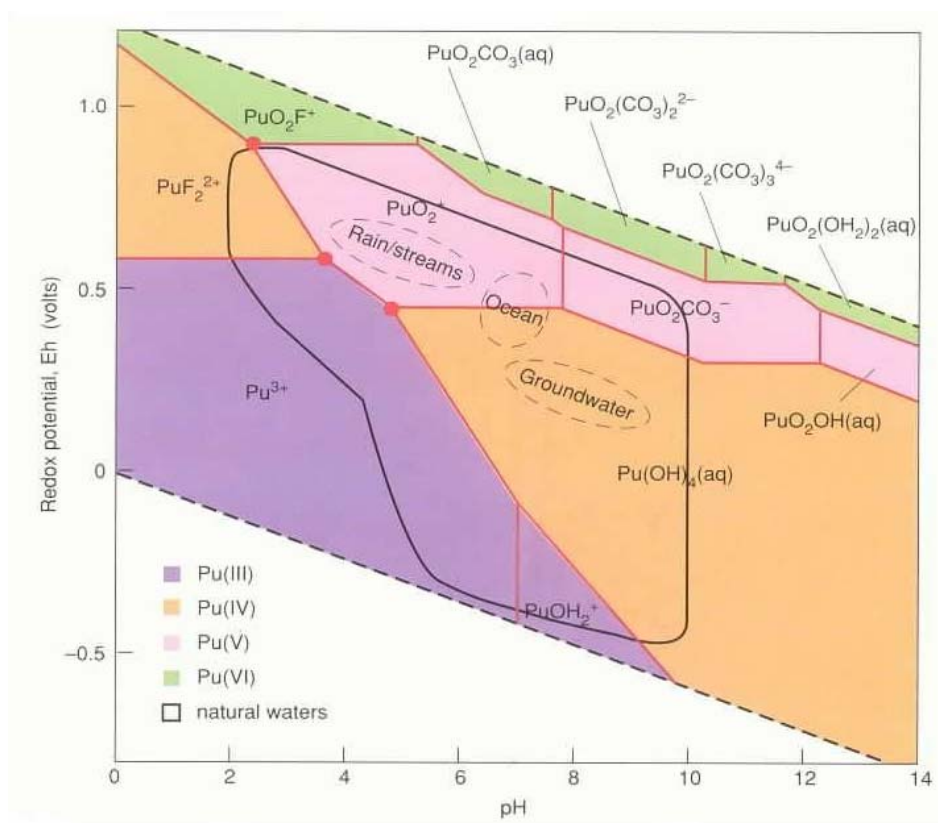
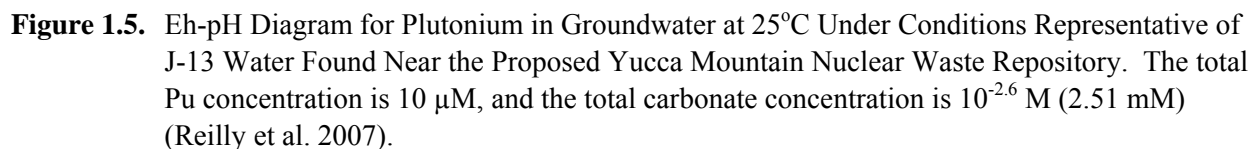


Figure 1.4. Eh-pH Diagram for Plutonium in Groundwater Containing Hydroxide, Carbonate, and Fluoride Ions. The ligand concentrations are comparable to those found in water from well J-13 at Yucca Mountain, Nevada (Runde 2000). The total Pu concentration is fixed at 10 μ M.



OAS is recognized as a direct noninvasive technique for studying Redox and complexation reactions of plutonium in solution. The applicability of conventional OAS is typically limited to a 10^{-5} to 10^{-3} M concentration range of Pu, depending on the oxidation state and the signal-to-noise ratio of the spectrophotometer (for measurements with 10-mm thick optical cells). The solubility of Pu compounds in neutral to moderately alkaline solutions is typically below 10^{-6} M, which precludes the application of conventional OAS for Pu speciation analysis.

1.8

The development of liquid-core waveguides over the last decade has allowed for the use of extremely long path lengths with small sample volumes and rapid sampling times (Waterbury et al. 1997). This method uses narrow-diameter capillary tubing for light transmission through a thick layer of solution under conditions of total internal reflection of the light from the tubing walls surrounding the solution. Cells of this type showed a good sensitivity in the analysis of trace transition metals, nitrate, and other analytes of interest in aquatic systems (Byrne et al. 2002). The first and so far the only application of a 100-cm long Liquid Waveguide Capillary Cell (hereafter LWCC) for plutonium detection and quantification was reported very recently (Wilson et al. 2005). Detection limits of 0.7 μM for Pu(VI), 16 μM for Pu(V), 5 μM for Pu(IV), and 8 μM for Pu(III) in acidic medium were achieved. The limits of detection represented increases of 18 to 33 times with respect to those achievable using a conventional 1-cm pathlength. To the best of our knowledge, no attempts were made to test the LWCC method for detection of lanthanides or actinides in an alkaline medium.

It should be mentioned that both LIPAS detection and LWCC detection achieve significant improvements in sensitivity in a limited spectral range from ~ 250 to ~ 750 nm. According to the LWCC manufacturer's specifications, the operation range of 100-cm LWCC is limited to 230 to 750 nm, and that of 500-cm cell narrows down to the 300- to 700-nm spectral window. This limitation is related to the absorbance spectrum of water (H_2O) as a solvent. The absorption coefficient of water is at its minimum of 0.015 to 0.030 m^{-1} in the 370- to 510-nm range. Beyond this range of wavelengths, it quickly grows both in ultraviolet (UV) and near infrared (IR) directions, and at 210 and 800 nm, it reaches a 2.0 m^{-1} value. An increase in water absorbance in the IR direction becomes even more dramatic starting from ~ 870 nm, which precludes reliable spectrophotometric measurements using LWCC detection in the near-IR range of the spectrum where a number of analytically important absorbance bands of Pu are possibly located in alkaline solution.

On the other hand, it is known that deuterated or heavy water (D_2O) has a very low and flat optical absorbance coefficient in the wide near-IR range of the spectrum. This difference in the optical properties of H_2O and D_2O could be exploited to perform Pu speciation analysis over a much wider optical window of several hundred nanometers (from ~ 300 to 1200 nm), provided that heavy water can be used as a solvent to prepare all the solutions for spectrophotometric analysis of Pu. No adverse effect by the use of D_2O instead of H_2O is expected in terms of measurable changes in the absorption peaks' positions and intensities of Pu(IV, V, & VI). This expectation is based on the very close similarity of absorption spectra of rare-earth ions in H_2O and D_2O solutions (Carnall 1979). Only one reference is found for actinide elements (Neck et al. 2001), which demonstrates that the peak position of tetravalent neptunium [Np(IV)] at 723 nm remains the same both in $\text{HClO}_4/\text{H}_2\text{O}$ and $\text{DClO}_4/\text{D}_2\text{O}$ solutions over pH (pD) range of 0 to 3.3.

The expected presence of chromate in alkaline solutions relevant to leachates originating from oxidative alkaline treatment of Hanford tank sludges (see next section for more details) might produce serious limitations to the window of optical transparency of water from near-UV to the visible range of the optical spectrum. This fact makes the application of D_2O as a solvent in studies of Pu speciation in chromate-containing solutions even more important to extend the operation range of LWCC toward the previously inaccessible near-IR region of the spectrum.

The main focus of this project is to determine the spectral features of Pu(IV), Pu(V), and Pu(VI) in a moderately alkaline medium ($\text{D}_2\text{O} + \text{NaOD}$) at low micromolar concentrations of Pu. These spectral features were compared whenever possible with the respective spectral signatures of Pu in a conventional

solvent both from the acidic side ($\text{H}_2\text{O} + \text{HNO}_3$) and the alkaline side ($\text{H}_2\text{O} + \text{NaOH}$) reported in the literature. In all cases when such comparison was possible, no differences were found in the positions or molar intensities of the respective absorbance bands. This proves that the presence of D_2O and OD^- in the primary coordination sphere of hydrolyzed Pu ions does not change their optical properties or the extent of their interaction with other complex forming agents, such as carbonate.

In regard to the isotopic effect on kinetics and thermodynamics of Cr(III), Pu(IV), and Pu(V) oxidation to their higher oxidation states by permanganate, it should be noted that the oxidation potentials of Mn(VII)/Mn(VI) and Pu(VI)/Pu(V) couples in deuterated alkaline media determined in the course of this project are in close agreement with the respective values reported for these couples in an ordinary solvent ($\text{H}_2\text{O} + \text{NaOH}$). This similarity suggests that the thermodynamics of the oxidative action of permanganate does not change when regular water is used instead of D_2O . The differences in the reaction rates of permanganate with Cr(III) and the lower oxidation states of Pu in D_2O vs. H_2O are likely to be more pronounced than the possible subtle differences in the magnitudes of oxidation potentials. However, all reactions studied in this project were found to reach equilibrium in less than 2 to 3 hrs. The rate constants of reactions of oxidizable compounds with permanganate in “protium” medium are typically higher than in deuterated medium. Consequently, it is believed that the oxidation processes in regular water should be less kinetically hindered and should approach a state of equilibrium even more rapidly.

1.5 Pu Solubilization and Speciation in the Process of Oxidative Alkaline Leaching of Hanford Tank Sludges

Chromium(III), one of the major components in Hanford tank sludge, originated mostly from the REDOX process. Chromium can interfere with high-level waste vitrification. Alkaline oxidative treatment of Hanford Site tank-waste sludges is currently under development to remove insoluble Cr(III) phases from the sludge by converting it into soluble Cr(VI) species.

Permanganate proved to be the best oxidizing agent among six candidates tested (hydrogen peroxide, ozone, persulfate, ferrate, peroxyxynitrite, oxygen, and permanganate, Rapko et al. 2004). One of its advantages compared with persulfate is moderate extent of TRU solubilization. It is expected that oxidizing conditions would partially dissolve co-precipitated Pu(IV) hydrous oxide present in the sludge by formation of anionic Pu(V) and/or Pu(VI) species.

Identification of Pu oxidation states in the sludge leachates is critical for understanding and predicting Pu behavior at the later stages of treatment of the leachate solutions including ^{137}Cs removal by ion exchange and regeneration of the resin.

1.6 The Project Goals

The following goals have been identified to achieve the project objectives as summarized in Table S.1. These goals are based on the description of the tests (Tasks 1 to 5) provided in the Test Plan TP-RPP-WTP-445.

- Determine the usable spectral range of 5-meter-long LWCC in alkaline H_2O and D_2O media in the presence of chromate.

- Demonstrate the applicability of LWCC-based optical absorbance spectroscopy for enhanced detection of various oxidation states of plutonium in alkaline media in the visible and near-IR range of the spectrum.
- Establish spectral signatures of Pu(IV, V, and VI) in weakly to moderately caustic solutions (0.1 M to 1 M hydroxide) at low micromolar concentrations of Pu. Determine detection limits of Pu for the respective oxidation states under these conditions.
- Evaluate the effect of carbonate on the spectral characteristics of Pu(IV, V, and VI) in alkaline media and estimate the extent of solubility enhancement of Pu(IV) in the presence of carbonate at 0.25 M of NaOD.
- Study redox stability of Pu(IV) and Pu(V) in the presence of chromate and permanganate in alkaline medium and examine redox-state perturbation upon acidification of initially alkaline solutions.
- Study Pu leaching from the $\text{Fe}(\text{OH})_3/\text{Cr}(\text{OH})_3/\text{Pu}(\text{OH})_4$ sludge simulant with homogeneously co-precipitated Pu as a function of time, Mn(VII)-to-Cr(III) ratio, and hydroxide concentration.

1.7 Quality Assurance and Quality Control

The following sections describe the quality assurance (QA) program and quality control (QC) measures applied to the conduct of work. The data represented in this report will refer to PNWD (in support of *Bechtel National, Inc. Support Project* [BNI-SP] before February 12, 2007) or PNNL (in support of *Waste Treatment Plant Support Program* [RPP-WTP] following February 12, 2007). Both of these projects performed work to the same QA program.

1.7.1 Application of RPP-WTP Quality Assurance Requirements

As of February 2007, the QA program is described as follows:

PNNL's QA program is based on requirements defined in DOE Order 414.1C, Quality Assurance and 10 CFR 830, Energy/Nuclear Safety Management, Subpart A—Quality Assurance Requirements (a.k.a., the Quality Rule). PNNL has chosen to implement the requirements of DOE Order 414.1C and 10 CFR 830, Subpart A by integrating them into the laboratory's management systems and daily operating processes. The procedures necessary to implement the requirements are documented through PNNL's Standards-Based Management System.

PNNL implemented the RPP-WTP quality requirements by performing work in accordance with the *River Protection Project – Waste Treatment Plant Support Program (RPP-WTP) Quality Assurance Plan* (RPP-WTP-QA-001, QAP). Work was performed to the quality requirements of NQA-1-1989 Part I, *Basic and Supplementary Requirements*, NQA-2a-1990, Part 2.7 and DOE/RW-0333P, Rev 13, *Quality Assurance Requirements and Descriptions* (QARD). These quality requirements are implemented through the *River Protection Project – Waste Treatment Plant Support Program (RPP-WTP) Quality Assurance Manual* (RPP-WTP-QA-003, QAM).

A matrix that cross-references the NQA-1, NQA-2a, and QARD requirements with PNNL's procedures for this work is given in Table A1. It includes justification for those requirements not implemented.

1.7.2 Conduct of Experimental and Analytical Work

Experiments that were not method-specific were performed in accordance with PNNL's procedures QA-RPP-WTP-1101 "Scientific Investigations" and QA-RPP-WTP-1201 "Calibration Control System," verifying that sufficient data were taken with properly calibrated measuring and test equipment (M&TE) to obtain quality results.

Spectrophotometric equipment was calibrated as described in Section 2.3. The oxidation-reduction-potential electrode and the pH electrode were calibrated with standard solutions as described in Section 2.7. The plutonium concentrations in simulants were measured according to the ASO procedure RPG-CMC-474, "Liquid Scintillation Counting," using a Perkin Elmer Tricarb model 3100 counter.

1.7.3 Internal Data Verification and Validation

PNNL addressed internal verification and validation activities by conducting an independent technical review of the final data report in accordance with PNNL's procedure QA-RPP-WTP-604. This review verified that the reported results were traceable, that inferences and conclusions were soundly based, and the reported work satisfied the Test Plan objectives. This review procedure is part of PNNL's RPP-WTP Quality Assurance Manual.

2.0 Experimental and Data Processing

This section discusses the experimental details of the experiments, including the reagents and solvents used; the preparation of Pu stock solutions; spectrophotometric equipment; calibration and speciation experiments with LWCC; the determination of Pu concentration in calibration solutions and leachates; the preparation of the sludge simulant and oxidative-leaching procedure; measurements of Eh and pH; the determination of Cr(VI), Mn(VII), and Mn(VI) concentrations in the oxidative-leaching experiments; the determination of baseline subtraction and net-peak intensity in calibration experiments; and the simulation and elimination of spectral interference in LWCC spectra.

2.1 Reagents and Solvents Used in Calibration, Sludge Preparation, and Oxidative-Leaching Experiments

The following solvents and chemicals were used in the course of this project:

- D₂O (99.8 atom % purity available from Aldrich) was stored in sealed vials inside of a dessicator and used directly before experiments.
- DNO₃ 65 wt% with an estimated molar concentration of 14.7 M.
- NaOD 40 wt% (99.5 atom% of D₂O); measured density of 1.527 g/mL; calculated molar concentration 14.9 M.
- Nd(NO₃)₃ 10,000 ppm (0.0693 M) stock solution in 5% HNO₃; (Ricca Chemical Company). Nd stock was converted from H₂O/HNO₃ medium to D₂O/DNO₃ medium by several cycles of evaporation-redissolution in 0.05 M of DNO₃.
- Na₄EDTA.
- Na₂CO₃.
- Na₂CrO₄·4H₂O.
- NaMnO₄·H₂O.
- Fe(NO₃)₃·9H₂O. Used for preparation of 1.33 M Fe(NO₃)₃ stock solution in 0.3 M HNO₃.
- Cr(NO₃)₃·9H₂O. Used for preparation of 1.0 M stock solution of Cr(III) nitrate in 0.3 M HNO₃.

All reagents used in calibration experiments in D₂O media were dried overnight at 140°C in a ventilated oven to remove moisture or hydration water before preparing their solutions in D₂O. In the case of Na₂CrO₄·4H₂O, complete dehydration of this substance was confirmed by excellent correspondence between calculated and observed weight loss.

2.2 The Preparation, Purification, and Valence-State Adjustment of Pu Stock Solutions

Pu Isotopic Composition and Admixtures of Other TRU. The plutonium stock material used in the course of this project had the following isotopic composition: ²³⁸Pu 0.014 atom%, ²³⁹Pu 93.48%, ²⁴⁰Pu 6.51%, ²⁴¹Pu 0.011%, and ²⁴²Pu 0.018%. These numbers correspond to the following alpha-activity fractions in

the total alpha-activity balance of this Pu sample: ^{238}Pu 3.04%, ^{239}Pu 75.6%, ^{240}Pu 19.2%, ^{241}Pu —none (beta emitter), and ^{242}Pu <0.001%. The specific alpha activity of this $^{238, 239, 240}\text{Pu}$ stock sample was calculated to be 2.79 MBq/mg. The main stock solution of $^{238, 239, 240}\text{Pu}$ was available as a 0.9 M solution of more than 99.5% pure Pu(IV) in ~4 M of HNO_3 . It was purified by ion-exchange from ^{241}Am (daughter product of beta-emitting ^{241}Pu) early in 2002. The estimated contribution of newly formed ^{241}Am to the total alpha activity of this Pu sample (over 5 years of storage since the last purification) is less than 0.13%. Admixtures of other oxidation states of Pu [Pu(III) and Pu(VI)] in the stock solution were not spectrophotometrically detectable.

Conversion of Pu(IV) Stock to Deuterated Acidic Medium. Pu(IV) in $\text{DNO}_3/\text{D}_2\text{O}$ was prepared by careful drying of an aliquot of an original Pu(IV) stock under vacuum at ~30°C for several weeks and redissolution of $\text{Pu}(\text{NO}_3)_4 \cdot x\text{H}_2\text{O}$ crystals in 4 M DNO_3 to make an 18 mM solution of Pu(IV). The cycle of vacuum drying and redissolution of dry residue in DNO_3 was repeated two times to minimize the admixture of H_2O of hydration in the final solution.

No attempt to prepare Pu(IV) alkaline stock solution in concentrated NaOD using an excess of holding reductant was made in this project because of problems with spectrophotometric characterization of this stock using LWCC.

Preparation of Pu(V) Stock in $\text{D}_2\text{O}/\text{NaOD}$. A solution of pentavalent Pu in concentrated NaOD was prepared by adding a small amount of Pu(IV) acidic stock solution to an excess of 14.9 M of NaOD. This was followed by continuous agitation of this mixture via magnetic stirring over 20 days with periodical spectrophotometric control of the oxidation state of soluble plutonium after centrifugation of insoluble Pu(IV) hydroxide. Finally, the Pu(V) solution was filtered through a 0.45- μm polysulfone syringe filter and stored in a sealed container to prevent its contamination with carbonate.

Preparation of Pu(VI) in $\text{D}_2\text{O}/\text{DNO}_3$. Hexavalent Pu was prepared by oxidation of Pu(IV) in near boiling 1 M DNO_3 with reflux during 4 hr followed by complete evaporation of all liquids and redissolution of the residue in 0.5 M of DNO_3 . The admixture of Pu(IV) in Pu(VI) was controlled spectrophotometrically [absence of major Pu(IV) peak at 476 nm] and was found not to exceed 1%. The Pu(VI) stock solution was regenerated periodically and used within 10 days since its oxidation to minimize the spontaneous reduction of Pu(VI) to Pu(IV) with time via the radiolytic decomposition of water.

2.3 Spectrophotometric Equipment

Two spectrophotometers were used to collect spectral data:

- SI Photonics 400 with scanning range from 200 to 950 nm and 1.19-nm spectral resolution
- Ocean Optics USB 2000 with scanning range from 550 to 1100 nm and 0.34-nm spectral resolution.

Optical fibers (400- μm core diameter ultraviolet-visible [UV-Vis] fibers from Ocean Optics) were used to conduct light to the LWCC and to collect the transmitted light and direct it to the spectrophotometer.

A 500-cm pathlength LWCC (World Precision Instruments) was used for enhanced Pu detection in deuterated solutions.

Plastibrand cells with a 1-cm pathlength (220- to 950-nm transparency range) were used to collect spectral data for calculating Mn(VI), Mn(VII), and Cr(VI) concentrations in oxidative leaching and homogeneous oxidation experiments.

The spectrophotometric equipment was calibrated daily using a NIST-traceable neutral density filter set RM-1N2N3N available from Starna.

2.4 Calibration and Speciation Experiments with LWCC (cold testing and Pu calibrations)

Constant Alkalinity (acidity) Single Macrocomponent Series with Growing Pu Concentration.

In a typical calibration experiment, a relatively large portion of a desired background solution was prepared, and six 2-mL portions of this solution were placed into 2-mL-capacity Nalgene plastic tubes. Targeted amounts of Nd or Pu stock solutions were added to each tube to create a desired range of Pu concentrations [e.g., 0.5 to 20 μM in Pu(VI) alkaline calibration experiments or 2 to 200 μM of Nd(III) in Nd(III)-EDTA calibration experiments]. Special care was taken to minimize matrix dilution by using smaller volumes of more concentrated Pu stock solutions. In the case of Pu(V) calibration experiments with relatively dilute Pu(V) stock solution available at high alkalinity (14 M of NaOD), the problem of maintaining constant alkalinity across the calibration series was solved by lowering the initial concentration of NaOD in background solutions when going from smaller to higher spike volumes of Pu(V) stock.

Speciation Series with Two Macrocomponents (mixed carbonate hydroxide systems) at Constant Hydroxide and Pu Concentration

In these series of experiments, one stock solution of pure NaOD was prepared first using volumetric dilution of 14.9 M of NaOD in D_2O . One half of this solution was then used to prepare an equimolar solution of Na_2CO_3 in NaOD (e.g., 1 M of Na_2CO_3 in 1 M of NaOD or 0.25 M of Na_2CO_3 in 0.25 M of NaOD). To create a variation of carbonate concentration at constant level of hydroxide, these two stock solutions were mixed in 100:0, 80:20, 60:40, 40:60, 20:80, and 0:100 volume ratios. These six mixtures were prepared in 8-mL amounts and later split onto four equal portions of 2 mL each. The first three portions were used as cold background solutions, and the last portion with the same $\text{CO}_3^{2-}/\text{OD}^-$ ratio was used to add stock solution of Pu(IV, V, or VI). It was necessary to inject three successive portions of the cold background solution of the same composition before injecting the Pu-containing sample to completely eliminate the LWCC memory effect of the previous sample with a different $\text{CO}_3^{2-}/\text{OD}^-$ ratio.

2.5 Determination of Pu Concentration in Calibration Solutions and Leachates

In Pu(VI) calibration experiments in an alkaline medium [0.5- to 20- μM concentration range of Pu(VI)], all Pu was assumed to be soluble, and the final Pu concentration was assumed to be equal to an initially added concentration. No subsamples were withdrawn for Pu concentration analysis by LSC.

In selected oxidative-leaching experiments with $\text{Pu}(\text{OH})_4$ and permanganate in acidic medium (Section 3.8), the concentration of total dissolved Pu was determined via the optical absorbance peak intensity of PuO_2^{2+} at 831 nm. The same procedure was used to estimate the extent of Pu(IV) to Pu(VI)

conversion in monomeric Pu(IV) oxidation experiments with Cr(VI) and/or Mn(VII) in nitric acid (Section 3.8).

In all other calibrations, speciation and oxidative-leaching experiments with Pu(IV) and Pu(V) in alkaline media with a dissolved Pu concentration were determined by LSC. All alkaline Pu-containing samples were acidified with HNO₃ or HCl within the first few hours after completing the experiment. HCl was used to acidify Mn(VII) and Mn(VI)-containing samples to destroy these highly colored species by their reduction with Cl⁻ to produce colorless Mn²⁺.

2.6 Preparation of the Fe(OH)₃/Cr(OH)₃/Pu(OH)₄ Sludge Simulant and Oxidative-Leaching Procedure

The Fe(III) to Cr(III) molar ratio in the sludge simulant was set at 1.0 to 0.7. The targeted amount of sludge was 5 g. The sludge amount was planned assuming six hydration waters, both for Fe(OH)₃ and Cr(OH)₃. To prepare 5 g of Fe(OH)₃ 6H₂O (F.W. = 215) and Cr(OH)₃ 6H₂O (F.W. = 211), a mixture of 3 g of Fe(III) hydroxide and 2 g of Cr(III) hydroxide should be mixed to achieve roughly the 1.0 to 0.7 molar ratio. This corresponds to $3 \times 56 / 215 = 0.78$ g of Fe (as element) and $\sim 0.78 \times 0.7 = 0.545$ g of Cr (as element).

The solution of 10.6 mL of 1.33 M Fe(III) stock mixed with 10.6 mL of 1.0 M Cr(III) stock (60-mL bottle) was transferred into a radiological fume hood. A stock solution of 28 μ L of 18 mM of Pu(IV) in 2M DNO₃ was added to the Fe(III)+Cr(III) mixture under stirring (targeted Pu concentration is 1×10^{-4} moles per kg of sludge). This mixture was neutralized under stirring with ~ 8.5 mL of 25% NaOH and aged for 3 days under continuous slow stirring. The precipitate color was dark brown. Three days after preparation, the sludge sample was centrifuged and supernatant (NaNO₃ solution) was discarded. The visually estimated volume of compacted sludge was 22 to 23 mL. The sludge was washed with water in three steps to remove most of the NaNO₃. Finally, ~ 37 mL of H₂O was added to the centrifuged sludge, and the sludge slurry was homogenized by shaking and then by stirring for 4 hr. The total visible volume of the agitated sludge slurry was about 60 ± 3 mL. Twelve equal portions of this slurry (3.0 mL each) were subsampled from the bottle into separate 2-dram-capacity vials with a 9.5-mm-diameter Spin-Plus stir bar placed inside. Sampling was performed within 6 to 8 seconds after terminating the intense stirring using a 5-mL pipette tip with $\sim 50\%$ of full depth immersion into the bottle. For each subsequent sampling, the stirring was resumed for another 2 to 3 minutes to make sure that the remaining bulk sample of the sludge got freshly mixed, and no fractionation of liquid and solid phases occurred due to sedimentation. All sludge-containing vials were centrifuged for 8 to 10 minutes. The visual volume of the compacted sludge was 1.1 ± 0.1 mL per vial, and it contained 40 mg Fe (as elemental Fe), 28 mg of Cr (as elemental Cr), and 6 μ g of Pu (as elemental Pu). The mass ratio of Pu to the sum of Fe and Cr in the sludge simulant was 8.8×10^{-5} g/g. The estimated interstitial liquid volume in this sludge sample was 0.8 mL ($\sim 75\%$ of the total visible volume). No attempts were made to remove interstitial water from the sludge by evaporation or vacuum drying to determine the fraction of free water in the wet sludge sample.

In a typical sludge leaching experiment, 3 mL of alkaline permanganate solution at a calculated concentration to achieve the desired Mn(VII)/Cr(III) ratio (from 0.66:1 to 1.45:1) was added to the sludge-containing vial. An approximate volume ratio of the leaching solution-to-sludge volume was 3:1. The estimated Cr(VI) concentration in the leachate in the case of complete oxidation of Cr(OH)₃ to chromate was 0.13 M. The estimated concentration of soluble Pu in the same leachate was 6 μ M,

assuming the hypothetical case of complete conversion of insoluble $\text{Pu}(\text{OH})_4$ to fully soluble $\text{Pu}(\text{VI})$ and neglecting the possible co-precipitation of $\text{Pu}(\text{VI})$ with the newly formed solid phase of MnO_2 . The mixture was put onto a stirrer, and full-speed stirring started ~20 to 30 sec after applying the stirrer motor. The 30-sec delay time was associated with difficulty in breaking the stir bar loose from the compacted sludge volume. The vial content was too dark to verify that the entire sludge volume was completely dispersed within the filled portion of the vial, but a deep and stable vortex pattern within the suspension volume indicated a very efficient mixing process in this heterogeneous mixture. In most cases, the first kinetic point was obtained by sampling 3 minutes after starting the full-speed stirring process. Typically, 60 μL of the sludge suspension were filtered through a 0.45- μm syringe filter, and 6 to 8 μL of the filtrate was diluted into 2000 μL of 0.24 M NaOH for determination of $\text{Cr}(\text{VI})$ and the remaining $\text{Mn}(\text{VII})$ or $\text{Mn}(\text{VI})$ concentration by UV-vis spectroscopy. Immediately after spectral measurement, 100 μL of 37% HCl were added to the diluted solution to acidify it and perform the same-day determination of soluble Pu concentration by LSC. For LSC measurements, 200 μL of the acidified solution were mixed with 5 mL of Ultima Gold liquid scintillation cocktail. All acidified samples were later submitted to ASO for Pu concentration determination via total alpha activity measurement by LSC.

2.7 Measurements of Eh and pH

Oxidation-reduction potentials in alkaline solutions from selected calibration and leaching experiments were measured with a combination oxidation-reduction potential (ORP) electrode (Orion) coupled with a Thermo Corporation ORION 5 star multimeter. A commercially available ORP standard solution (ORION 967961) was used for the electrode calibration. In most of our samples containing strong oxidizers (permanganate and/or manganate) and solid phases [MnO_2 , $\text{Fe}(\text{OH})_3$], the measured ORPs showed a slow drift with time. In diluted homogeneous permanganate-manganate mixtures, the ORP drift was invariably negative with time, which correlated with a progressive decrease of permanganate concentration due to its oxidative interaction with plastic surfaces of a stir bar and a polyethylene vial used for ORP measurements (Section 3.9.1). In these cases, the potential observed within the first 3 to 4 minutes from the moment of the electrode immersion into solution was accepted. In all other cases, when the stable ORP reading could not be achieved, the potential observed after 10 to 15 minutes was accepted. The uncertainty of ORP measurements performed in this project is typically ± 10 mV.

For pH measurements of selected alkaline solutions, an ORION 8103 combination electrode was used. The electrode was calibrated using standard pH = 4.00 and pH = 10.01 buffer solutions. The electrode performance after calibration was checked using a series of NaOH and NaOD solutions in the hydroxide (deuteroxide) concentration range from 0.001 M to 1.0 M. It was observed that starting from 0.1 M of hydroxide concentration, the electrode response showed prolonged drifts in pH and little difference in pH (pD) readings between 0.1 M, 0.25 M, and 1.0 M of NaOH (NaOD) concentrations. Re-checking the electrode response with the standard pH buffers after its exposure to the NaOH (NaOD) solutions showed significant positive deviations from the expected pH values with an extended negative drift (often exceeding one pH unit) to lower pH values. For these reasons, pH (pD) measurements were not applied systematically to measure the alkalinity of Pu-containing solutions in calibration and leaching experiments at 0.25 M to 1 M NaOD concentrations.

2.8 Determination of Cr(VI), Mn(VII), and Mn(VI) Concentrations in the Course of Oxidative-Leaching Experiments

An Mn(VII) stock solution in D₂O was prepared by dissolving a known amount of NaMnO₄·H₂O in D₂O, and the concentration of Mn(VII) was determined by spectrophotometric analysis by comparing the 528 nm peak intensity with the respective value of a standard permanganate solution with an Mn(VII) concentration known from titration with oxalate.

The Mn(VI) concentration in leaching experiments with Pu(OH)₄ and Fe(OH)₃/Cr(OH)₃/Pu(OH)₄ sludge simulant was determined spectrophotometrically using a major absorbance band of manganate at 603 nm with $\epsilon = 1598 \text{ M}^{-1} \text{ cm}^{-1}$ (Gmelin 1975, pp. 17-42).

In the case of mutual presence of manganate and permanganate, the extent of Mn(VII) conversion to Mn(VI) in the course of reduction by Pu(IV), Pu(V), and Cr(III) was calculated by normalizing the net gain in optical absorbance at 603 nm onto the difference between the molar absorptivities of Mn(VI) and Mn(VII) at this wavelength position

$$\Delta\epsilon_{603} = \epsilon_{603 \text{ Mn(VI)}} - \epsilon_{603 \text{ Mn(VII)}} = 1598 \text{ M}^{-1}\text{cm}^{-1} - 216 \text{ M}^{-1}\text{cm}^{-1} = 1382 \text{ M}^{-1} \text{ cm}^{-1}.$$

2.9 Baseline Subtraction and Net Peak Intensity Determination in Nd and Pu Calibration Experiments

To minimize the effects of baseline irreproducibility in LWCC measurements on peak-intensity calculations in the spectra of Nd(III) and Pu(V, VI), baseline corrections were made as follows:

Nd(III): The baselines in Nd spectra were approximated with a parabolic function using five to six groups of anchor points in the spectral regions with no absorbance from f-f transitions of Nd, and this was subtracted from the raw spectrum.

Pu(V): The net intensities of 653-nm and 809-nm peaks of pentavalent Pu were determined by subtracting calculated baseline positions at the peaks' maxima from the raw spectrum of Pu(V). Baselines in the regions of interest were approximated by linear functions with anchor points at 646 and 660 nm for the 653-nm peak and at 776 and 835 nm for the 809-nm peak as illustrated in Figure 2.1.

Pu(VI): The major peak of Pu(VI) at 625 nm was treated in the same manner as peaks of Pu(V) by using linear baseline calculation with anchor points at 563 and 710 nm.

2.10 Simulation and Elimination of Waveform-Shaped Spectral Interference in LWCC Spectra Burdened with Low-Frequency Noise

In spectral measurements with LWCC, special care was taken to match chemical composition and concentrations of major components in blank and sample solutions to suppress baseline distortions associated with chemical-composition differences. In most cases, this procedure resulted in good-quality spectral measurements with minimal baseline perturbations. However, in some measurements, the spectral signal was burdened by oscillating waveform-shaped distortions with a wavelength-dependent periodicity (fewer oscillations at higher wavelength values). This pattern is frequently observed in thin-film spectroscopy when the wavelength interval between two adjacent minima or maxima can be used to

calculate the film thickness of the tested material. In this project, no films were intentionally introduced or created along the light-propagation pathway in the process of solution injection, but they could be inadvertently formed within the liquid-core waveguide in the process of not completing the displacement of previously injected solution with a new one with a slightly different refractive index or chemical composition. The exact nature of this spectral distortion remains unclear, but an attempt was made to simulate this interference so it can be subtracted from the distorted spectrum to improve its quality.

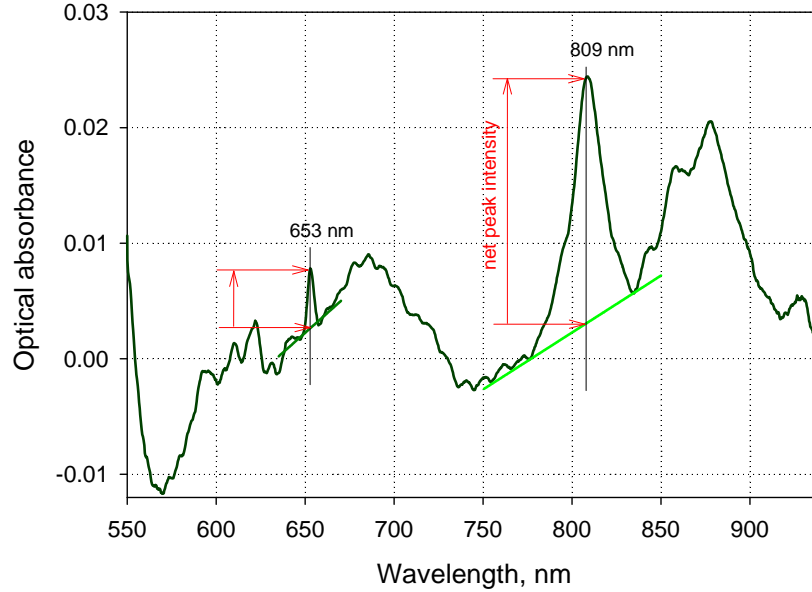


Figure 2.1. Net Peaks' Intensity Determination in Pu(V) Spectra

The following functional expression was used to simulate the waveform interference:

$$A(\lambda) = a + b \cdot \sin(c/\lambda + d) + e \cdot \sin(c/2\lambda + f) \quad (2.1)$$

where λ is the wavelength, and a , b , c , d , e , and f are variable parameters that allow the waveform bias (a), the amplitude (b and e), the frequency (c), the phase shift (d and f), and skewedness (b/e) of the background oscillations to be adjusted. This approach was used to suppress waveform distortions in the spectral analysis of Pu(V) interaction with Mn(VI) (Figure 2.2).

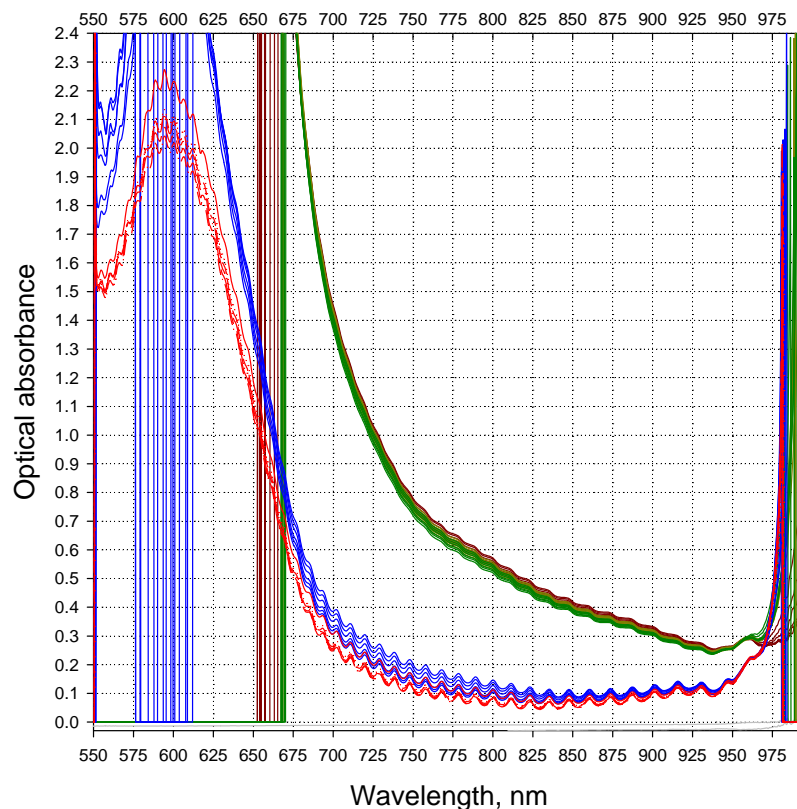


Figure 2.2. Manganate Reduction After Adding Pu(V). Initial Mn(VI) and Pu(V) concentrations are 15 μM and 12.5 μM , respectively. Green series: a number of repeated injections of 15 μM cold solution of Mn(VI) aimed at saturation of Mn(VI) reducing sites within the capillary cell and Mn(VI) signal stabilization. Blue and red series: first and second injection of the same Pu-containing solution 5 and 10 minutes after mixing Pu(V) and Mn(VI).

3.0 Results and Discussion

This section discusses the light-transmission efficiency of LWCC; the demonstration of the identity of spectral features of Nd(III) in H₂O and D₂O; the cold testing of LWCC; Pu(VI) and Pu(V) calibration and speciation experiments; spectral measurements, oxidative dissolution, and oxidation of Pu(IV); interaction of Pu(V) with low levels of manganate; and the oxidative leaching of sludge simulant with permanganate.

3.1 Light-Transmission Efficiency of LWCC

According to the manufacturer's specifications, the 5-m-long LWCC employed for this project had the usable spectral range from 350 to 700 nm due to the limited optical transparency range of H₂O. The main idea of this project was to use deuterated water instead H₂O to extend the operation range of LWCC all the way to 1100 nm. Therefore, the first testing of the LWCC was performed with D₂O without any other solutes present to make sure that the assumption about the possibility of the scanning range extension could be realized in practice. For this testing, a near-IR optimized spectrophotometer from Ocean Optics with a scanning range capability from 550 to 1200 nm (as claimed by the manufacturer) was used, which was coupled with LWCC and a light source using two optical fibers. The first experiment performed with 99.8% pure D₂O injected into the LWCC showed that the amount of light reaching the spectrophotometer after passing through a 500-cm layer of D₂O dropped down very sharply, starting from ~930 nm to practically immeasurable levels in the 975- to 1060-nm window (Figure 3.1). This "black window" effect cannot be attributed to optical absorbance of the solvent known to be highly transparent all the way to 1200 nm. A small admixture of H₂O in D₂O (0.2%) should have some minor attenuation effect in the 950- to 1070-nm spectral range, but its calculated magnitude can account only for $[1 - 1/(10^{0.2 \times 0.002 \times 500})] \times 100 = 37\%$ of light intensity loss at the major absorbance peak maximum of H₂O at 975 nm. Clearly, this minor attenuation due to the presence of H₂O cannot explain the drastic blackening-out effect in the 975- to 1060-nm window shown in Figure 3.1. Possibility of light attenuation by -OH moieties on the interior of the quartz fiber was also considered but this effect should be significant only in a relatively narrow spectral range from 925 to 975 nm (based on a high OH fiber attenuation curve presented in the Ocean Optics catalog).

In the second experiment, the spectrophotometer was coupled with a standard 1-cm plastic cell filled with the same solvent to see whether the observed effect originates from the spectral characteristics of the LWCC itself or is associated predominantly with the limited spectral range of the spectrophotometer. According to Figure 3.2, switching to the standard pathlength-measurement mode results in a significant extension of the usable spectral range to ~1100 nm, which demonstrates that the black-window effect cannot be explained by limitations in the scanning range of the Ocean Optics Instrument.

Finally, the spectrophotometer was tested in a direct coupling mode with a light source without using any optical fibers to exclude the possible effect of optical fiber material on the light-transmission efficiency. Results of this test shown in Figure 3.3 confirm that there are no limitations in the spectral characteristics of both the light source and the spectrophotometer, which might be responsible for the appearance of the light cut-off effect starting from 970 nm.

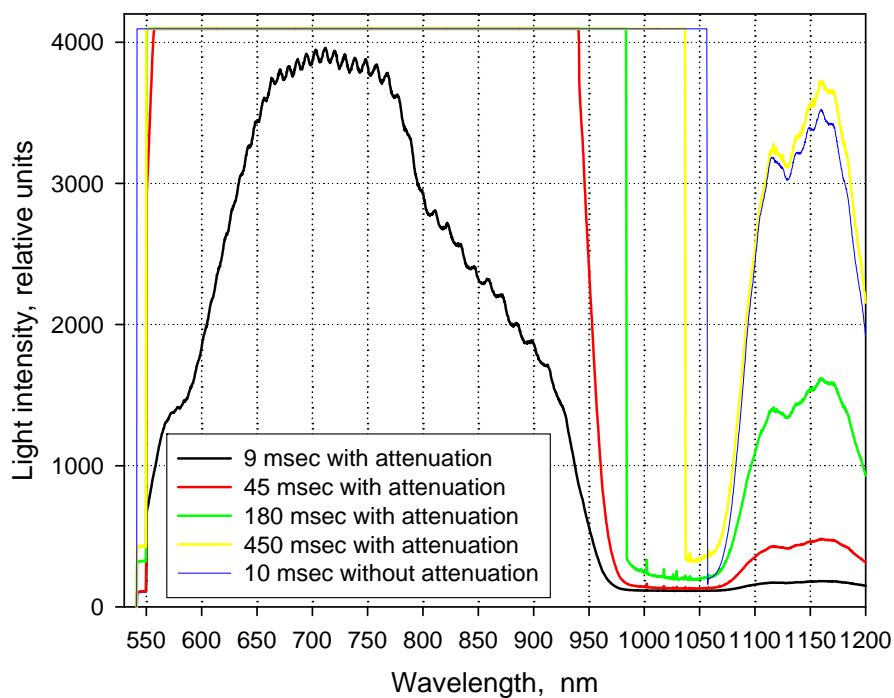


Figure 3.1. Light Intensity Spectra After Exiting a 5-m LWCC Filled with 99.8% D₂O. The legend shows different integration times used to acquire light-intensity spectra.

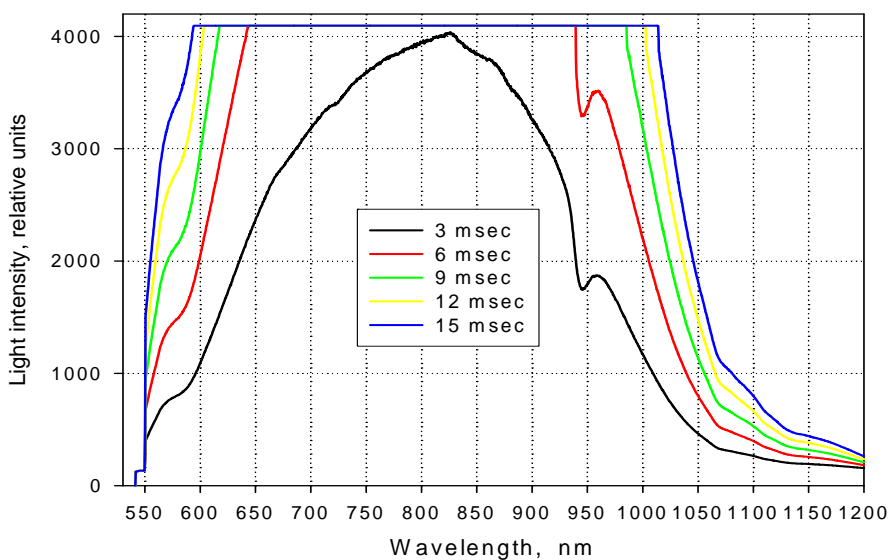


Figure 3.2. Light-Intensity Spectra After Passing Through a 1-cm Quartz Cell Filled with 99.8% D₂O. The legend shows different integration times used to acquire light-intensity spectra.

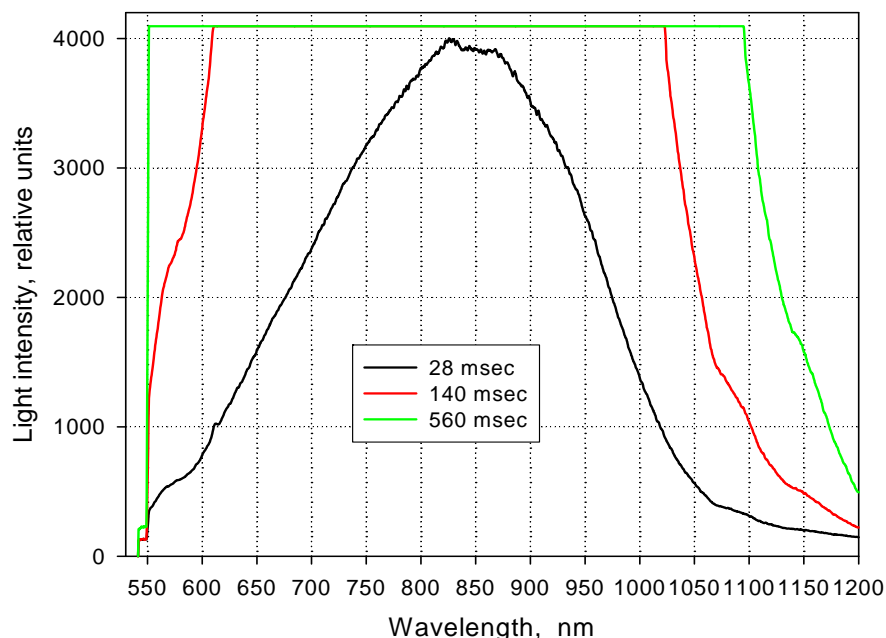


Figure 3.3. Light-Intensity Spectra with Direct Light Coupling to the Spectrophotometer (without any spectrophotometric cells or optical fibers). The legend shows different integration times used to acquire light-intensity spectra.

All the data shown in this section were sent to technical experts at World Precision Instruments (WPI) where the LWCC was manufactured with a request to express their opinion on what might be the reason of the blackening-out effect in the 970- to 1070-nm region of the spectrum when using LWCC measurements in the D₂O medium. Some comments from their representative are reproduced below as they were received in the summer of 2006:

This black-window effect you are speaking of is most likely the intrinsic water absorption. What light source are you using? The silica tubing glass is clear, and light percent throughput is 95%, so 5% is lost via the glass.

Note: Type 1 material is no longer available. However, this will not make a difference theoretically as intrinsic absorbance of the water effect is the same no matter what the material of the waveguide is.

We do not have any experience with using LWCC in the range, so a modification will more than likely be out of the question in this case.

In conclusion, if the WPI comments on the attribution of this effect to the intrinsic absorption of water are correct, then the application of higher-purity D₂O should extend the usable range of LWCC deeper into the IR region of the spectrum, but this possibility was not explored in the course of this project.

3.2 Demonstration of Identity of Spectral Features of Nd(III) in H₂O and D₂O

A number of questions were raised by the test-plan reviewers at the project planning stage as to what extent the spectral features of plutonium measured in D₂O solvent could be applicable to Pu solutions in H₂O in terms of the equivalency of the absorbance peaks' positions and the molar absorptivities in the both solvents. The first attempt to answer this question was a cold experiment based on comparing the spectral features of Nd(III) in D₂O and H₂O. A trivalent neodymium cation with three electrons on the 4f electronic energy level (i.e., 4f³ valence electronic configuration) can be considered as an iso-electronic analog of Pu(V), which possesses a 5f³ electronic configuration. This experiment was performed with ~350-fold diluted Nd(III) stock solution both in D₂O and H₂O solvents at a low concentration of nitric acid using LWCC detection. The results are presented in Figure 3.4. One can see that while the deuterated medium allows all five absorbance bands of Nd(III) in the 550- to 900-nm range to be detected, spectral measurement in the H₂O solvent results in the disappearance of the last three bands at 740, 794, and 865 nm from the spectrum due to an insufficient amount of light reaching the detector starting from 700 nm. Therefore, only two bands of Nd(III) are available to evaluate the solvent effect. As Figure 3.4 shows, the spectral shapes and intensities of both 575 nm and 683 nm are practically undistinguishable from each other, regardless of the solvent's nature. Hot experiments conducted with Pu(IV, V, and VI) solutions (see subsequent sections) further served as an additional proof of this spectral equivalence.

The molar absorptivity of the Nd(III) peak at 576 nm, which was estimated from the peak intensity, indicated that the Nd concentration and the optical pathlength of 500 cm was 6.1 M⁻¹cm⁻¹, which corresponds to 85% of the 7.2-M⁻¹cm⁻¹ value reported in the literature (Carnall 1979). Two possible reasons for this discrepancy should be mentioned: 1) insufficient spectral resolution of the spectrophotometer due to an entrance aperture that was too wide (50-μm slit); 2) collection of a small portion of light that did not travel through the liquid medium, but through the quartz walls of the capillary cell, which could result in lowering effective optical absorbances measured by the spectrophotometric detector.

It should be mentioned here that the absorbance peak at ~1152 nm observed in the both spectra was initially believed to represent a real absorbance band of Nd(III). However, it turned out that it is not listed among other peaks of Nd in the band register for lanthanide (aquo) ions in H₂O-D₂O (Carnall 1979), or in other words, Nd(III) does not have any absorbance bands centered at this wavelength. After discussing this finding with technical experts from Ocean Optics, the following comments were received:

One of the problems with the USB2000 spectrometer detectors is that they are not very efficient in the range that you are looking at. What this means is that you would need a very good signal to be able to see anything there and it seems that you have a very weak one. Another thing that looks strange is that you are able to detect a signal after 1100 nm, those peaks look like secondary peaks or harmonics which could mean that we made a mistake and did not install the OFL-OF550. It would be good if you can send us the spectrometer so we can verify that the filter is there or if it got loose for some reason.

Based on the above comment and taking into account that the 1152-nm peak position corresponds to a double value (harmonic) of the 576-nm peak position of Nd(III), and their intensities match, it has to be

concluded that the 1152 peak is just an overtone of the 576-nm peak. Any spectral features detected beyond 1100 nm with this instrument represent artifacts.

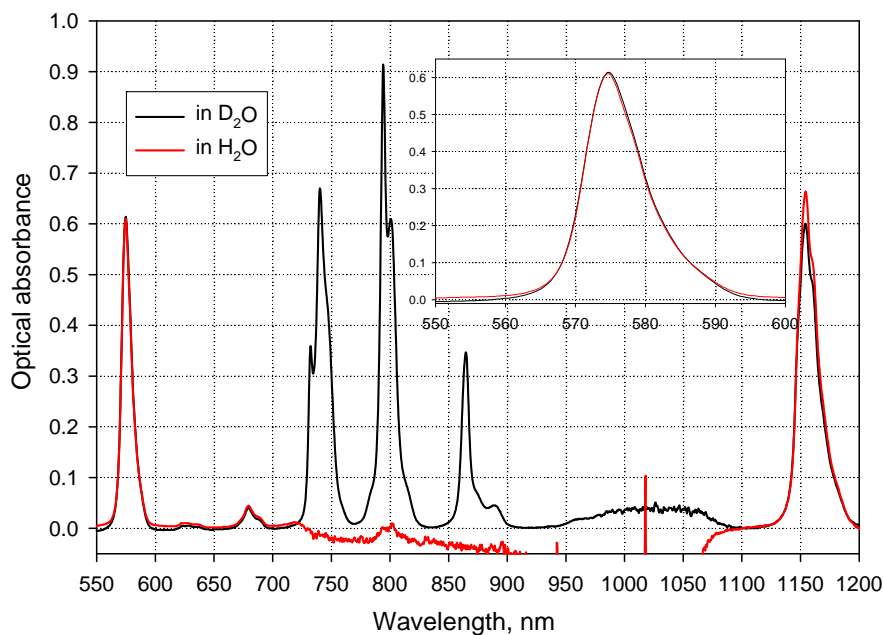


Figure 3.4. Spectra of 0.2 mM $\text{Nd}(\text{NO}_3)_3$ Solution in D_2O and H_2O in 0.015% HNO_3 and DNO_3 , Respectively, Using LWCC Detection

3.3 Cold Testing of LWCC Using Nd(III) Complex with EDTA in 0.1 M NaOH and 0.1 M NaOD

For a more systematic evaluation of the capabilities of enhanced detection of weak absorbance bands of f-elements in alkaline aqueous solution, several series of calibration experiments were performed using an alkaline solution of Nd in the presence of EDTA. EDTA was used as a holding complexing agent to prevent Nd(III) precipitation as $\text{Nd}(\text{OH})_3$ from solution in the presence of hydroxide. These experiments were performed both in chromate-free solutions and in the presence of 50 mM of chromate. As a preliminary experiment, absorbance spectra of chromate in D_2O (with no Nd and EDTA present) were taken to see to what extent the tailing effect of the major absorbance band of chromate (with a peak maximum at 372 nm) propagates into the visible range of the spectrum, starting from 550 nm, and possibly interferes with absorbance bands of interest. The results of this measurement are shown in Figure 3.5. As follows from these data, the presence of chromate up to 40 mM in concentration exhibits only a minor effect of optical absorbance in the 550- to 570-nm range of the spectrum. This leaves practically the entire range of the optical transparency of D_2O (up to 960 nm with present instrumentation) suitable for enhanced detection of characteristic absorbance bands of Nd and Pu.

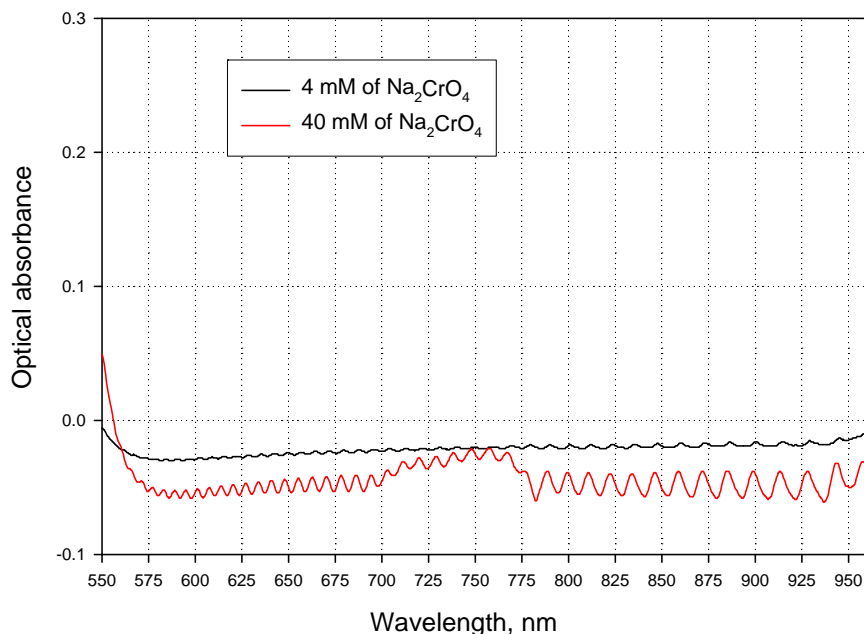


Figure 3.5. Spectra of Na_2CrO_4 Solution in D_2O at 4 mM and 40 mM of Cr(VI). Pure solvent was used for baseline acquisition.

Nd-EDTA calibration experiments were conducted both in H_2O and D_2O medium in the presence of 0.1 M of NaOH and 0.1 M of NaOD, respectively. The spectral data from these experiments are shown in Figure 3.6. Similar to the Nd spectral detection in a weakly acidic medium, the usable window of optical transparency in $\text{H}_2\text{O}/\text{NaOD}$ solvent was found to be limited to 550 to 700 nm, whereas spectral measurements in $\text{D}_2\text{O}/\text{NaOD}$ allow spectral information to be collected in a much broader range up to 960 nm. Calibration curves show good linearity both in H_2O and D_2O solvents, and their slopes show little or no difference within each series with or without chromate present in solution for the first three peaks of Nd at 581, 628, and 683 nm. Detection limits for Nd-EDTA peaks with molar absorptivities of $6 \text{ M}^{-1}\text{cm}^{-1}$ and higher (including three additional major bands of Nd in the 720- to 880-nm range in D_2O medium) were found to be in the submicromolar range of Nd concentrations. Two peaks of Nd at 576 nm ($\epsilon = 9.1 \text{ M}^{-1}\text{cm}^{-1}$) and 801 nm ($\epsilon = 10.2 \text{ M}^{-1}\text{cm}^{-1}$) showed exceptionally low detection limits, in the 0.04 to 0.08- μM range, mostly due to very low background signal fluctuations in the blank spectra in these spectral regions. Table 3.1 summarizes results of all four calibration series shown in Figure 3.6.

Overall, cold testing of LWCC using Nd-EDTA complexes in an alkaline media showed promising results and demonstrated the possibility of much more sensitive detection of relatively weak but well defined absorbance bands of f-elements in the visible and near-IR range of the spectrum. Most importantly, the presence of up to 50 mM chromate in these solutions (if properly compensated via blank signal acquisition) did not produce any adverse effects on the sensitivity of LWCC detection or spectral signal perturbations in a wide range of the spectrum starting from $\sim 560 \text{ nm}$.

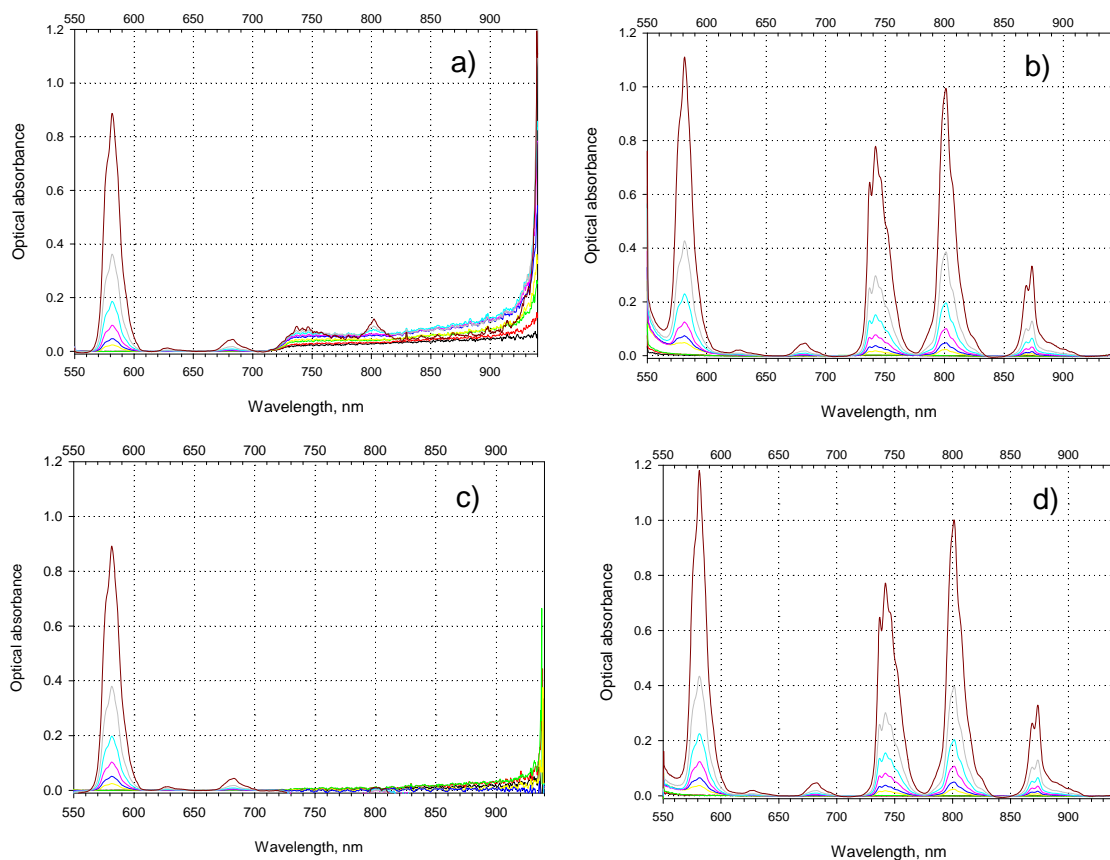


Figure 3.6. Calibration of LWCC Using Nd(III) Solution in the Presence of 0.25 M of Na_4EDTA in 0.1 M of Sodium Hydroxide:

- a) $\text{NaOH}/\text{H}_2\text{O}$ no chromate
- b) $\text{NaOD}/\text{D}_2\text{O}$ no chromate
- c) $\text{NaOH}/\text{H}_2\text{O}$ + 50 mM of Na_2CrO_4
- d) $\text{NaOD}/\text{D}_2\text{O}$ + 50 mM of Na_2CrO_4

Table 3.1. Summary of Calibration Experiments with 5-m LWCC Using Nd-EDTA Complex in NaOH and NaOD

Solvent	Peak Position, nm	Peak Detectability	Calibration Curve Slope, M ⁻¹		Molar Absorptivity, M ⁻¹ cm ⁻¹		Detection Limit, μ M	
			No Cr(VI)	50 mM of Cr(VI)	No Cr(VI)	50 mM of Cr(VI)	No Cr(VI)	50 mM of Cr(VI)
H ₂ O + 0.1 M NaOH	581.4	Yes	4512	4543	9.02	9.09	0.078	0.038
	627.75	Yes	64	66	0.13	0.13	2.11	4.61
	682.83	Yes	222	222	0.44	0.44	2.39	1.77
	737.21	No	-	-	-	-	-	-
	742.01	No	-	-	-	-	-	-
	801.25	No	-	-	-	-	-	-
	868.98	No	-	-	-	-	-	-
	873.53	No	-	-	-	-	-	-
D ₂ O + 0.1 M NaOD	581.4	Yes	5583	5950	11.2	11.9	0.94	0.29
	627.75	Yes	104	96	0.21	0.20	7.3	8.2
	682.83	Yes	237	239	0.47	0.48	5.4	4.2
	737.21	Yes	3272	3290	6.5	6.6	0.8	0.8
	742.01	Yes	3949	3920	7.9	7.8	0.64	0.57
	801.25	Yes	5056	5095	10.1	10.2	0.08	0.05
	868.98	Yes	1331	1340	2.7	2.7	1.1	1.1
	873.53	Yes	1700	1670	3.4	3.3	1.7	1.1

3.4 Pu(VI) Calibration and Speciation Experiments in DNO₃ and NaOD

3.4.1 Pu(VI) Calibration Experiment in DNO₃

Pu(VI) in an acidic medium is known to have the most intense and sharp absorbance band of any of the other actinide metal cations. The peak maximum is at 830.5 nm in acidic aqueous solutions and (as shown in this work with stock solution of Pu(VI), Figure 3.7) has the same λ_{max} in D₂O/DNO₃. The peak position beyond the 700-nm border of the transparency of H₂O makes it undetectable in the 500-cm LWCC in H₂O. Therefore, it was of interest to demonstrate the detectability of this peak in deuterated aqueous solvent and to determine its molar absorptivity, linearity of the calibration curve, and detection limit.

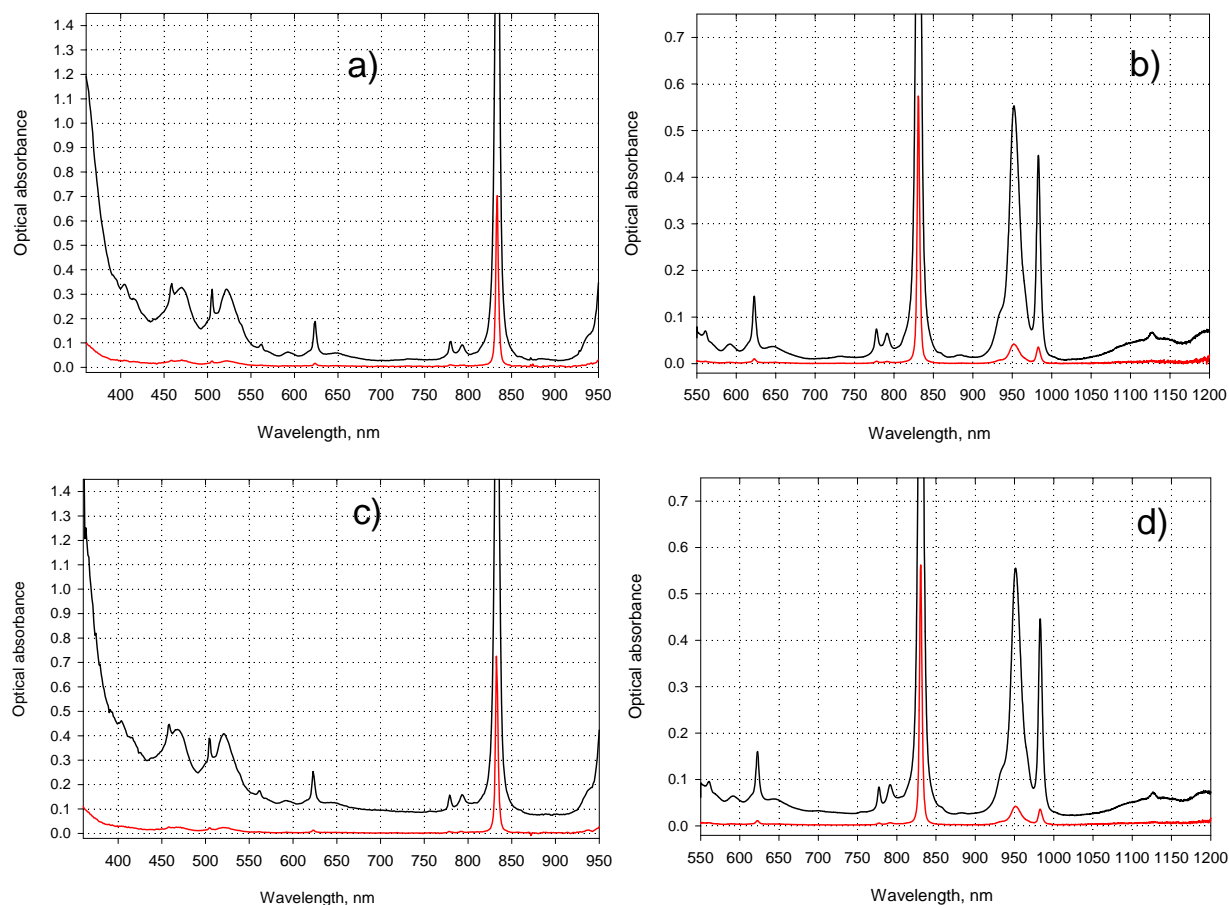


Figure 3.7. Pu(VI) Acidic Stock Solution Spectra in 0.5 M of HNO_3 [a) and b)] and 0.5 M of DNO_3 [c) and d)]. Black trace: 26.4 mM of Pu(VI); red trace: 0.306 mM of Pu(VI). Spectral sets a) and c) are recorded with SI-400 spectrophotometer (360- to 950-nm scanning range); spectral sets b) and d) are recorded with an Ocean Optics spectrophotometer (550- to 1100-nm scanning range). A 1-cm plastic cell was used in all spectral measurements.

Figure 3.8 shows results of this calibration experiment performed in $\text{D}_2\text{O}/\text{DNO}_3$ solution. The linear regression data are summarized in the upper section of Table 3.2. The detection limit achieved in this experiment is 5.6 nM of Pu(VI). The peak position of Pu(VI) and its molar absorptivity are in excellent correspondence with previously published data on Pu(VI) detection by visible spectroscopy using 100-cm LWCC in H_2O medium (Wilson et al. 2005). It is noteworthy that, because of selecting a D_2O medium for spectroscopic measurements, a 125-fold improvement in the detection limit of Pu(VI) was achieved by increasing the optical pathlength by just five times. The invariability of the Pu(VI) peak position and its intensity by the nature of the aqueous solvent serves as another proof that D_2O does not perturb spectral features of 5f metal cations in solution compared with conventional H_2O solvent.

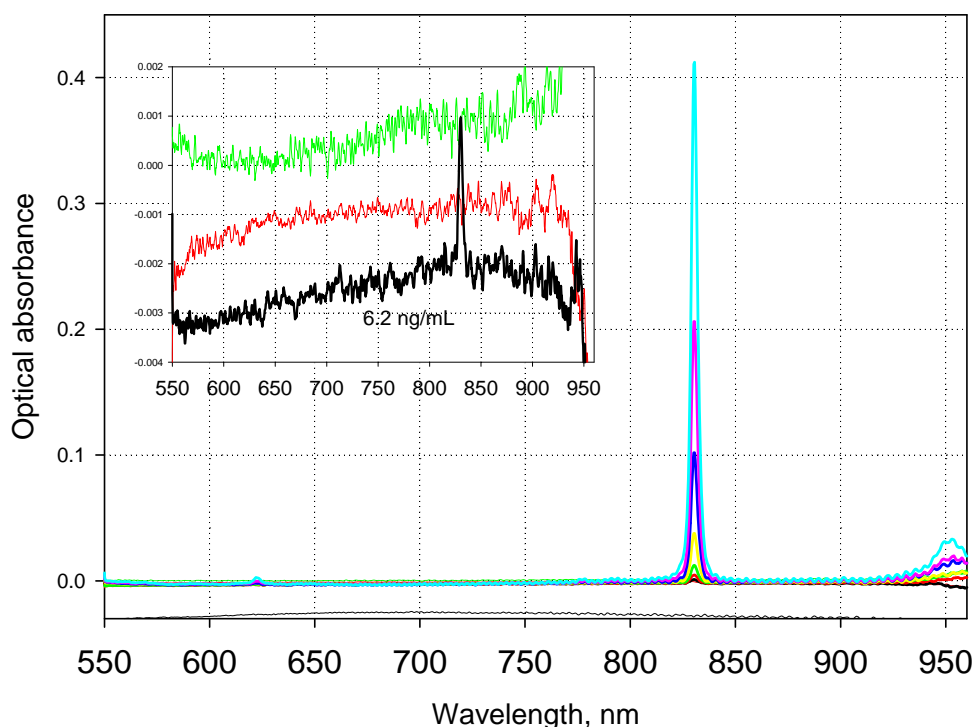


Figure 3.8. Calibration Experiment with Pu(VI) in 0.1 M of DNO₃ Using 500 cm LWCC. The Pu(VI) Concentration Range Is from 0.021 μ M (6.2 ng/L, black trace) to 2.12 μ M (pale blue trace). Red and green traces in the inset show typical baseline spectra obtained with a blank solution of 0.1 M of DNO₃.

Table 3.2. Summary of Calibration Experiments with Pu(VI) in 0.1 M of DNO₃, 0.1 M and 1 M of NaOD

Medium	Solution Age, hr	Concentration Range, μ M	Calibration Curve Linearity, R^2	Slope, M^{-1}	Extent of Reduction to Pu(V)	Detection Limit, μ M
0.1 M of DNO ₃	1.5 ± 0.5	0.021 – 2.12	0.9999	190060 ± 660	Pu(V) is not detected	0.0056
0.1 M of NaOD	1.5 ± 0.5	0.53 – 15.6	0.995	5530 ± 130	< 2%	0.47
	72 ± 3	0.53 – 15.6	0.980	4670 ± 270	< 2%	0.71
1.0 M of NaOD	1.5 ± 0.5	0.53 – 15.6	0.995	5740 ± 170	8%	0.55
	72 ± 3	0.53 – 15.6	0.949	4650 ± 440	12%	1.03

3.4.2 Pu(VI) Calibration Experiments in NaOD

Literature data on the spectral features of Pu(VI) in alkaline medium are contradictory. One of the first spectral measurements of Pu(VI) in alkaline medium was performed and published by Spitsyn and co-authors (Spitsyn et al. 1969). Their spectrum of Pu(VI) in 1 M KOH shows a very prominent band at

870 nm ($\epsilon = 300 \text{ M}^{-1}\text{cm}^{-1}$) and a broader and much less intense peak at $\sim 640 \text{ nm}$ ($\epsilon = 70 \text{ M}^{-1}\text{cm}^{-1}$). Both peaks can be considered as red-shifted transforms of the peaks of cationic PuO_2^{2+} at 830 nm and 616 nm, respectively, as result of Pu(VI) hydrolysis and the formation of anionic hydroxocomplexes. The similar but less symmetrical and $\sim 40\%$ less intense peak of Pu(IV) was reported by Ray and colleagues in 0.05 M NaOH (Ray et al. 1988). On the other hand, a much more recent publication from the former Spitsyn's institution (Budantseva et al. 1997) indicated that in 2M NaOH and higher, the 870-nm band of Pu(VI) is barely detectable and has a molar absorptivity of $\sim 10 \text{ M}^{-1}\text{cm}^{-1}$ while the 630-nm band is about 60% more intense, but still a factor of 4.2 lower than Spitsyn's value for the same peak. In a study by Bourges (1972), electrochemically generated Pu(VI) in 1 M NaOH did not exhibit the 870-nm spectral feature at all. Therefore, it was of interest to take advantage of the higher sensitivity offered by LWCC detection and the wide spectral window in D_2O solvent for re-examination of the spectral characteristics of Pu(VI) in NaOD. If the very intense and clearly defined 870-nm absorbance band of Pu(VI) reported by Spitsyn could be confirmed in this study, that feature would be very beneficial for a much more sensitive detection of alkaline Pu(VI) in the low-nanomolar concentration range.

A series of Pu(VI) solutions in 0.1 M of NaOD was prepared in duplicate by spiking tiny amounts of acidic Pu(VI) solution in 0.025 M of HNO_3 into an excess of 0.1 M of NaOD. The perturbation of the initial NaOD concentration with this preparation was less than 0.75% for the highest amount of acidic stock of Pu(VI) added. The solutions were quickly homogenized by shaking, and the first series was spectrally measured 1 to 1.5 hr after preparation. The results of this experiment are shown in Figure 3.9 (plot **a**). The net intensity of the major peak of Pu(VI) at 625 nm was calculated using the spectral treatment described in Section 2.9, and the respective calibration plot is shown as plot **b**) in the same Figure. A good proportionality between Pu(VI) concentration and the peak intensity is observed for all concentration points with a slightly lower slope of the calibration curve for the first three points (0.65 to 3.25 μM). The same tendency of the calibration slope decrease at a lower metal concentration was observed previously with acidic Pu(VI), and in both cases this effect may be attributed to the presence of low concentrations of unidentified reductant in the prepared solutions. This reductant might be introduced with solvent (D_2O), NaOD, or DNO_3 , or it may come into solution from plastic containers used to store the samples.

Duplicate portions of the same solutions were stored without additional agitation over 3 days before spectral measurement. The results are shown in Figure 3.9 (**c** and **d**). Comparing spectral sets **a**) and **c**) shows that Pu(VI) is stable in a 0.1 M NaOD medium for at least 3 days with spectral features observed in the freshly prepared series clearly identifiable in the aged series at higher Pu concentrations. However, in the lower range of Pu(VI) concentrations, no positive signal of Pu(VI) could be discriminated against the 570- to 660-nm baseline. This observation may indicate that a slight deficiency in the Pu(VI) signal in the low concentration region of the freshly prepared series becomes more pronounced with time because of the partial reduction of Pu(VI) to one of the lower oxidation states. As regards the 870-nm peak reported as the major spectral feature in 1 M of KOH (Spitsyn et al. 1969) and in 0.05 M of NaOH (Ray et al. 1988), our data do not confirm those findings (see Section 3.4.3 for correct attribution of the 870 nm peak of Pu(VI)).

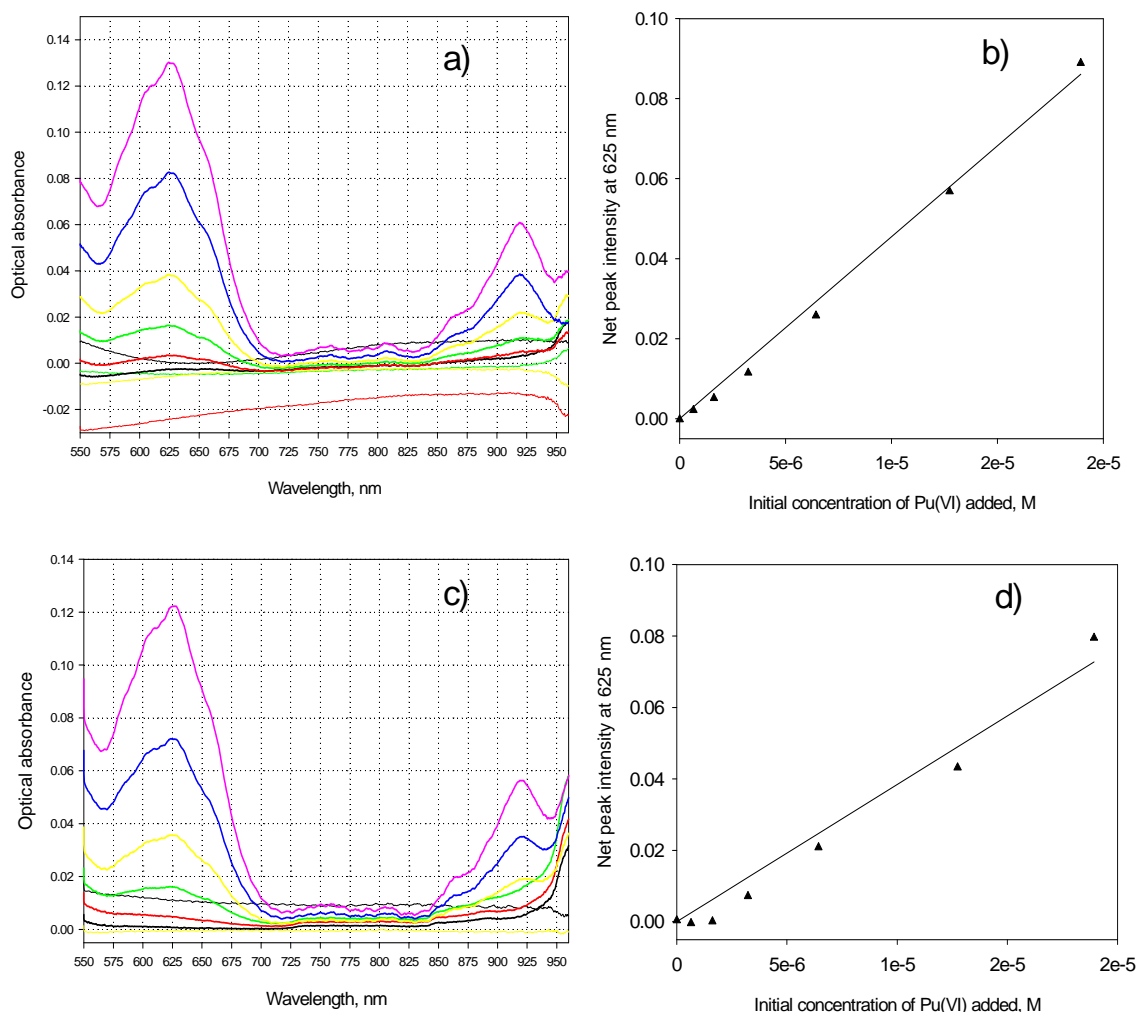


Figure 3.9. Calibration Experiments with Pu(VI) in 0.1 M of NaOD. Freshly prepared series a) and b), and 3 days between solution preparation and measurement c) and d). Initial concentrations of Pu(VI) are 0.53, 1.33, 2.66, 5.30, 10.5, and 15.6 μM for black, red, green yellow, blue, and pink spectral traces, respectively.

The same experimental approach was used to prepare and study Pu(VI) speciation in 1 M NaOD. The results obtained with freshly prepared series are shown in Figure 3.10 [plots a) and b)]. There are very minor (if any) changes in the major absorbance peak shape and intensity compared with the 0.1 M NaOD data. More noticeable changes were observed in the 800- to 950-nm spectral range. First, a very weak spectral feature initially observed at 808 to 812 nm is now more pronounced and manifests itself as a narrow and nearly symmetrical peak centered at 809 nm. What is more interesting, kinetic monitoring of the intensity of this band at 15.6 μM of initially added Pu(VI) indicates that the 809-nm peak intensity slowly increases with time, while the 625-nm peak of Pu(VI) simultaneously decreases (black, red, green, yellow, and blue traces in Figure 3.11). The 809-nm peak position and spectral shape are in excellent correspondence with the Pu(V) spectrum reported previously in the literature for higher hydroxide concentrations (Delegard 1987). Therefore, the observed spectral changes are consistent with the partial conversion of Pu(VI) to Pu(V) by an unidentified reductant. Overall, the extent of Pu(VI) conversion to

Pu(V) is approximately 6 to 8% over the first 60 minutes of the kinetic sequence. It was not possible to continue kinetic measurements with this solution over a longer period of time because of the aggressive nature of the 1 M NaOD medium on contact with the inner wall of the liquid waveguide capillary made from quartz. Measuring the same concentration point in a 3-day-old series in 1 M of NaOD (bold dark yellow trace in the same Figure) indicates that the Pu(V) signal grew ~ 1.5 times with the decrease in intensity of the Pu(VI) peak to approximately same extent. No new spectral features appeared in the aged sample. These data indicate that most likely, it is the stock solution of NaOD that supplies reductant to reduce Pu(VI) to Pu(V).

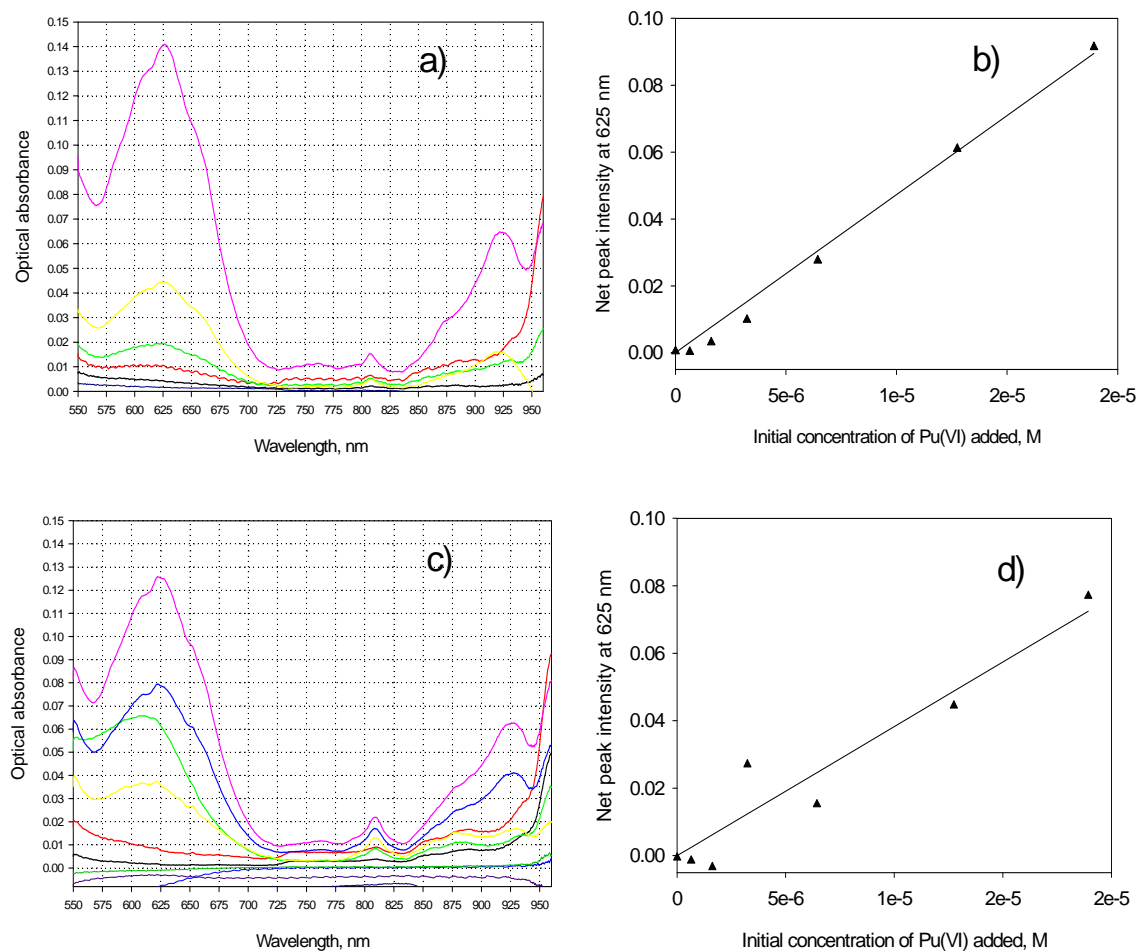


Figure 3.10. Calibration Experiments with Pu(VI) in 1 M NaOD. Freshly prepared series a) and b), and 3 days between solution preparation and measurement c) and d). Initial concentrations of Pu(VI) are 0.53, 1.33, 2.66, 5.30, 10.5, and 15.6 μM for black, red, green yellow, blue, and pink spectral traces, respectively.

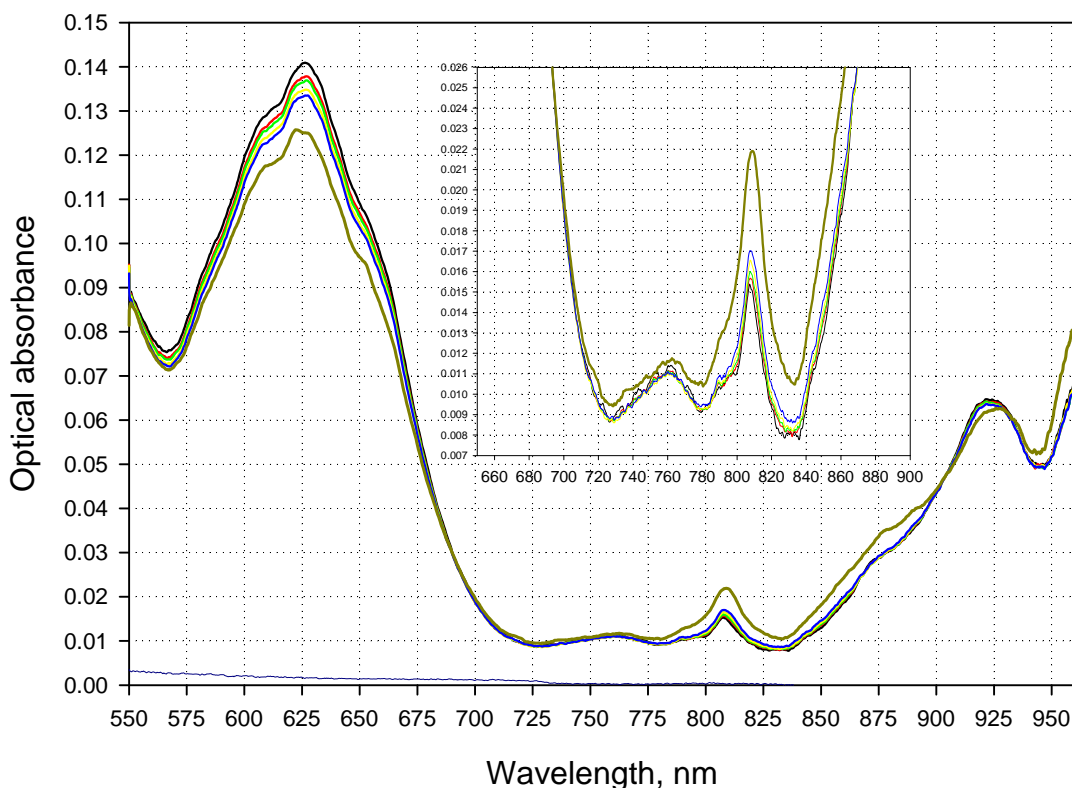


Figure 3.11. Spectral Evidence of Partial Reduction of Pu(VI) to Pu(V) in 1 M NaOD with Time. $C_{\text{Pu(VI)}}^0 = 15.6 \mu\text{M}$. Black trace: 2 minutes after injection. Red, green, yellow, and blue traces: 10, 20, 30, and 50 minutes after the first scan. Dark yellow bold trace: duplicate solution of identical composition measured 3 days after preparation.

As regards the linearity and slopes of the calibration curves, the freshly prepared 1 M NaOD series shows more pronounced negative deviations for the 625-peak intensity at lower Pu concentrations compared with the 0.1 M NaOD data. This effect is most noticeable for the first three concentration points. Aging 1 M NaOD solutions for 3 days [Figure 3.10, plots **c**) and **d**)] makes this deviation even more pronounced with all six points going down in intensity and with the first two concentration points showing no positive signal of Pu(VI) at all.

The second largest peak of Pu(VI) centered at 920 nm in 0.1 M NaOD undergoes a 4- to 5-nm red shift in its position and broadens in 1 M NaOD solution.

Overall, the data scattering and additional partial reduction of Pu(VI) to Pu(V) in 1 M NaOD aged series results in elevated fluctuations in the spectra of blank solutions and a reduced slope of the calibration curve, which leads to a 1.5 times higher detection limit of Pu(VI) under these conditions.

No attempts were made to repeat these four series of calibration experiments with Pu(VI) in the presence of Cr(VI). It is expected that Cr(VI) cannot perturb the oxidation state of Pu(VI) by oxidizing it to Pu(VII), nor can it compete with hydroxide for the Pu(VI) metal center to form mixed hydroxy-chromate complexes of Pu(VI). By analogy with a lack of chromate interference in detecting Nd(III)-EDTA

species in the 570- to 685-nm spectral range, it can be predicted that Cr(VI) should not have any adverse effect on the quality of spectral detection in the 625-nm peak of Pu(VI).

A Pu(VI) calibration experiment in the 0.25 M NaOD medium was not performed, but one spectrum was taken at 13 μ M of Pu(VI). The spectrum served as a starting point in studying Pu(VI) speciation in mixed 0.25 M NaOD-Na₂CO₃ media (Section 3.4.3, Figure 3.12, plot **b**), and it does not show any unusual spectral features compared to those already observed and discussed in this section for 1 M NaOD.

Again, no evidence of the intense spectral feature of Pu(VI) at 870 nm was observed in 1 M NaOD. Therefore, the prior published Pu(VI) spectrum (Spitsyn et al. 1969) was not confirmed in this study. The 625-nm peak appears to be the major spectral feature of Pu(VI) in a purely hydroxide medium in the concentration range from 0.1 M to 1 M NaOD. Unfortunately, the peak is too broad to be discriminated reliably from other light absorbing species with absorbance maxima in this region of the spectrum. On the positive side, the peak location below 700 nm should make it detectable in a H₂O/NaOH medium, provided no other spectral interferences are present in the same solution.

3.4.3 Pu(VI) Spectra in the Presence of Carbonate at Constant Concentration of Hydroxide

The formation of mixed hydroxy-carbonate complexes of Np(VI) and Pu(VI) of unidentified composition was reported by Varlashkin and co-workers (Varlashkin et al. 1984a; Varlashkin et al. 1984b) who used optical absorbance spectroscopy to observe significant spectral changes in the spectrum of a triscarbonate complex of Pu(VI) in 2 M of Na₂CO₃ after adding NaOH up to 1.44 to 2.0 OH⁻/CO₃²⁻ molar ratio. The spectra were measured at a high concentration of Pu(VI) (16 mM). A relatively low solubility of PuO₂(OH)₂ in moderately alkaline solutions (\leq 1 M NaOH) did not allow the authors to study this process from a purely alkaline (carbonate-free) side. The most pronounced spectral changes were found in the 850- to 890-nm range of the spectrum where a sharp and intense absorbance band developed and reached its maximum intensity at 0.6:2 molar ratio of OH⁻ to CO₃²⁻. The exact peak position and molar intensity was not reported explicitly in the paper, and it is difficult to deduce these parameters from the published spectra with an arbitrarily drawn vertical scale and a very compressed horizontal scale. Qualitatively, the mixed ligand spectrum resembles the 870-nm peak of Pu(VI) in 1 M KOH reported by Spitsyn and colleagues (1969).

The study of fundamental complexation chemistry of mixed hydroxy-carbonate complexes of Pu(VI) was beyond the scope of this project, but it was of practical interest to find conditions in an NaOH-Na₂CO₃ solution under which the spectral signature of Pu(VI) could be maximized to allow more sensitive and selective detection of Pu(VI) in alkaline solutions relevant to the oxidative-leaching process. Moreover, even if carbonate is not to be added for leaching of alkaline solutions, it is always present as a minor contaminant in stock solutions of NaOH. More carbonate enters the leaching solutions and leachates with time as a result of their exposure to air.

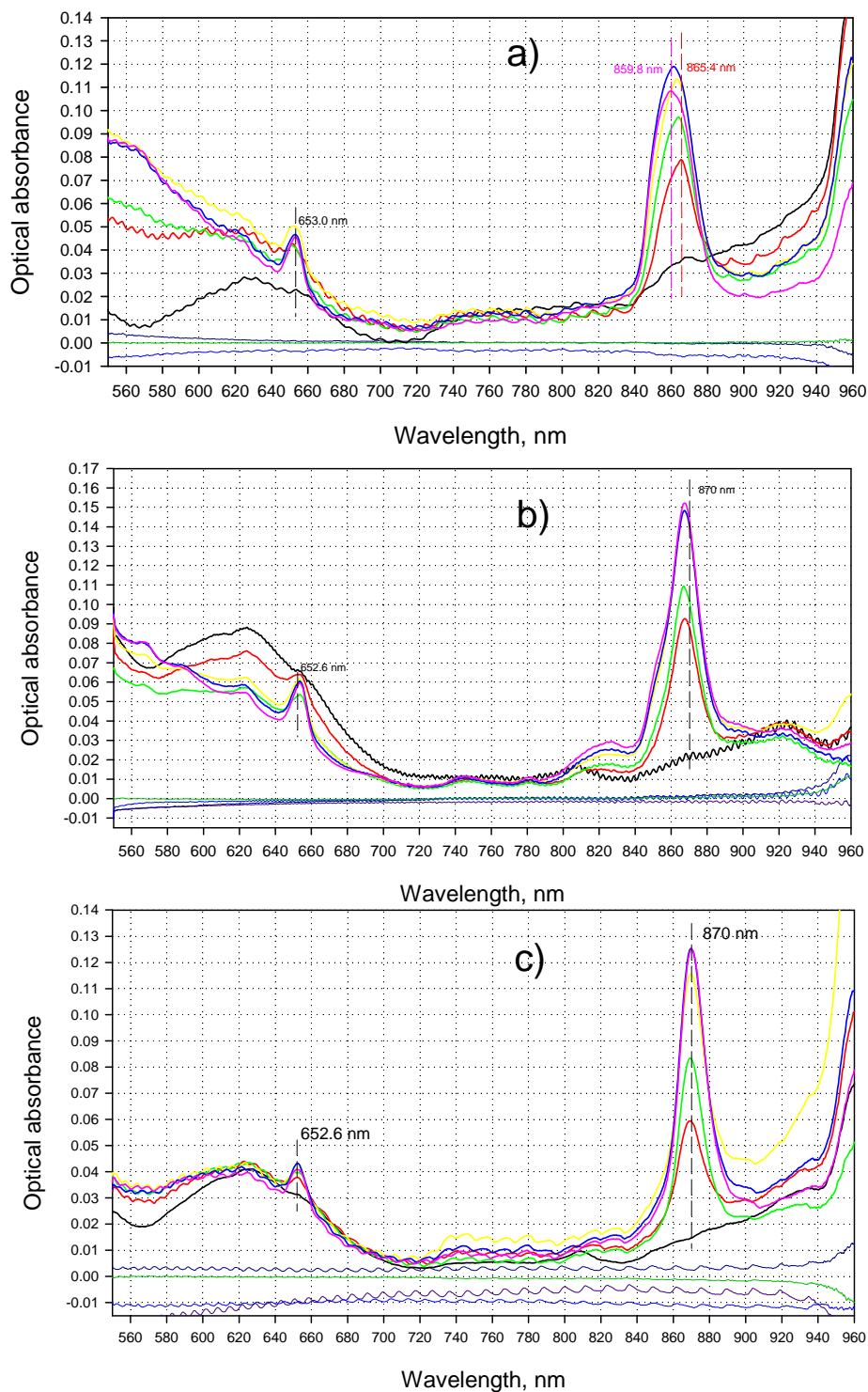


Figure 3.12. Pu(VI) Spectra in 0.1 M NaOD a), 0.25 M NaOD b), and 1 M NaOD c) in the Presence of Carbonate. In all cases, the carbonate concentration varies from 0% to 100% with 20% increments relative to the respective molar concentration of hydroxide for black, red, yellow, green, blue, and pink spectral traces, respectively. The Pu(VI) concentration is fixed at 8 μM for sets a) and c) and at 13 μM for set b).

In this study, the effect of carbonate on the spectral features of alkaline Pu(VI) was studied at three constant levels of NaOD. The carbonate concentration was varied in five increments up to the equimolar ratio for the given hydroxide level. The results are presented in Figure 3.12.

The 0.1 M NaOD data [plot a)] show significant spectral changes after adding the first portion of carbonate up to 0.02 M. The most prominent new spectral feature emerges at 865 nm, and at a higher concentration of carbonate, its intensity grows. The peak position gradually shifts to higher energy, and at 0.08 M of carbonate, the peak maximum is at 860 nm. Its molar absorptivity is approximately $30 \text{ M}^{-1} \text{ cm}^{-1}$. There is a slight decrease in the peak intensity with a further 20% increase in carbonate concentration. Another evidence of the formation of mixed complexes in this system is a weaker but sharper absorbance band at 653 nm. Its position remains the same regardless of the CO_3^{2-} to OD^- ratio.

The 0.25 M NaOD spectral data [plot b)] show less complex behavior of the major peak in the region of 840 to 890 nm. This peak position is more red shifted (868 nm) compared with the 0.1 M NaOD data set, and the peak maximum value does not change as a function of carbonate concentration. It appears that the peak intensity reaches a maximum at 0.20 M of carbonate and does not change further with an additional increase in carbonate concentration to 0.25 M. The molar absorptivity of this peak is $23.5 \text{ M}^{-1} \text{ cm}^{-1}$. The peak is not quite symmetrical as it contains a weak shoulder at $\sim 855 \text{ nm}$. The secondary peak maximum remains at 653 nm (no change vs. a 0.1 M NaOD spectral set).

The 1.0 M NaOD spectral set [plot c)] shows an additional red shift in the major absorbance band of the mixed complex by 2 nm compared with the 0.25 M NaOD data. The peak intensity grows more slowly for the same $\text{CO}_3^{2-}/\text{OD}^-$ ratio as it was observed at 4 times lower alkalinity and reaches a maximum value in the 0.8- to 1.0-M concentration range of carbonate. Its molar absorptivity is $31.3 \text{ M}^{-1} \text{ cm}^{-1}$. The secondary peak position remains unchanged at 653 nm, although its intensity is two times less compared with the lower alkalinity experiments.

In summary, all newly observed spectral features indicate that the formation of mixed hydroxyl-carbonate complexes is a complicated process that depends not only on the carbonate to hydroxide ratio but is governed by absolute levels of their concentrations. Evidence of at least three complex species is obtained from spectral data.

For practical applications, the major peak intensity of the mixed complex with a molar absorptivity of $\sim 30 \text{ M}^{-1} \text{ cm}^{-1}$ may offer a 2.5 times better sensitivity for Pu(VI) detection in mixed hydroxy-carbonate media. Unfortunately, the peak position in the 860- to 870-nm range would require conversion of the analyzed solution to a deuterated medium to allow its detection by LWCC.

3.5 Pu(V) Calibration and Speciation Experiments in NaOD

3.5.1 Preparation and Characterization of Pu(V) Solution in 14 M of NaOD

Alkaline solutions of Pu(V) were first produced via electrochemical reduction of Pu(VI) in 4 M of NaOH and spectrally characterized by Bourges (1972). Later, it was shown by Delegard (1987) that the same oxidation state of Pu in solution can be prepared by a prolonged exposure of the suspension of freshly formed $\text{Pu}(\text{OH})_4$ to an aerated solution of 15 M of NaOH. The highest concentration of Pu(V) that can be

prepared in this way was found to be 0.884 mM. The spectrum of this solution (Figure 3.13 bottom) matched closely the spectrum of Pu(V) observed by Bourges (1972; shown in the same Figure as the top spectrum). The relative easiness of preparing a Pu(V) stock solution from Pu(IV) without using any redox reagents prompted us to study a possibility of Pu(V) generation in concentrated NaOD. Delegard (1987) also observed that initially homogeneous solutions of 4 mM of Pu(VI) in 15 M of NaOH after a few weeks produced a solid phase of Pu(IV) hydrated oxide, and the concentration of soluble Pu dropped down to the concentration levels of Pu(V) found in tests begun by Pu(IV) nitrate added to NaOH. However, the solutions with Pu(VI) addition were not characterized spectrally to identify the oxidation state of Pu in them. Therefore, a parallel experiment based on Pu(VI) addition to 14.9 M of NaOD was conducted in search of an alternative and possibly quicker way to produce Pu(V) stock solution for subsequent experiments.

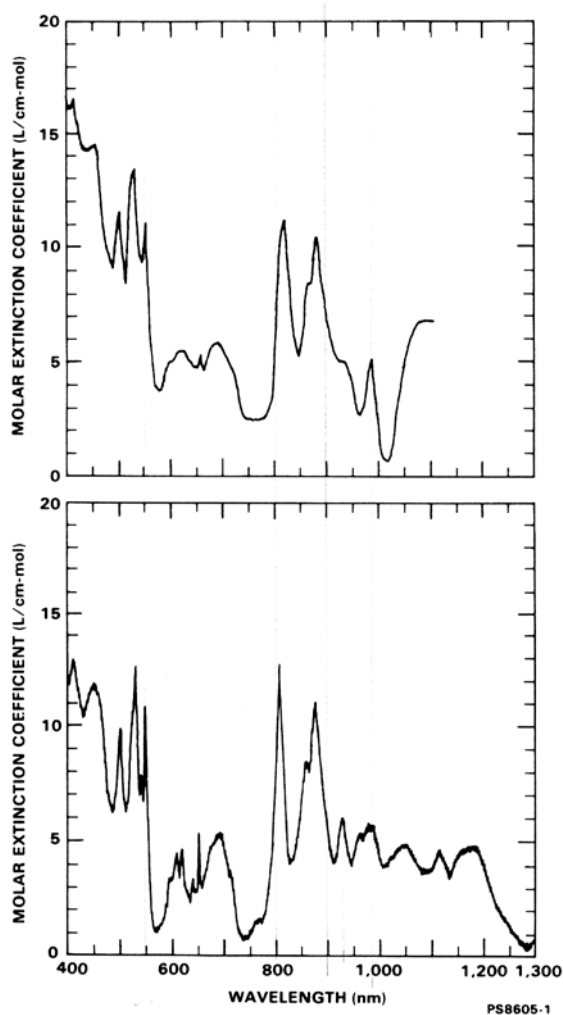


Figure 3.13. Literature Data on Pu(V) Spectra in Concentrated Sodium Hydroxide. Pu(V) spectrum in 4 M NaOH (top) (Bourges 1972) and 15 M NaOH (bottom) (Delegard 1987).

In the first experiment, 65 μL of 18-mM acidic stock solution of Pu(IV) in 2 M DNO_3 was added to 1.1 mL of 14.9 M NaOD. Simultaneously, 92 μL of 10.7 mM Pu(VI) solution in 0.5 M DNO_3 was spiked into the same volume of concentrated NaOD. Both preparations were made directly in 1-cm plastic

spectrophotometric cells equipped with stir bars, and in both cases, the targeted concentrations of Pu were selected to be close to 1 mM if no precipitation occurs. The cells were sealed to minimize the penetration of CO₂ from the atmosphere and its reaction with excess NaOD to form carbonate. Stirring started just before Pu solutions were added and continued for 3 days before the first spectral measurement. Both solutions appeared to contain small amounts of colloidal matter of unidentifiable color; therefore, centrifugation was applied to obtain better quality spectra (data not shown). Stirring continued for several weeks with periodical interruption for centrifugation and spectral measurement. The first signs of characteristic peaks of Pu(V) at 620, 653, 809, 877, and 930 nm were detected after 1 week of stirring. The stirring-centrifugation-spectral measurement-reagitation-stirring cycle was repeated several more times until no statistically significant difference between peak intensities of Pu(V) in both solutions were found after 15 and 20 days of observation. After that, the solutions were filtered through a 0.45-μm Supor (polyethersulfone; Pall Corporation) membrane, and their spectra were measured multiple times to improve the signal-to-noise ratio. The results of these measurements are shown in Figure 3.14. One can see that both spectra look very similar to each other, and their peaks' positions, shapes, and relative intensities are in good correspondence with the spectrum of Pu(V) in 15 M NaOD reported by Delegard (1987; Figure 3.13).

Assuming that the molar absorptivities found in 15 M NaOH can be applied to 14 M NaOD solutions in this study, the calculated concentrations of Pu(V) were estimated as 0.53 mM and 0.49 mM for the Pu(IV) and Pu(VI) samples, respectively, based on the 809-nm peak. LSC analysis, however, returned somewhat higher values [0.81 mM and 0.88 mM for the Pu(IV) and Pu(VI) solutions respectively]. This discrepancy can be explained by incomplete spectral resolution of sharp Pu(V) peaks in spectral measurements using the Ocean Optics spectrophotometer. The fact that Pu(V) produced using Pu(VI) as the starting material, has an ~5% less-intense peak at 809 nm but 8% more plutonium concentration compared with Pu(IV)→Pu(V) conversion might also indicate that not all Pu(VI) was converted to Pu(V) in this sample.

In all subsequent calibration and speciation experiments, Pu(V) stock prepared by spontaneous oxidation of Pu(IV) was used to prepare diluted solutions of Pu(V).

It was of interest to compare the original spectrum of undiluted Pu(V) stock in 14 M NaOD measured with a 1-cm cell (Figure 3.14 a) with the spectrum of a 34-fold diluted sample of the same solution at a 1 M NaOD concentration measured by LWCC. Figure 3.15 shows results of this comparison. It can be seen that many spectral features observed at higher alkalinity remain mostly unchanged in 1 M NaOD. There are two spectral regions where the changes are more noticeable: **a)** 670- to 740-nm region where an ~12-nm red shift of the broad absorbance band of Pu(V) initially at 682 nm is observed with an increasing concentration of hydroxide; **b)** 910- to 940-nm region where the 930-nm peak of Pu(V) undergoes an ~6- to 7-nm blue shift as the NaOD concentration grows. These minor changes indicate that the coordination sphere of the Pu^{VO}₂⁺ cation is practically saturated with hydroxide ligands already in 1 M NaOD solution and further 14-fold increase in deuteroxide concentration causes only a minor equilibrium shift from PuO₂(OD)_{n-1}ⁿ⁻² to PuO₂(OD)_nⁿ⁻¹ species, where n is the number of deuteroxide ligands around the metal center at the higher OD⁻ concentration. The spectrum of Pu(V) measured with LWCC detection represents the first spectrum of this oxidation state of Pu measured at such a low Pu(V) concentration in 1 M NaOD.

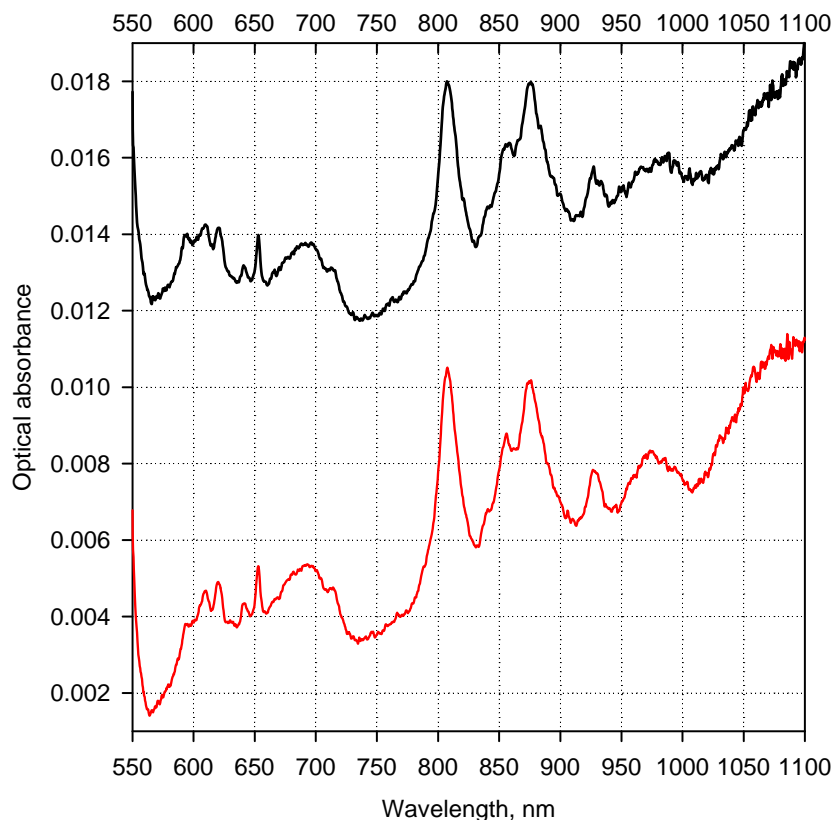


Figure 3.14. Pu Spectra in 14 M NaOD 20 Days After Adding Acidic Pu(IV) (red trace) and Pu(VI) (black trace) to an Excess of 14.9 M NaOD. Both solutions were filtered through a 0.45- μ m Supor membrane filter to remove insoluble Pu phases. The spectra represent the averages of 10 individual scans. A 1-cm plastic cell was used for measurements, and 14 M of NaOD was used as a blank solution. Pu concentrations in solutions that started from Pu(IV) and Pu(VI), which were determined by LSC counting, are 0.81 mM and 0.88 mM, respectively.

3.5.2 Pu(V) Calibration and Speciation Experiments in NaOD

Chromate-Free Medium.

Preparing diluted series of Pu(V) solutions in 0.25 M and 1 M NaOD required more careful planning compared with Pu(VI) calibration experiments due to a much lower concentration of Pu(V) stock available and the very high alkalinity of this stock. To maintain constant alkalinity through the calibration series, the concentration of NaOD in cold solutions before spiking them with Pu(V) was individually adjusted for each concentration point of Pu(V). The 1 M NaOD series was studied first to take advantage of a better stability of Pu(V) solutions, which are prone to disproportionation at a sodium hydroxide concentration lower than 8 M. Similar to the Pu(VI) calibration experiments, two series of solutions were prepared the same day with the first series spectrally measured within the first 60 to 90 minutes after adding Pu(V), and the second series was stored for 3 to 4 days and measured after that. Figure 3.16 shows spectral data from this testing along with respective calibration plots based on the net signal intensity of the two most characteristic peaks of Pu(V) at 653 and 809 nm as a function of the

initially added Pu(V) concentration. The freshly prepared series [plots a) and b)] exhibit all characteristic spectral features of Pu(V) up to the highest concentration of Pu(V) of 23.6 μM and excellent linearity of the calibration plots for both peaks of Pu(V). This proves that all Pu is present in solution as Pu(V), and no disproportionation or other redox processes accompanied by precipitation of lower oxidation states of Pu occurs under these conditions. The 4-day-old series, however, shows a very interesting redox behavior of Pu at the highest concentration of initially added Pu(V). As can be seen by comparing the blue and pink spectral traces in plot c), there is a sudden drop in the intensities of Pu(V) peaks while the newly emerged broad absorbance band at 625 nm is clearly attributable to Pu(VI) (compare this spectrum with spectral sets of Pu(VI) shown in Figure 3.16). The LSC analysis of total Pu concentration indicates that only 11 μM (46% of initially added Pu) remains in solution. This observation is consistent with the disproportionation of Pu(V) at a higher concentration. It is not clear, though, why this process is so concentration sensitive because going down in Pu(V) concentration just two times (blue trace) preserves most Pu as Pu(V). One possible explanation of this effect may involve the precipitation of $\text{Pu}(\text{OH})_4$ as one of the disproportionation products that forms in solution initially as a soluble anionic complex of Pu(IV) and precipitates out with time as its concentration reaches some critical value. More research is needed to explore the kinetics and thermodynamics of this process.

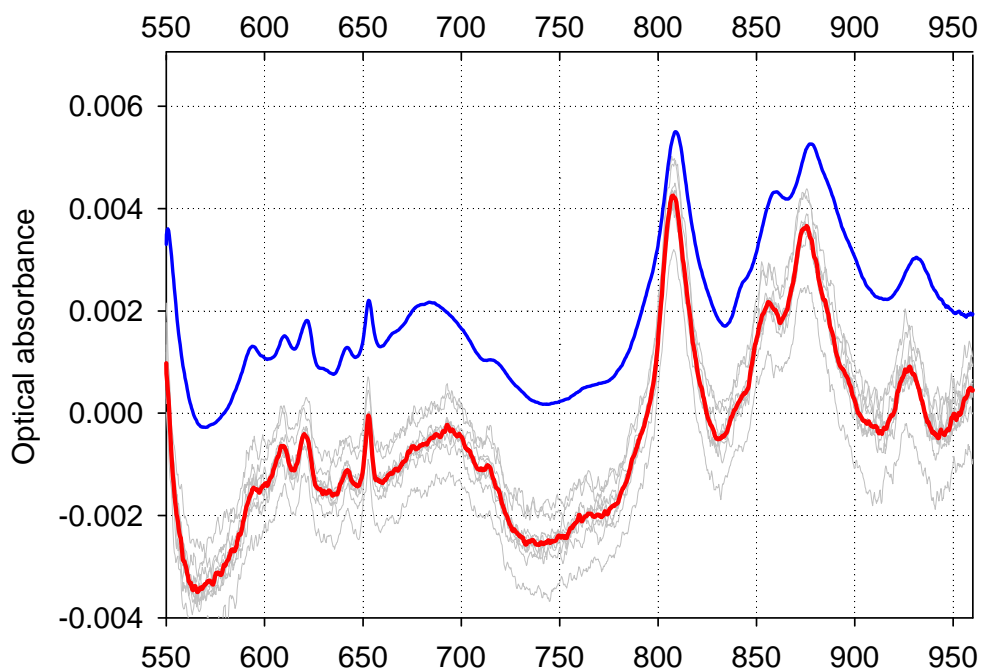


Figure 3.15. Comparison of the Stock Solution of 0.811 mM Pu(V) in 14 M NaOD Measured with 1-cm cell (red trace) with 23.6- μM Pu(V) Solution Spectrum in 1 M NaOD Measured by LWCC (blue trace). The latter spectrum was scaled down 35 times to fit the vertical scale. Gray traces around red spectrum are single scans used for averaging to improve the signal-to-noise ratio in the Pu(V) stock solution spectrum.

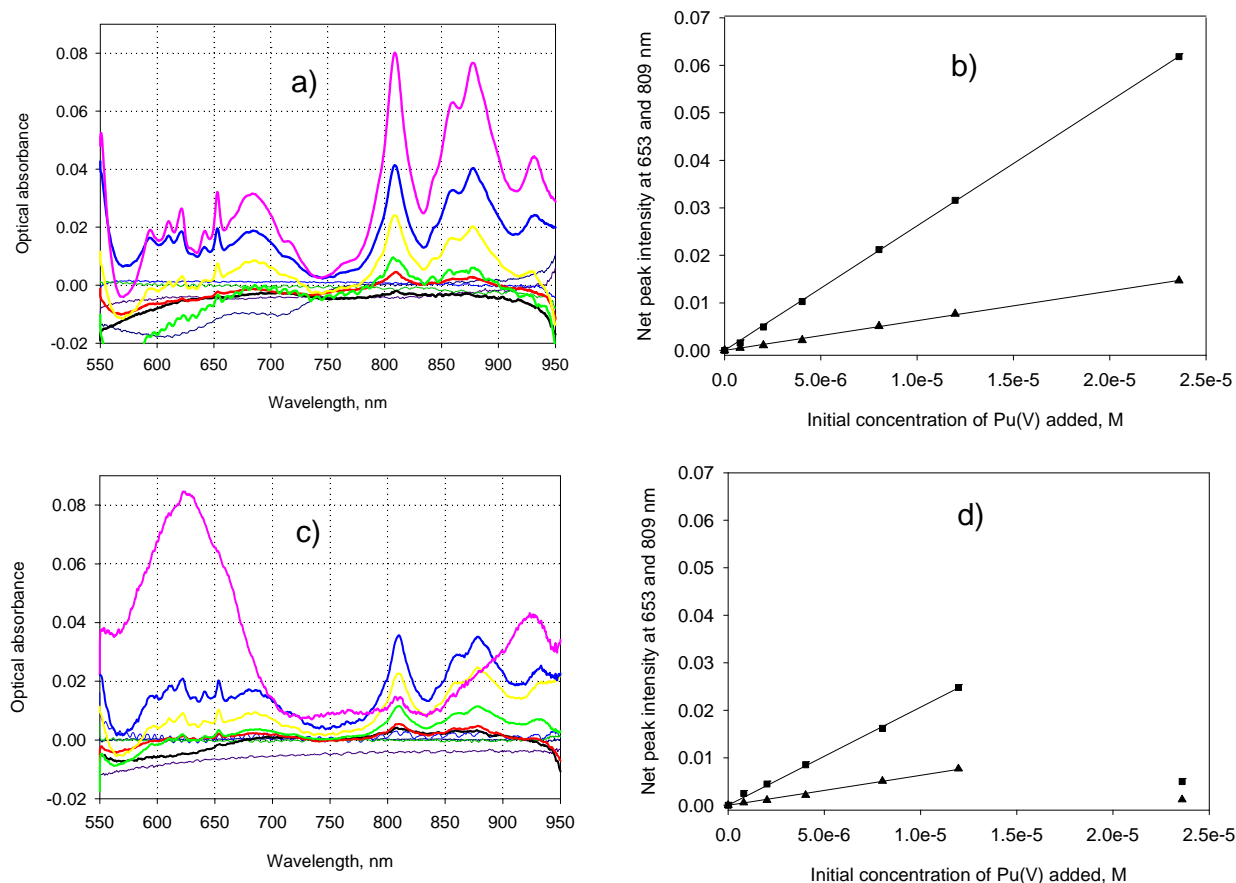


Figure 3.16. Calibration Experiments with Pu(V) in 1 M NaOD. Initial concentrations of Pu(V) are 0.81, 2, 4, 8, 12, and 24 μM for the black, red, green, yellow, blue, and pink spectral traces, respectively. Freshly prepared series a) and b); 4 days between solution preparation and measurement c) and d). In plots b) and d), triangles denote the net peak intensity at 653 nm while squares refer to the peak at 809 nm.

Similar experiments were performed at a 0.25 M concentration of NaOD. In this system, even for freshly prepared and measured series of samples, significant negative deviations between the total initial concentration of Pu(V) added and observable peak intensities of Pu(V) were found [Figure 3.17 a) and b)]. The magnitude of this effect becomes more pronounced at higher total Pu concentration. A limited linearity of the calibration curve is observed for the first two additions of Pu(V) stock. Spectral features of the last three additions of Pu(V) clearly indicate the presence of Pu(VI) in the solutions. Total concentrations of soluble Pu (by LSC analysis) in this series indicate that the percentage of remaining soluble Pu decreases as the initially created concentration of Pu increases. These results are consistent with the redox transformation of Pu(V) into higher [Pu(VI)] and lower [Pu(IV)] oxidation states at this alkalinity. The aging of Pu(V) solutions in 0.25 M NaOD for 3 days [Figure 3.17 c) and d)] shows significant additional decreases of the Pu(V) spectral intensities to very low levels, regardless of the initial level of Pu(V) concentration. The spectral intensities of Pu(VI) peaks remain approximately at the same level as found in the freshly spiked and measured series. Soluble Pu levels were found to go further down by -25%, 51%, 16%, 10%, 9%, and 1% compared with the freshly added Pu(V) series (the negative value

of -25% is most likely associated with pipetting irreproducibility for the 1st concentration point). This drop is consistent with a decrease in solubility of Pu(IV) with time.

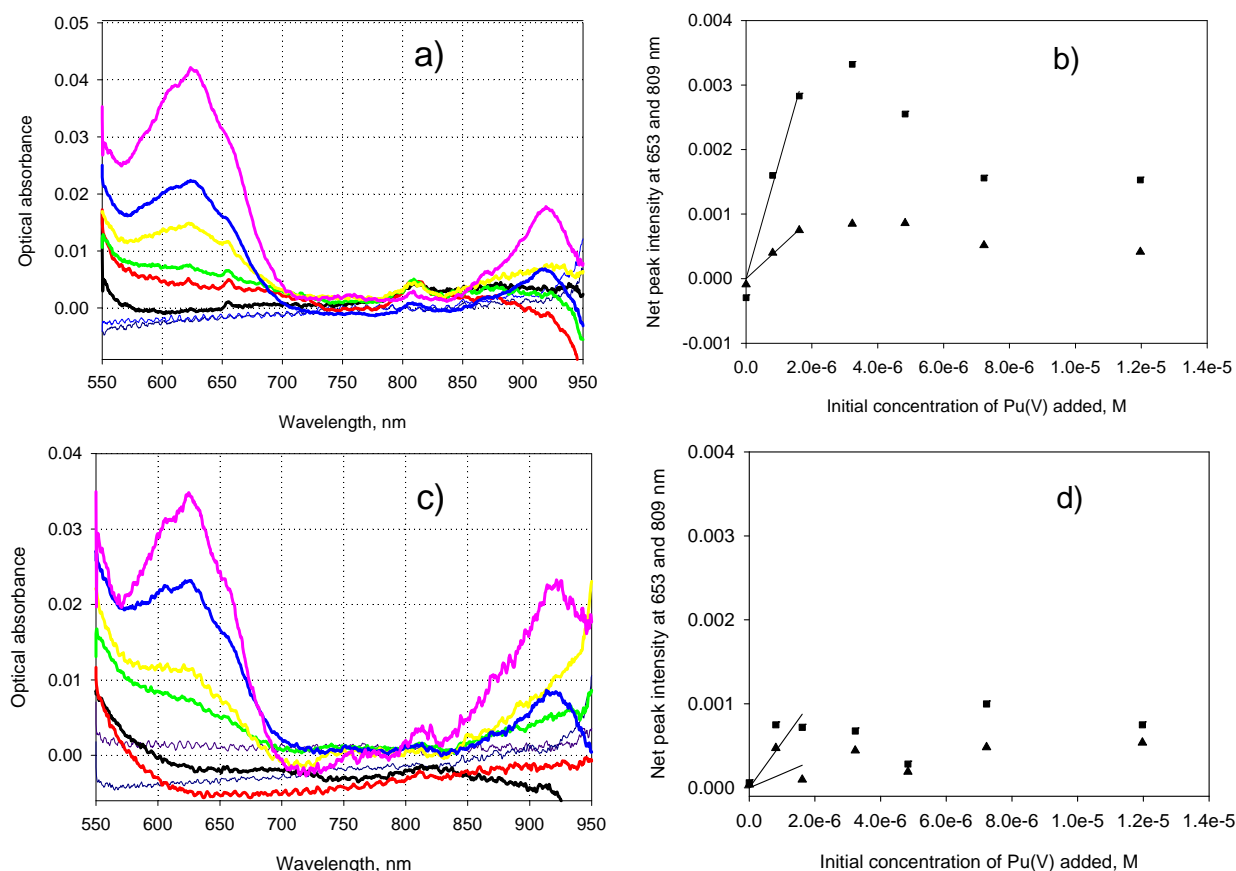


Figure 3.17. Calibration Experiment with Pu(V) in 0.25 M NaOD. Initial concentrations of Pu(V) are 0.81, 1.6, 3.2, 4.8, 7.2, and 12 μM for the black, red, green, yellow, blue, and pink spectral traces, respectively. Freshly prepared series a); 3 days between solution preparation and measurement b). In plots b) and d), triangles denote the net peak intensity at 653 nm while squares refer to peak at 809 nm.

Effect of Chromate on Pu(V) Redox Speciation

As pentavalent Pu represents an intermediate oxidation state between Pu(IV) and Pu(VI), its redox speciation in alkaline solution may be affected not only by levels of NaOD, but also by the presence of other redox reagents. Chromate is expected to be present in alkaline solutions as a soluble product of the oxidation of Cr(III) phases present in Hanford tank sludge after their oxidative leaching with permanganate. Cr(VI) is known to be a moderately strong oxidizer in an acidic medium where it is present as dichromate, but its oxidation ability in alkaline solutions is not well explored. Therefore, it was of interest to investigate Pu(V) redox behavior in 0.25 M and 1 M NaOD media in the presence of Cr(VI). The experiments were executed in the same manner as those conducted in the Cr(VI) free-alkaline medium. Cr(VI) in all four experiments described in this section was fixed at 50 mM.

The 1 M NaOD spectral and calibration series with freshly measured samples (Figure 3.18 a) and b) below) show practically no difference compared with the Cr(VI)-free experiment described above. All Pu added as Pu(V) remains as Pu(V) under these conditions. A slight deviation of the Pu(V) signal intensity for the 809 nm peak is probably related to increased waveform noise level in the pink spectrum (plot a), which distorted the peak shape and intensity. Allowing more time for the Cr(VI) and Pu(V) to interact with each other in the same solution [Figure 3.18 c) and d)] does not lead to any additional conversion of Pu(V) to Pu(VI) by the action of Cr(VI). The level of the Pu(VI) signal observed in the most concentrated solution corresponds to the one observed in the chromate-free experiment and can be explained solely by partial disproportionation of Pu(V). Therefore, it can be concluded that Cr(VI) does not show any oxidizing effect with respect to Pu(V) in 1 M NaOD.

Experiments in 0.25 M NaOD in the presence of 50 mM Cr(VI) with freshly spiked Pu(V) [Figure 3.19 a) and b)] show very similar behavior of Pu(V) to the respective Cr(VI)-free series.

The 3-day-old series at the same alkalinity [Figure 3.19 c) and d)] shows approximately the same levels of residual Pu(V) as in the Cr(VI)-free series, but practically no Pu(VI), which was spectrally observed before as a broad spectral feature with a maximum at 625 nm [compare Figure 3.17 c and Figure 3.19 c)]. For technical reasons (an emergency response to fire alarm), the solution with the highest concentration of added Pu(V) was not spectrally measured. No explanation of the absence of a Pu(VI) signal in the Cr(VI) tests can be offered at this time. It is possible that the Cr(VI) used in this work contained a trace amount of Cr(III), which acted slowly as a three-electron reductant to convert the Pu(VI) that was initially formed via the disproportionation of Pu(V) to practically insoluble Pu(IV). Even a 0.01% admixture of Cr(III) in a 50 mM Cr(VI) solution [which would correspond to 5 μM of Cr(III) in the solution] would be sufficient to seriously perturb the yield of Pu(VI) in this system with a total initial Pu concentration below 20 μM . The results of determining the total soluble Pu concentration in this series confirm a significant drop in Pu concentration for all samples compared with the chromate-free series.

All results obtained in the course of the eight calibration experiments described above are summarized in Table 3.3 with an emphasis on the linearity ranges, slopes, and detection limits.

3.5.3 Pu(V) Spectra in the Presence of Carbonate at Constant Concentration of Hydroxide

A significant effect of the presence of hydroxide on the optical absorbance spectrum of the triscarbonate complex of Pu(V) in concentrated Na_2CO_3 solution was noted by Varlashkin and co-workers (1984b). This effect can be explained by the formation of mixed hydroxy-carbonate complexes of Pu(V). The most pronounced spectral changes were found in the 640- to 1000-nm range of the spectrum where a number of absorbance peaks of $\text{Pu}^{\text{V}}\text{O}_2(\text{CO}_3)_3^{5-}$ changed their peak positions and intensities as one or more carbonates were displaced by a growing hydroxide concentration. Unfortunately, the authors did not try (or were limited by solubility problems) to study Pu(V) speciation in the presence of carbonate, starting from a purely hydroxide medium, and in their experiments, the $\text{OH}^-/\text{CO}_3^{2-}$ ratio was at or below 2.29:2. In this project, it was considered important to study redox and complexation speciation of Pu(V) in an alkaline media in the presence of carbonate for two reasons. First, the presence of carbonate may affect the redox speciation of Pu(V) with its partial conversion to other oxidation states, which in turn may impact the solubility of Pu. Second, in searching for more intense and clearly defined spectral features of

Pu(V) in an alkaline medium, the presence or artificial addition of carbonate could be beneficial to improve the sensitivity of its detection by optical absorbance spectroscopy.

In this study [similar to Pu(VI) speciation in a mixed hydroxy-carbonate medium, Section 3.4.3], the effect of carbonate on the spectral features of alkaline Pu(V) was studied at two constant levels of NaOD. The carbonate concentration was varied in 5 increments up to the equimolar ratio for the given hydroxide level. The results are presented in Figure 3.20.

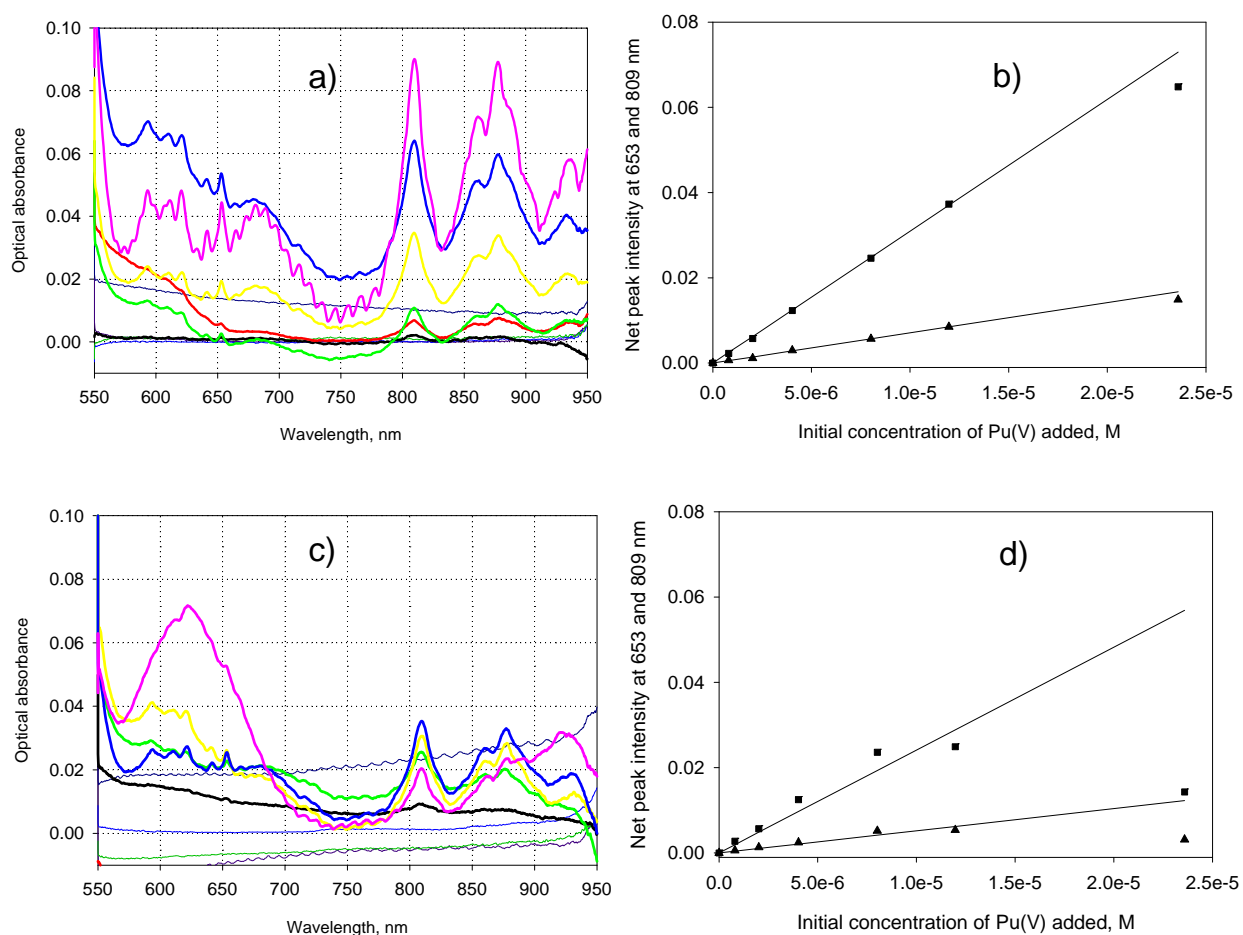


Figure 3.18. Calibration Experiments with Pu(V) in 1 M NaOD in the Presence of 50 mM Chromate. Freshly prepared series a); 3 days between solution preparation and measurement b). Initial concentrations of Pu(V) (0.81, 2, 4, 8, 12, and 24 μM) are the same as those indicated in caption to Figure 3.16.

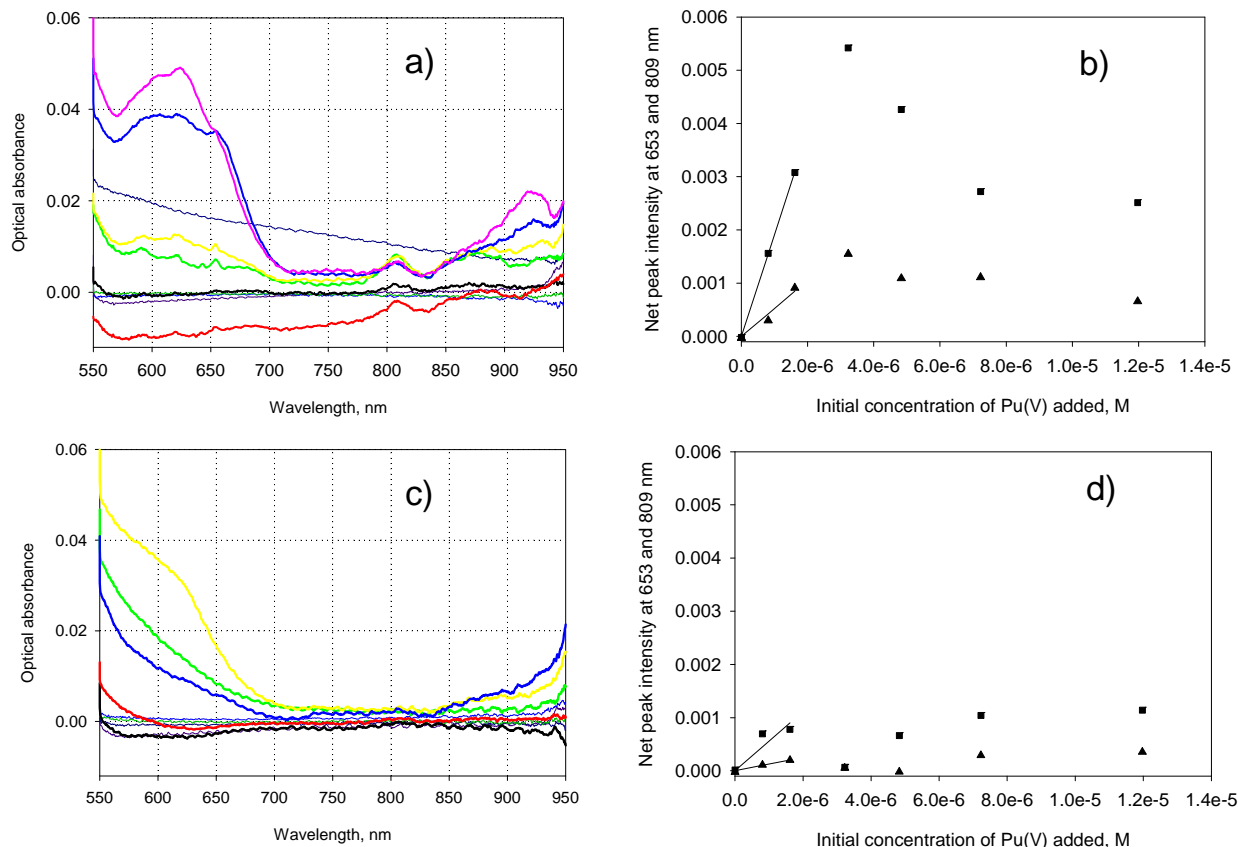


Figure 3.19. Calibration Experiments with Pu(V) in 0.25 M NaOD in the Presence of 50 mM Chromate. Freshly prepared series a); 3 days between solution preparation and measurement b).

At the 1 M NaOD concentration [plot b)], the carbonate-free spectrum (black trace) shows that Pu(V) is the only oxidation state in solution that is consistent with previously discussed results on Pu(V) stability up to 3 days at this concentration of Pu(V). The very first addition of carbonate induces significant spectral changes, which progress further as the carbonate concentration grows. The most sensitive range of the spectrum of Pu(V) to the presence of carbonate is the 720- to 770-nm where a new peak at ~735 nm becomes clearly visible, even at the very first addition of carbonate. The major peak of Pu(V) at 809 nm also shows significant changes as it red shifts to 822 nm as result of complexation with carbonate, but no intensification of the new absorbance band occurs in this case. Another very characteristic band of Pu(V) at 653 nm gets ~2.5 times more intense at the one-to-one $\text{OD}^-:\text{CO}_3^{2-}$ molar ratio. Spectral analysis does not give any indication of the conversion of Pu(V) species to the Pu(VI) complex, which should be clearly visible as a separate peak at 870 nm even in case of the partial conversion of Pu(V) to Pu(VI).

Table 3.3. Summary of Calibration Experiments with Pu(V) in 0.25 M and 1 M NaOD

Medium		Concentration Range, μM	Solutions Age, hr	Pu(V) Peak Used for Calibration, nm	Calibration Curve Linearity ^(a) , R^2	Slope, M^{-1}	Detection Limit, μM
1 M NaOD	No Cr(VI)	0.81–23.6	1.5 ± 0.5	653	$0.999_2 (6)$	624 ± 7	0.24
				809	$0.999_9 (6)$	2620 ± 14	0.38
			96 ± 3	653	$0.999_5 (5)$	480 ± 12	0.054
				809	$0.998_8 (5)$	2020 ± 34	0.36
	50 mM Cr(VI)	0.81–23.6	1.5 ± 0.5	653	$0.999_1 (5)$	709 ± 10	0.19
				809	$0.999_7 (5)$	3090 ± 20	0.33
			72 ± 3	653	$0.967 (5)$	521 ± 43	0.59
				809	$0.969 (5)$	2410 ± 190	0.13
0.25 M NaOD	No Cr(VI)	0.81–11.9	1.5 ± 0.5	653	$0.988 (2)$	470 ± 37	0.71
				809	$0.989 (2)$	1800 ± 130	0.40
			72 ± 3	653	$0.379 (2)$	170 ± 150	1.7
				809	$0.884 (2)$	540 ± 140	1.3
	50 mM Cr(VI)	0.81–11.9	1.5 ± 0.5	653	$0.976 (2)$	520 ± 60	0.50
				809	$0.999 (2)$	1910 ± 11	0.31
			72 ± 3	653	$0.985 (2)$	126 ± 11	2.4
				809	$0.931 (2)$	560 ± 110	1.5
(a) Number in brackets corresponds to numbers of concentration points of Pu used for linear regression: 6 points correspond to full range of Pu(V) additions; 5 points correspond to first 5 additions of Pu (0.810- to 11.9 μM range); 2 points correspond to first two additions (0.81- to 1.62 μM range).							

The 0.25 M NaOD spectral series [plot a)] represents a more complicated case because of the partial conversion of Pu(V) to Pu(VI) at this reduced level of hydroxide observed in a carbonate-free medium. It should be noted that in all OD^- - CO_3^{2-} experiments, including this one, a series of six solutions with a varying carbonate-to-hydroxide ratio was prepared first, and then equal amounts of Pu(V) stock solution in 14 M of NaOD were spiked into each solution, followed by mixing and equilibration for 1 to 1.5 hr before spectral measurement. In other words, it was not a titration experiment with an increasing amount of carbonate added to the same solution, but a series of separately prepared solutions used to collect spectral information after all samples were allowed sufficient and approximately equal time for equilibration.

In the very first spectrum [black trace in plot a)], Pu is present as a mixture of 57% of Pu(VI) and 43% of Pu(V) (this estimate is approximate as it based on the assumption that the molar absorptivity of the Pu(V) peak at 809 nm remains the same in the 0.25 M NaOD medium as was found to in 1 M NaOD). However, in the presence of 0.05 M of carbonate (red trace), very drastic spectral changes were noted:

- Very prominent spectral features of the mixed Pu(V) hydroxy-carbonate complex at 735 and 820 nm were observed.
- Their spectral intensities were comparable with those observed in the 1 M NaOD + carbonate experiment at the highest concentration of Na_2CO_3 (1 M).
- No characteristic absorbance band of mixed hydroxy-carbonate complex of Pu(VI) at 868 nm was present, which should be clearly visible at an $\sim 8\text{-}\mu\text{M}$ concentration of Pu(VI).

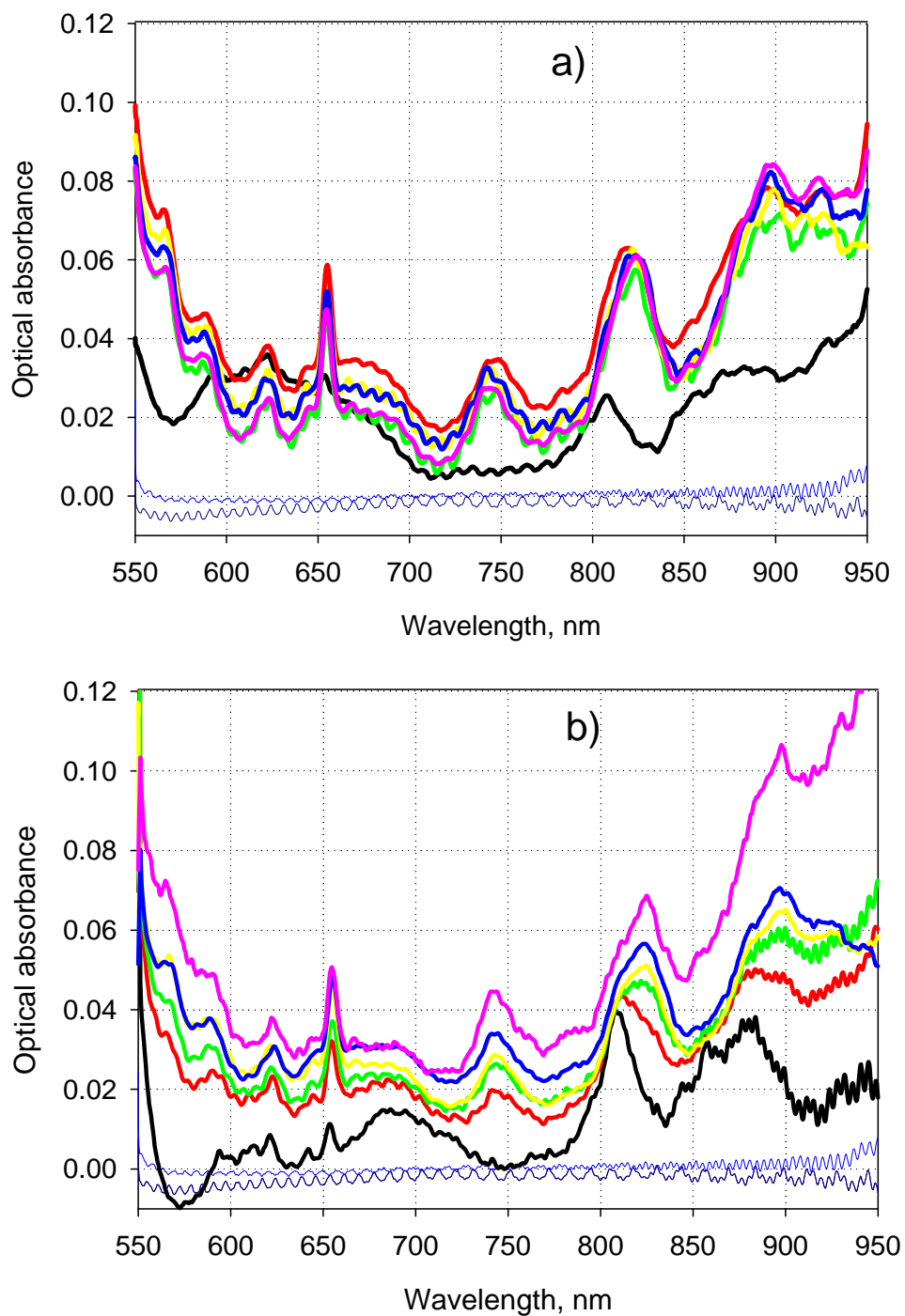


Figure 3.20. Pu(V) Spectra in 0.25 M NaOD a), and 1 M NaOD b) in the Presence of Carbonate. In all cases, the carbonate concentration grows from 0% to 100% with 20% increments relative to the respective molar concentration of hydroxide for black, red, yellow, green, blue, and pink spectral traces, respectively. The Pu(V) concentration is fixed at 14.3 μM and at 12 μM for the 0.25 M and 1.0 M NaOD series, respectively.

A further increase in carbonate concentration (0.1, 0.15, 0.20, and 0.25 M) produced only minor changes in absorbance spectra compared with the very first addition of this ligand.

All of these observations indicate that carbonate plays an important role in stabilizing Pu(V) in its initial oxidation state at 0.25 M hydroxide concentration, most likely via suppression of the disproportionation reaction of Pu(V) to Pu(IV) and Pu(VI), which would be followed by the precipitation of Pu(IV) as poorly soluble Pu(IV) hydroxide.

3.5.4 Pu(V) Redox Speciation After Acidification of Initially Alkaline Pu(V) Solution by DNO₃ at a Low Micromolar Concentration of Pu(V)

As has been shown in Section 3.4, Pu(VI) detection in an acidic medium by optical absorbance spectroscopy is ~100 times more sensitive than in an alkaline medium. The spectrum of Pu(V) in acid is reported to have two relatively sharp and intense absorbance bands centered at 569 nm and at 775 nm (Cohen 1961). At a millimolar concentration range of Pu(V), this oxidation state has a limited lifetime due to the disproportionation at pH below 2. On the other hand, it is known that the rate of the disproportionation reaction of Pu(V) is a sensitive function of the initial concentration of Pu(V). Therefore, the disproportionation of Pu(V) is slowed considerably at a low micromolar concentration. In this project, it was of interest to determine under what conditions the acidification of an initially alkaline Pu(V) solution may produce a stable spectrum of Pu(V) without significant perturbation of its redox equilibrium with other oxidation states possibly present in the same alkaline solution. Two simple tests were performed: 1) acidification of Pu(V) alkaline stock by slight excess of DNO₃ to achieve ~0.05 M acidity level; 2) repetition of the same experiment in the presence of 5 mM chromate.

Chromate Free Medium

Fifty μ L of 0.81 mM alkaline Pu(V) stock solution in 14 M NaOD were spiked into 2 mL of 0.4 M DNO₃ solution in D₂O. The estimated acidity of the resulting mixture is 0.06 M of DNO₃. The acidified Pu(V) solution was injected into LWCC 3 to 4 minutes after the solution was homogenized, and a kinetic series of 22 spectra was taken. The solution was left inside the cell overnight, and one more spectrum was taken the next morning. Figure 3.21 shows the results of this experiment. Only four spectral scans are shown for simplicity (6 minutes, 28 minutes, 60 minutes, and 17 hours after acidification). The very first spectral scan (black trace), taken ~6 minutes after acidification, shows four absorbance bands of Pu(V) at 569, 775, 848, and 895 nm as well as a prominent peak of Pu(VI) at 831 nm. The estimated fraction of Pu(VI) for this spectrum is 8% of the total Pu present in solution. This percentage slowly increases with time [17% and 33% of Pu(VI) were found in solution after 60 minutes and 17 hours of exposure to acidic conditions, respectively]. The remaining fraction of Pu is present as Pu(V). No absorbance bands of Pu(IV) and Pu(III) could be distinguished in the overnight spectrum. For this reason, we believe that the observed process of a slow build-up of Pu(VI) from Pu(V) is purely oxidation rather than disproportionation. Both nitric and nitrous acids (the latter is always present as a trace admixture in untreated nitric acid solutions) might be acting as mild oxidizing agents. It would be desirable to repeat this experiment using DCl as a non-oxidizing acidifying agent to understand the role of nitrous and/or nitric acid in this process.

The 8% admixture of Pu(VI) in Pu(V) solution 6 minutes after acidification most likely is result of a relatively quick oxidation of Pu(V) by the oxidizing components of the acidic mixture. More careful

analysis of kinetic data is needed to extrapolate the 6-min data back to zero time to determine the actual level of Pu(VI) (if any) in the Pu(V) stock solution.

In the Presence of 5 mM Chromate

A similar experiment was conducted but in the presence of 5 mM chromate. The chromate solution converts to 2.5 mM dichromate in acid. In this case, a 100% conversion of Pu(V) to Pu(VI) was observed already at the moment of the very first spectral scan (black trace in Figure 3.22). Five more spectral scans with ~2-min time intervals (only the second scan is shown in the figure for simplicity) showed no further spectral changes. This experiment proves that the technique of acid strike can not be used to determine the ratio between Pu(V) and Pu(VI) by acidification of an initially alkaline solution if the solution contains chromate. Dichromate appears to be too strong an oxidizer in an acidic medium for Pu(V) to survive in its presence. Another problem with dichromate in terms of the LWCC detection range is its much stronger optical absorbance in the 550- to 600-nm spectral range compared to chromate. This is noticeable even at a relatively low 2.5 mM concentration of this species. The detection range of LWCC is expected to be narrowed even further with 10- to 20-fold higher concentrations of dichromate.

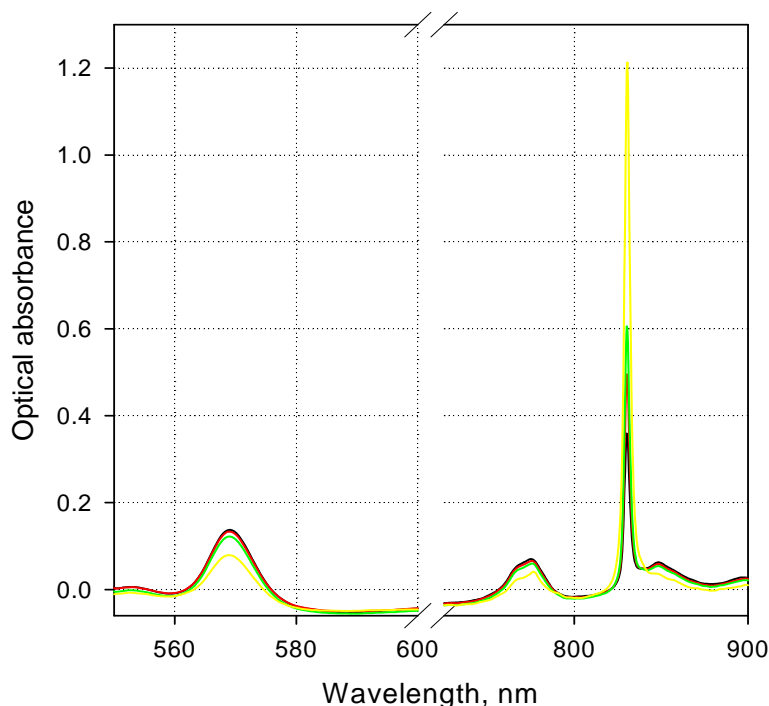


Figure 3.21. Spectra of Pu(V) After Acidic Strike of Small Amount of Pu(V) Stock in 14 M NaOD with a Slight Molar Excess of 0.4 M DNO₃ Solution. The total concentration of Pu is 19.7 μ M. Black, red, green, and yellow spectral traces correspond to 6-minute, 28-minute, 60-minute, and 17-hour exposures of alkaline Pu(V) to an acidic medium.

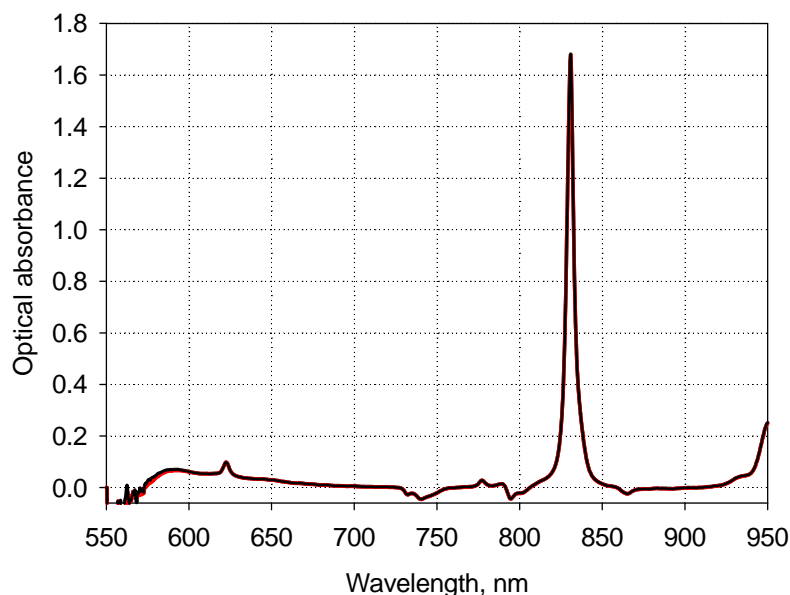


Figure 3.22. Spectra of Pu(V) After Acidic Strike of Tiny Amount of Pu(V) Stock in 14 M NaOD into a Slight Molar Excess of 0.4 M DNO₃ Containing 5 mM of Chromate (physically present as 2.5 mM dichromate). Black trace: ~ 10 minutes after acidification. Red trace: 30 minutes later.

3.5.5 Determination of Formal Electrochemical Potential of Pu(VI)/Pu(V) Couple in 0.25 M to 1.0 M NaOD Using Direct Potentiometric Measurement with an ORP Electrode

Experiments on Pu(VI) speciation in NaOD described in Section 3.4.2 showed that a 1 M NaOD Pu(VI) solution contained a spectrophotometrically detectable concentration of Pu(V) (see Pu(V) peak at 809 nm in Figure 3.11). Knowing the initial concentration of Pu(VI) that was added to the alkaline solution and calculating the Pu(V) concentration from the 809-nm peak intensity should make it possible to calculate the remaining concentration of Pu(VI) in equilibrium with Pu(V). The ratio of [Pu(VI)]/[Pu(V)] can be incorporated then into the Nernst equation, which describes the relationship between the measured potential in the Pu(VI) + Pu(V)-containing solution and the formal potential of the Pu(VI)/Pu(V) couple as shown below:

$$E_{\text{measured}} = E^{\circ}_{\text{formal}} + RT/nF \cdot \log \{ [Pu(VI)]/[Pu(V)] \} \quad (3.1)$$

where the RT/nF term is equal to 0.0592 V at 25°C (for $n = 1$) after conversion of the natural logarithm scale (\ln) to the base-10 logarithm scale (\log).

There are a limited number of studies of the determination of the electrochemical potential of the Pu(VI)/Pu(V) redox couple as summarized by Barney and Delegard (1999) with no data available in the low alkalinity range (<1 M NaOH). According to a recent paper on Np electrochemistry (Gelís et al. 2001), the corresponding Np(VI)/Np(V) couple becomes irreversible at NaOH below 1.3 M, presumably due to the formation of solid Np(V) hydroxide in an initially homogeneous solution from the process of cyclic voltammetry measurements under these conditions. Therefore, it was of interest to perform one more

set of spectral experiments with a Pu(VI) solution in a lower alkalinity range of NaOD concentrations with simultaneous measurement of the oxidation-reduction potential in a portion of the same solution. Six solutions of NaOD were prepared in the deuteroxide concentration range from 0.25 M to 1.0 M, followed by adding a small volume of weakly acidic Pu(VI) solution to make a 20- μ M Pu concentration. Solutions were homogenized and stored for 1 to 2 hr before spectral measurements. ORP measurements were performed simultaneously with spectral measurements of the same Pu-containing solution split into two equal 2-mL portions. The ORP readings were taken within the first 7 to 10 minutes after the solution made contact with the electrode to minimize a positive temperature drift due to a prolonged intense stirring during ORP measurements.

The spectral data that were used to determine the extent of Pu(VI) spontaneous conversion to Pu(V) are shown in Figure 3.23, and the ORP measurements are presented in Table 3.4. As follows from these data, a higher alkalinity favors a higher percentage of Pu(V) in equilibrium with Pu(VI), but the measured ORP potential is not a simple monotoneous function of the Pu(V) fraction in total Pu balance as it goes through a minimum at 0.55 M of NaOD. Accordingly, the formal potential calculated from these data also shows a minimum at this alkalinity. This complex behavior of the magnitude of a formal potential might be associated with the effect of non-constant ionic strength, but it might also indicate a lack of structural “identity” between Pu(VI) and Pu(V) species in this range of hydroxide concentrations [see Gelis et al. 2001 for more details about this effect for the Np(VI)/Np(V) couple]. The formal potential determined in 1.0 M NaOD (+0.145 V) is in satisfactory agreement with the value of +0.233 V reported for Pu(VI)/Pu(V) at 0.9 M NaOH for much higher Pu concentration (Peretrukhin et al. 1982). The difference between these two values can be partially explained by the liquid-junction potential between the working electrode (filled with saturated KCl) and the electrolyte solution (1 M NaOH).

From a practical point of view, the most important result of this study is the finding that the formal potential of the Pu(VI)/Pu(V) couple is about 400 mV lower than potentials of Mn(VII)/Mn(VI) and Mn(VI)/Mn(IV) couples in an alkaline medium. This indicates that any Pu(V) possibly present in solution before oxidative alkaline treatment is expected to be quantitatively oxidized by an excess of permanganate and/or manganate to Pu(VI).

3.6 Pu(IV) Spectral Measurements in DNO₃ and NaOD

3.6.1 Verification of Identity of Spectral Features of Pu(IV) in 4 M of HNO₃ and 4 M of DNO₃

A stock solution of Pu(IV) in 4 M DNO₃ was prepared by careful evaporation of Pu(IV) solution in 4 M HNO₃ under vacuum at room temperature and redissolution of Pu(NO₃)₄ in DNO₃. The cycle of evaporation-redissolution was repeated two times to minimize the admixture of H₂O in D₂O. The spectrum of 18 mM of Pu(IV) is shown in Figure 3.24. All peak positions and their relative intensities are in excellent correspondence with the spectrum of Pu(IV) at the same Pu concentration in 4 M of HNO₃ (black spectral trace in the same Figure). Therefore, the entire body of spectral data [Nd(III), Nd(EDTA), Pu(VI), Pu(V), and Pu(IV)] accumulated so far proves that there is no effect of H₂O, HNO₃ substitution by D₂O, and DNO₃ on the spectral features of light-absorbing species of lanthanide and actinide metal cations and their complexes.

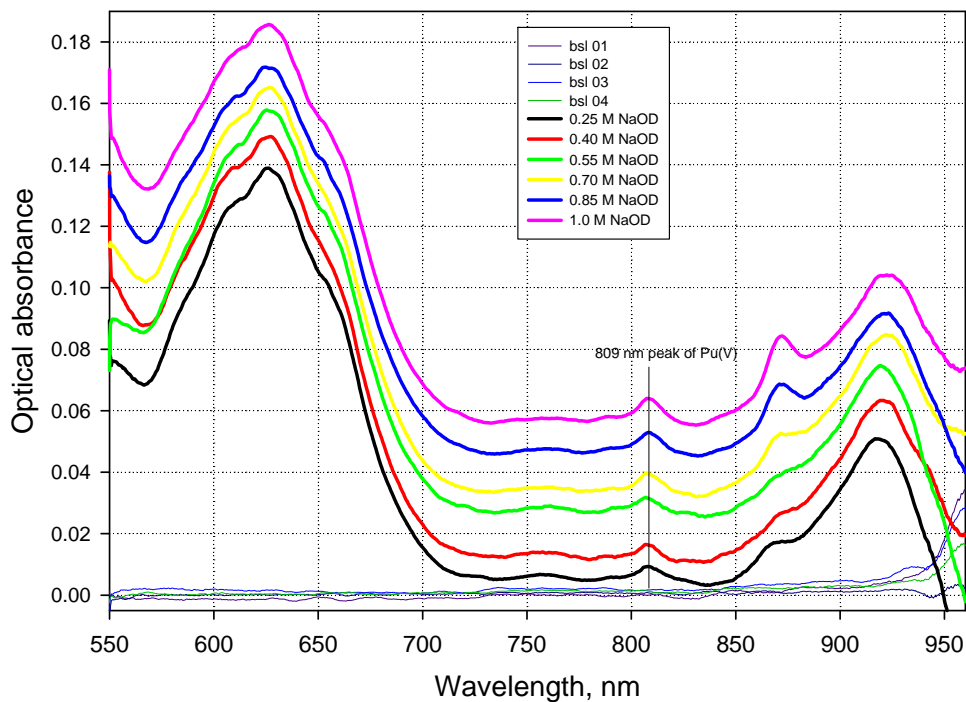


Figure 3.23. Spectra of Pu(VI)+Pu(V) Solutions in NaOD Solutions at Total Concentration of Pu at 20 μM . Admixture of Pu(V) is seen as a minor peak at 809 nm. Spectra are vertically offset by 0.00, +0.007, +0.023, +0.026, +0.04, and +0.05 absorbance units for 0.25-, 0.40-, 0.55-, 0.70-, 0.85-, and 1.0-M NaOD concentrations, respectively.

Table 3.4. Calculation of Formal Potentials of the Pu(VI)/Pu(V) Couple in NaOD Solution

C_{NaOD} , M	A_{809} , a.u.	$C_{\text{Pu(V)}}$, μM	C_{Pu} total, μM	$C_{\text{Pu(VI)}}$, μM	$C_{\text{Pu(VI)}/C_{\text{Pu(V)}}$	Fraction of Pu(V), %	Log term { $59.2 \times$ $\log[C_{\text{Pu(VI)}/C_{\text{Pu(V)}}]$ }, mV	E_{measured} , mV	E_{formal} , mV
0.25	0.0051	1.92	20	18.1	9.4	9.6	57.4	182	125
0.40	0.00477	1.80	20	18.2	10.1	9.0	59.3	173	114
0.55	0.00505	1.90	20	18.1	9.5	9.5	57.7	165	108
0.70	0.00627	2.36	20	17.6	7.5	11.8	51.5	169	117
0.85	0.00679	2.56	20	17.4	6.8	12.8	49.2	193	143
1.00	0.00759	2.86	20	17.1	6.0	14.3	45.9	191	145

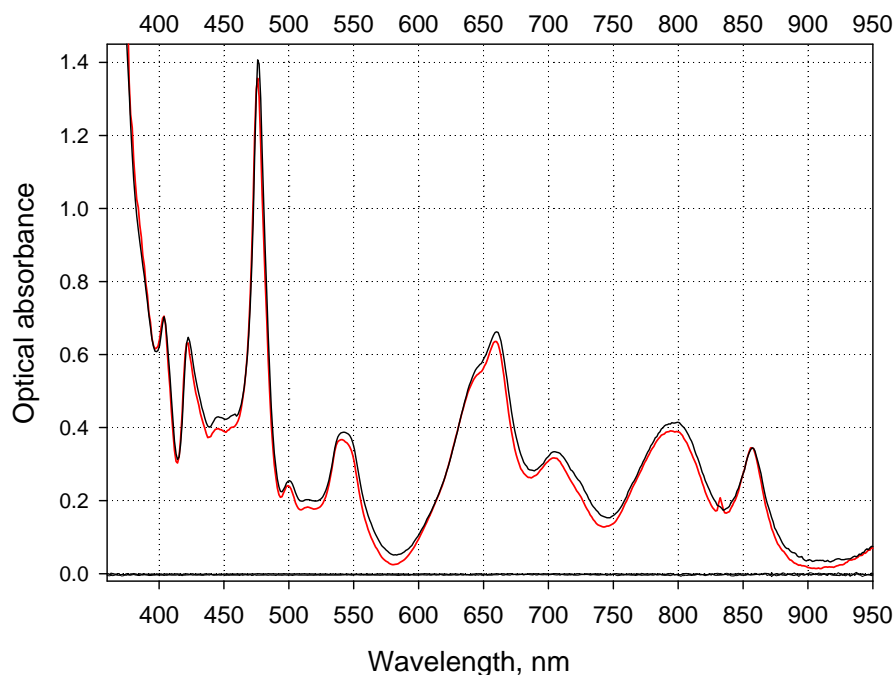


Figure 3.24. Optical Absorbance Spectra of 18 mM Pu(IV) in 4.0 M HNO₃ (black trace) and 4.0 M DNO₃ (red trace). The black spectrum is upshifted by 0.025 absorbance units for clarity.

3.6.2 Pu(IV) Calibration Experiment in 0.75 M of DNO₃

It was of interest to determine the detection limit of Pu(IV) in an acidic medium using LWCC detection before performing experiments with Pu(IV) from the alkaline side. The acidification of an initially alkaline solution possibly containing multiple oxidation state species of this metal was expected to provide better detection limits [as has been already demonstrated with Pu(VI)]. Conventional optical absorbance spectroscopy (with 1-cm optical pathlength) offers a limited sensitivity for Pu(IV) detection in an acidic medium with a detection limit on the order of 160 μM using a major peak of Pu(IV) at 476 nm (Wilson et al. 2005). In this project, the 476-nm peak was inaccessible with the near-IR optimized Ocean Optics instrument coupled with LWCC. For this reason, the second major peak of Pu(IV) at 660 nm was selected for calibration experiment in 0.75 M DNO₃. The reduced level of acidity was considered to be still sufficient for suppressing the hydrolysis of Pu(IV) and preventing its disproportionation to Pu(III) and Pu(VI). A series of diluted Pu(IV) solutions in 0.75 M of DNO₃ was prepared and spectrally measured to cover the concentration range of Pu from 0.18 μM to 8.8 μM . The results of this measurement are shown in Figure 3.25. The net signal intensity of the 660-nm peak measured against its valleys at 585 nm and 692 nm was used to establish a correlation between its magnitude and the Pu concentration in solution (data not shown). The calibration plot showed good linearity ($R^2 = 0.9971$) and high sensitivity (slope = 11500 M^{-1}). The detection limit was found to be 27 nM, which is just five times worse than the 5.6 nM value found earlier for Pu(VI) in acidic solution. Therefore, the technique of acid strike (using deuterated acid and solvent) might be useful to establish the presence of Pu(IV) and Pu(VI) in an initially alkaline solution if both oxidation states are present at low submicromolar concentration levels. However, the conversion of soluble hydrolyzed forms of Pu(IV) into its monomeric cationic form of $\text{Pu}^{\text{IV}}(\text{NO}_3)_2^{2+}$ is expected to be quick and quantitative only if the hydrolyzed form is monomeric itself. If alkaline Pu(IV) is present as low-nanometer-sized colloidal particles (which can easily penetrate

through 200- or 450-nm pore-size membrane filters and thus qualify as a soluble fraction), then depolymerization of this material may take a much longer times and would require much higher acid concentrations for completion.

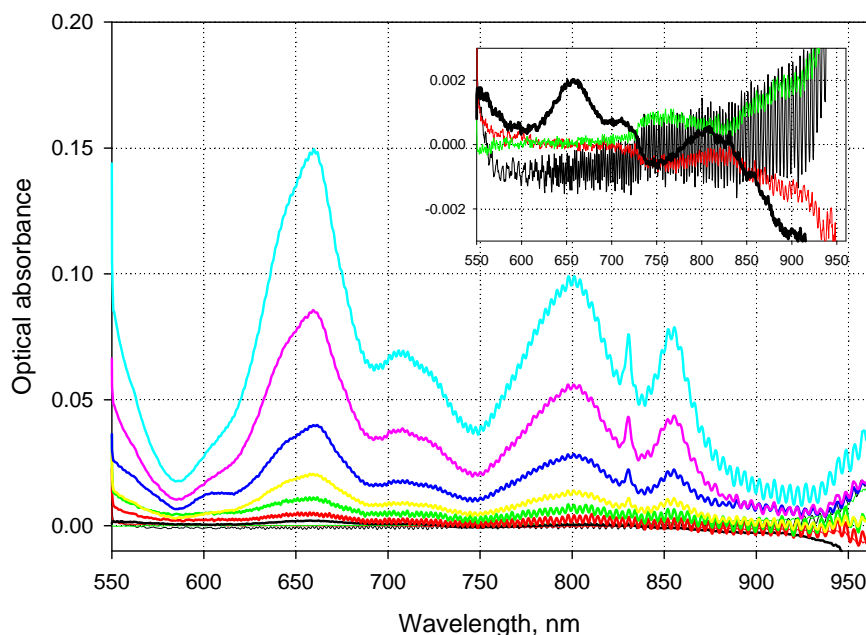


Figure 3.25. Calibration Experiment with Pu(IV) in 0.75 M of DNO_3 Using a 500-cm LWCC. Pu(IV) concentrations are as follows: black—0.18 μM ; red—0.36 μM ; green—0.72 μM ; yellow—1.43 μM ; blue—2.86 μM ; pink—5.32 μM ; pale blue—8.8 μM . The inset shows the lowest concentration of the Pu(IV) spectrum vertically magnified along with typical blank spectra (thin black, red, and green traces).

3.6.3 Pu(IV) Speciation and Solubility in 0.25 M NaOD

The alkaline chemistry of Pu(IV) remains poorly explored, mainly because of the very low solubility of this oxidation state of Pu in NaOH solution. The total Pu concentration in equilibrium with $\text{Pu}(\text{OH})_4$ in deaerated and carbonate-free weakly alkaline solutions is reported not to exceed 10 nM. (Rai et al. 1999; Neck et al. 2007). Indirect redox speciation analysis by solvent extraction indicates that the fraction of Pu(IV) in the total balance of soluble Pu does not exceed a few percent, which corresponds to subnanomolar levels of tetravalent Pu. Even under these well-controlled conditions of solubility studies performed in inert atmosphere gloveboxes, it was noted that partial conversion of Pu(IV) species to other oxidation states occurred over long equilibration times (more than one week).

In this project, no technical capability existed to protect alkaline solutions of NaOD from dissolved oxygen and atmospheric CO_2 . For this reason, we chose to minimize the time between the preparation of the alkaline solution of Pu(IV) and the spectral measurement to 10 minutes for the freshly prepared sample and 3 days for “aged” sample. The alkaline solution of Pu(IV) in 0.25 M NaOD was prepared by spiking 5 μL of 0.36 mM Pu(IV) acidic stock in 2 M DNO_3 into 2 mL of 0.25 M NaOD. The estimated perturbation of the initial alkalinity via Pu(IV) introduction did not exceed 2%. The total amount of added Pu(IV) corresponded to 9 μM of total Pu concentration under the assumption that all added Pu

remains in solution. The results of spectral measurements of the “fresh” and “aged” sample are shown in Figure 3.26. One can see that the spectrum of the fresh sample (bold black trace) does not exhibit any peak-like spectral features in all the spectral ranges available for scanning. A monotonous elevation of optical absorbance toward shorter wavelengths starting from ~740 nm was not observed before with Pu(VI) and freshly prepared Pu(V) solutions at the same alkalinity, but the similar spectral trend was noted for aged Pu(V) samples [see Figure 3.19 plot c)]. For the aged sample (bold red trace), two weak and broad peaks at 700 nm and ~820 nm were detected, but this spectral measurement is heavily distorted by negative fluctuations of baseline from the both ends of the spectrum. The monotonous elevation of the background signal is more pronounced for the aged sample than for the freshly spiked specimen, which would be consistent with a higher presence of the same unidentified form of soluble Pu in the aged sample. However, according to LSC analysis, concentrations of total soluble Pu in these samples amounted to 0.027 μM and 0.016 μM for fresh and aged samples, respectively. These levels of concentrations are well below detection limits for Pu(VI) and Pu(V). Therefore, the presence of neither Pu(VI) nor Pu(V) could be established by these spectra even in a hypothetical case of 100% conversion of Pu(IV) to any of these oxidation states. In addition, no reliable spectrum of a Pu(IV) dissolved species was observed.

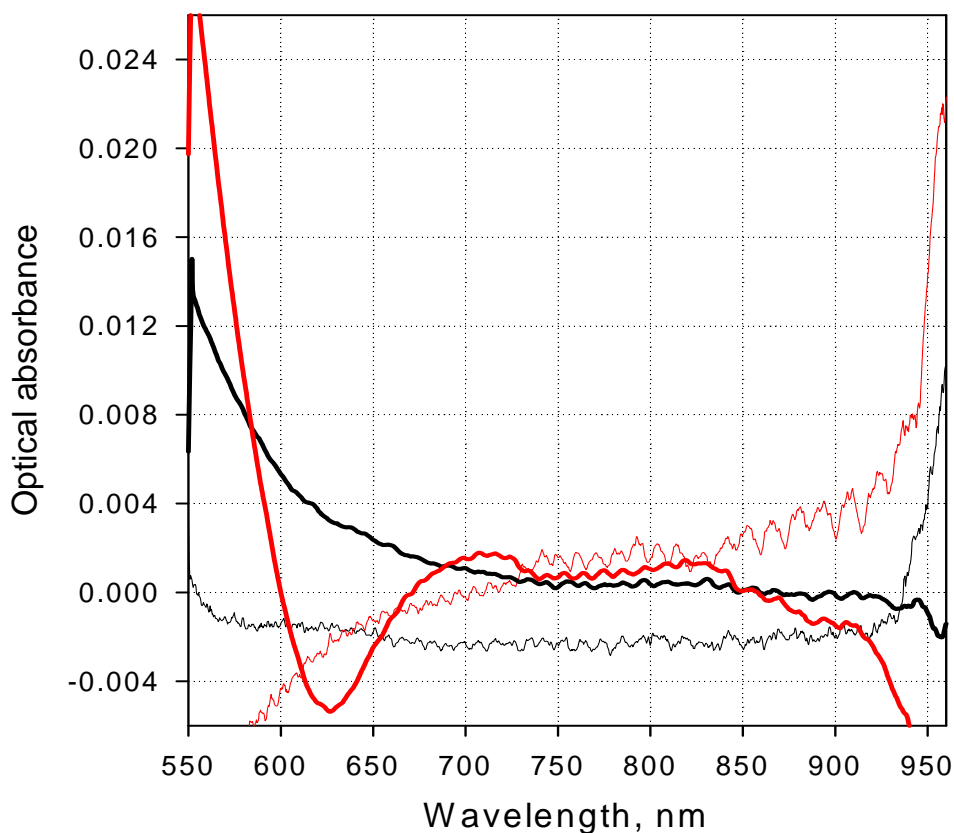


Figure 3.26. Pu(IV) Spectra in 0.25 M NaOD for Freshly Spiked (bold black trace, 0.027 μM of total Pu) and 3-Day-Old Solution (bold red trace; 0.016 μM of total Pu). Thin black and red traces represent the spectra of blank solutions (0.25 M of NaOD before injection of Pu-containing samples).

3.6.4 Pu(IV) Speciation and Solubility in 0.25 M NaOD in the Presence of Carbonate

Carbonate is known as a strong complexing agent for tetravalent plutonium (Lierse and Kim 1986; Clark et al. 1995; Yamaguchi et al. 1994; Rai et al. 1999; Neck et al. 2007). Its presence in a weakly alkaline medium (0.01 M KOH) starting from 0.1 M of carbonate was reported to enhance the solubility of Pu(IV) many orders of magnitude up to 0.003 m in a 6.2 m K_2CO_3 solution. At this high concentration, the carbonate complex of Pu(IV) was characterized by a number of techniques (including optical absorbance spectroscopy) and proved to have five carbonate ions coordinated around a metal center: $\text{Pu}^{\text{IV}}(\text{CO}_3)_5^{6-}$ (Clark et al. 1995). The same species predominates in a concentrated solution of bicarbonate (1.04 m of KHCO_3). At a lower carbonate concentration, the stoichiometry and the spectral features of mixed hydroxy-carbonate complexes of Pu(IV) could not be established because of an insufficient concentration of these species. Solubility curve analysis using a thermodynamic model developed by Rai and co-workers indicated that just one hydroxyl-carbonate species of Pu(IV) of the 2:2 stoichiometry $[\text{Pu}(\text{OH})_2(\text{CO}_3)_2]^{2-}$ needs to be included in the model in addition to the limiting pentacarbonate complex to explain the observed solubility behavior of $\text{PuO}_2(\text{am})$ in bicarbonate systems. However, the same two-species model did not describe adequately the solubility curve of Pu(IV) in a carbonate solution at a carbonate concentration less than 1 m. This discrepancy indicated that additional species are needed to better fit the carbonate data. Yamaguchi et al. determined the solubility of $\text{PuO}_2(\text{am})$ in relatively low ionic strength solutions (0.1 M) at total carbonate concentrations of < 0.1 M and at pH values ranging from 9.4 to 13.0. The authors interpreted their data assuming the formation of $\text{Pu}(\text{OH})_2(\text{CO}_3)_2^{2-}$ in the bicarbonate region and the formation of $\text{Pu}(\text{OH})_4(\text{CO}_3)_2^{4-}$ in the carbonate region. However, these species were found to exist at concentrations too low to be verified by spectroscopic techniques.

For oxidative alkaline leaching that was proposed for chromium dissolution from Hanford tank sludges, carbonate is not considered as one of the intentionally added chemicals to the leaching solution, but it can be present in solution as an impurity or contributing component in sodium hydroxide, or it can accumulate in leaching solutions and leachates upon their exposure to an ambient air atmosphere with ~ 300 ppm of CO_2 . Therefore, in this project, the effect of carbonate on the solubility and speciation of Pu(IV) was studied at a constant concentration of NaOD at 0.25 M and a variation of carbonate concentration from 0 to 0.25 M. Solutions were prepared in duplicate with the first series spectrally measured 10 minutes after adding Pu(IV) acidic stock to the excess of NaOD+ Na_2CO_3 . The second series was measured 3 days after Pu introduction to the solutions. Acidic Pu(IV) was added to achieve a Pu concentration at the 9 μM in case all added Pu should remain in alkaline solution. Both experiments were conducted under aerobic conditions. Concentrations of soluble Pu in these solutions were determined by LSC analysis after acidification of the filtered samples with an HCl excess immediately after the spectral measurement. The spectral data are shown in Figure 3.27, and the solubility data are plotted in Figure 3.28. The freshly prepared and measured series [plot a)] does not show any peak-like spectral features regardless of the carbonate concentration except the previously observed monotonous increase of optical absorbance in the short-wavelength range of the spectrum. The solubility of Pu shows a modest enhancement at increasing carbonate levels (from 0.027 μM in carbonate-free solution to 0.14 μM in 0.25 M Na_2CO_3). The magnitude of the spectral elevation at 560 nm does not correlate with total soluble Pu levels in these series. No spectral features of Pu(V) and Pu(VI) previously established in mixed hydroxy-carbonate media can be distinguished in this spectral set regardless of carbonate level.

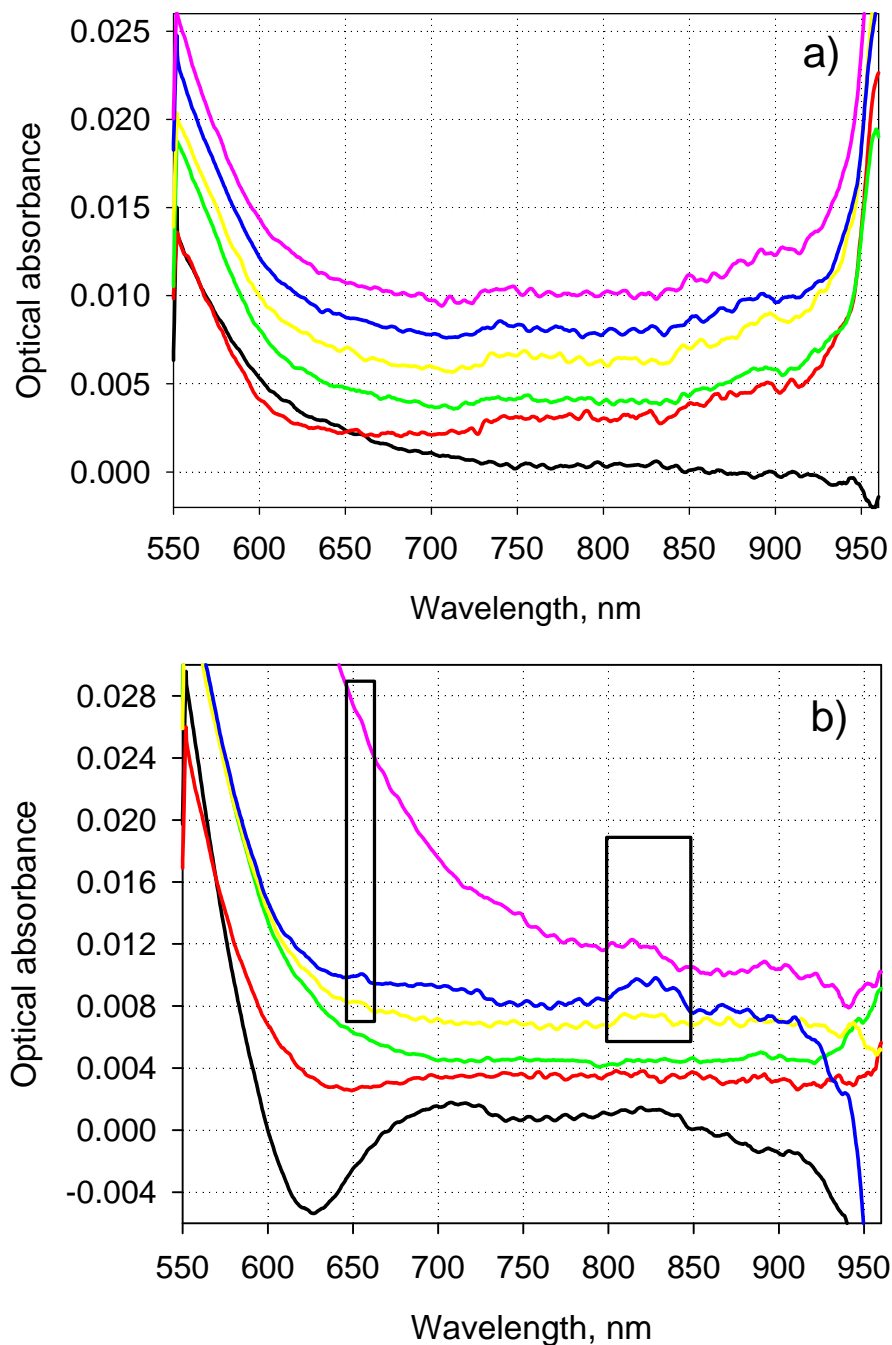


Figure 3.27. Pu(IV) Spectra in 0.25 M NaOD in the Presence of Carbonate. Freshly prepared series a); 3-day-old series b). Carbonate concentration is 0-, 0.05-, 0.10-, 0.15-, 0.20-, and 0.25-M black, red, yellow, green, blue, and pink spectral traces, respectively. The expected initial concentration of Pu(IV) is 9 μ M assuming all added Pu remains in solution. Black rectangular frames in plot b) show regions of weak spectral features at 653 nm and 825 nm.

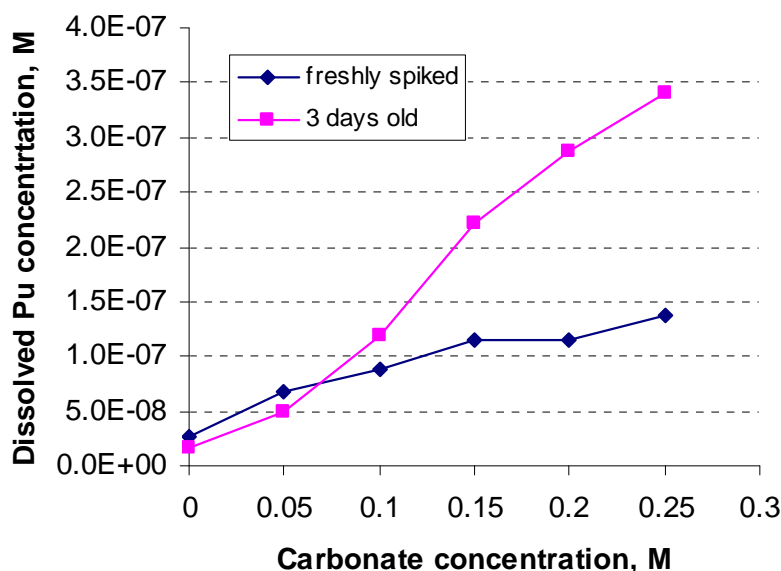


Figure 3.28. Effect of Carbonate on the Solubility of Pu(IV) in 0.25 M NaOD

The 3-day-old series of Pu(IV) solutions showed somewhat different data, both spectrally and in terms of the concentration of soluble Pu. The first three levels of carbonate concentration [0, 0.05, and 0.10 M with black, red and green spectral traces, respectively, in plot b)] did not produce any new spectral features compared with featureless spectra of these solutions observed in the freshly spiked series. The only spectral difference between freshly spiked and 3-day-old spectra for these carbonate concentrations is a more pronounced monotonous increase of optical absorbance in the short wavelength range of the spectrum. Solubility data (Figure 3.28, first three points in the pink curve) indicate that only at 0.10 M of carbonate, the total concentration of soluble Pu increased about 35% compared with a freshly prepared sample of the same composition. At lower carbonate concentrations, an opposite effect was observed, which can be explained by aging of initially fresh $\text{Pu}(\text{OH})_4$ solid.

At higher carbonate concentrations [0.15, 0.20, and 0.25 M with yellow, blue, and pink spectral traces, respectively, in plot b)], weak but sufficiently distinct peaks at 653 ± 1 nm and 823 ± 3 nm can be identified on the spectra. These peaks' positions are in good correspondence with the spectra of Pu(V) in 0.25 M of NaOD with an increasing concentration of carbonate [Figure 3.20, plot a)]. The 823-nm peak intensity in the blue spectrum (0.20 M of CO_3^{2-}) has an approximate net intensity of 0.002 ± 0.0004 absorbance units. If it is assumed that the mixed hydroxy-carbonate complex of Pu(V) is the only species that accounts for the total dissolved Pu concentration in this solution (0.29 μM), then the expected peak intensity should amount to $0.04 \times 0.29 / 14.3 = 0.0008$ absorbance units [0.04 is net peak intensity of Pu(V) complex shown in Figure 3.20 a) at a 14.3 μM concentration of Pu(V)]. Therefore, the observed magnitude of the $\text{Pu}^{\text{V}}(\text{OD})_x(\text{CO}_3)_y$ complex absorbance is ~ 2.5 times higher than can be predicted from the molar absorptivity observed in the mixed complex study (Section 3.5.3). The reason for this discrepancy is difficult to understand unless the tenuous assumption is made that the molar absorptivity of the mixed hydroxyl-carbonate complex of Pu(V) increases at lower concentrations of Pu(V).

The data on Pu(IV) solubility in a mixed NaOD- Na_2CO_3 medium were plotted in a log-log scale and analyzed in terms of the slope of this dependence (the plot is not shown). Originally, this treatment was applied by Yamaguchi and co-workers who studied the solubility of Pu(IV) in aqueous carbonate solution

at pH 9 to 10 (bicarbonate region) and at pH 12 and 13 (carbonate region). Their measured solubility of Pu(IV) for the higher pH region was found to be proportional to the square of the carbonate concentration (slope = 2 in the log-log plot), which was sufficient in their opinion to conclude that the predominant soluble species of Pu(IV) had the following composition: $\text{Pu}(\text{OH})_4(\text{CO}_3)_2^{4-}$. The similar treatment applied to the present work data returned the following values of the slope: 0.45 ± 0.03 ($R^2 = 0.983$) for the freshly spiked series and 1.24 ± 0.07 ($R^2 = 0.989$) for the 3-day-old series. Caution should be exercised in the attempt to derive the mixed complex stoichiometry from these slopes. The 3-day-old series cannot be analyzed this way because of the significant presence of Pu(V) in solution. The fresh series was measured quickly enough to minimize Pu(IV) to Pu(V) oxidation, but a significant variation of the ionic strength as a function of the sodium-carbonate concentration at a constant level of 0.25 M of NaOD (from 0.25 M to 1 M) may distort the real stoichiometry because the assumption of the steady value of the equilibrium constant for the mixed complex formation under these conditions was not valid. Nevertheless, the similar value of the fractional slope was derived by the author of this study from the recently published report on the solubility of $\text{ThO}_2 \cdot x\text{H}_2\text{O}(\text{am})$ in a carbonate solution at $[\text{OH}^-] = 0.1$ M (Altmaier et al. 2005). The solubility of Th derived from one of the plots in that publication was estimated to be $10^{-8 \pm 0.5}$ M, $10^{-8.2 \pm 0.3}$ M, and $10^{-8.4 \pm 0.3}$ M at carbonate concentrations of 0.1 M, 0.04 M, and 0.015 M, respectively (closed-system experiment). These data allow the slope value of 0.47 to be derived, formally corresponding to less than one carbonate ion per Th ion in the mixed complex formula, but in terms of the speciation diagram, this represents an equilibrium between $\text{Th}(\text{OH})_4^0$ and $\text{Th}(\text{OH})_4\text{CO}_3^{2-}$. Excellent correspondence between the slope value obtained by Altmaier and colleagues (2005) for the redox stable Th(IV) and the respective parameter found in this study for the freshly prepared Pu(IV) solubility series in 0.25 M NaOD + Na_2CO_3 indicates that soluble Pu(IV) in our experiments did not get oxidized to any significant extent to more soluble Pu(V).

A recent solubility study of Pu and Am in alkaline salt solutions representative of SRNL tank waste (Rudisill et al. 2004) identified hydroxide and carbonate as the two most significant factors determining the Pu solubility in these six-component media containing also aluminate, sulfate, nitrate, and nitrite as their sodium salts. The functional dependence established in that study can be expressed as follows:

$$[\text{Pu}] = -7.48 \times 10^{-8} + 1.2 \times 10^{-6} [\text{OH}^-] + 4.9 \times 10^{-6} [\text{CO}_3^{2-}] \quad (3.2)$$

The derived coefficients are valid for OH^- and CO_3^{2-} concentrations expressed in molar scale. This relationship was established using experimental points in the range of 0.45 to 15 M of NaOH and of 0.001- to 0.95 M CO_3^{2-} concentrations, and it is based on solubility data obtained from 40 to 90 days of equilibration. It is of interest to test the predictive power of this equation for conditions used to determine the solubility of Pu in the test described in this section (i.e., a constant level of 0.25 M NaOD and variable carbonate). Table 3.5 compares predicted values with experimentally-determined solubilities.

Comparing predicted and actually observed solubilities shows that the SRNL model overestimates Pu solubilities observed in this work for freshly spiked series by a factor of 8.8 ± 1.4 (the average number and standard deviation for all six points). It should be mentioned again here that the SRNL equilibration times (40 to 90 days) were much longer than those used in this work, which, on the one hand, should produce Pu(IV) hydrous oxide with a higher degree of microcrystallinity and, hence, a lower concentration of soluble Pu(IV) in equilibrium with $\text{PuO}_2 \cdot x\text{H}_2\text{O}$. On the other hand, longer equilibration times should allow a slow Pu(IV) oxidation by dissolved oxygen to proceed to a much higher extent, resulting in significant conversion of poorly soluble Pu(IV) to more soluble Pu(V). Comparing the

freshly spiked series with the 3-day-old series indicates that the rate of this reaction increases in the presence of higher levels of carbonate. This conclusion is based on comparing the model overestimation factors for the first three levels of carbonate (9.8 ± 3.9) with the last three experimental points (4.3 ± 0.1). More experiments in more detail are needed to examine the kinetics of Pu(IV) to Pu(V) conversion at various levels of hydroxide and carbonate.

Table 3.5. Comparison of Experimentally Determined Solubilities of Pu in Mixed Hydroxy-Carbonate Medium at Constant Level of 0.25 M NaOD/D₂O with Predictions of the SRNL Pu Solubility Model (Rudisill et al. 2004)

Carbonate, M	Pu _{predicted} , μM	Pu _{fresh} observed, μM	Pu _{fresh} /Pu _{predicted}	Pu _{3 days old} observed, μM	Pu _{3 days old} / Pu _{predicted}
0	0.225	0.0268	0.119	0.0163	0.072
0.05	0.470	0.0669	0.142	0.0491	0.104
0.10	0.715	0.0886	0.124	0.119	0.166
0.15	0.960	0.0115	0.120	0.221	0.230
0.20	1.21	0.115	0.095	0.288	0.239
0.25	1.45	0.138	0.095	0.340	0.235

In summary, we believe that our experimental data represent the solubility of Pu(IV) in equilibrium with freshly precipitated PuO₂ · xH₂O more correctly than can be assessed through the SRNL model prediction, which produces highly overestimated values presumably because of the significant conversion of Pu(IV) to Pu(V).

3.7 Oxidative Dissolution of Pu(IV) Hydroxide Suspension by Permanganate and Manganate in 0.25 M NaOD

3.7.1 Oxidative Dissolution of Pu^{IV}(OH)₄ Suspension by NaMnO₄ in 0.25 M NaOD

The Pu(OH)₄ solid was prepared by neutralizing the Pu(IV) solution in nitric acid with a slight excess of the 0.25 M NaOD solution. The brown-greenish precipitate was formed immediately after neutralization and aged under the mother liquid for 3 days. The amount of Pu(OH)₄ used in the oxidative leaching experiments was controlled volumetrically by sampling out a known volume of continuously stirred suspension [with a formal Pu(IV) concentration of 4.5 mM] and delivering it to a reaction vessel containing oxidizer.

The first experiment was performed in a 0.25 M NaOD medium at 3.38-fold molar excess of permanganate with respect to Pu. In earlier experiments on permanganate stability in alkaline solutions, it was observed that permanganate undergoes a slow reduction to manganate in the process of spectrophotometric monitoring when the solution is in contact with a plastic wall of a 1-cm spectrophotometric cell. Therefore, to make a distinction between permanganate consumption in the process of Pu(IV) oxidation to Pu(V) or Pu(VI) and permanganate decomposition by water and/or plastic material of the cell, a control experiment was run in parallel with the Pu-dissolution experiment. Both experiments were started at the same time by placing equal portions of 0.2 mM NaMnO₄ solution in 0.25 M NaOD into two identical spectrophotometric cells equipped with Teflon stir bars and taking the spectra

of these identical solutions (spectral traces 00 in the Figure 3.29). At time zero, an aliquot of $\text{Pu}(\text{OH})_4$ suspension was added to one of the cells, and stirring was continued for 5 minutes before the first spectral measurement with Pu present. Both cells were returned to the stirrer, and stirring continued for another 5 minutes before the next spectral scan. No centrifugation or filtration was applied to separate unreacted $\text{Pu}(\text{OH})_4$ before spectrophotometric measurements. In total, 12 spectral scans were taken with hot and cold samples before taking an aliquot of hot solution for filtration and LSC analysis to determine the concentration of dissolved Pu. The spectral data are shown in Figure 3.29. The cold series (shown in green color) is plotted as is, while the hot series (red color) is upshifted by 0.175 absorbance units for clarity.

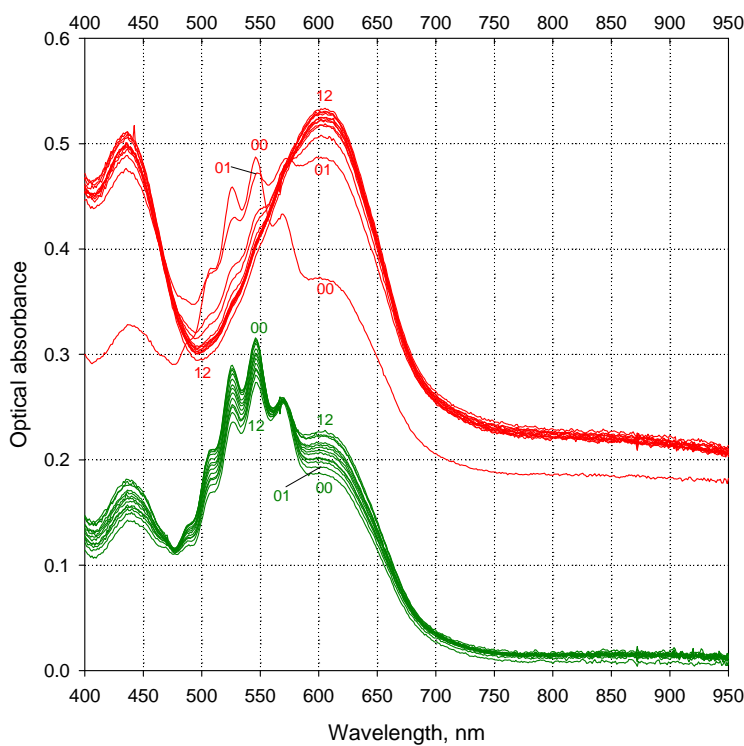


Figure 3.29. Spectral Monitoring over Mn(VII) Conversion to Mn(VI) in the Presence of Added $\text{Pu}(\text{OH})_4$. Green series: control experiment without $\text{Pu}(\text{OH})_4$; red series: identical solution and volume of 0.2 mM Mn(VII) after addition of 30.1 μg of Pu (as metal) in a form of $\text{Pu}(\text{OH})_4$ (solid). The red series is upshifted by 0.175 absorbance units for clarity. The molar ratio of permanganate to plutonium is set to 3.38:1. Time intervals between consecutive spectral scans within each series are 7.5 ± 0.5 minutes.

Qualitatively, the hot sample changed its color from purple-gray to green-gray very quickly in the first 5 to 6 minutes after Pu addition, whereas no appreciable color changes were noticed for the cold sample. Spectrally, this difference can be illustrated by comparing 00 and 01 spectra in both series. It can be seen that significant conversion of Mn(VII) to Mn(VI) occurred within the first few minutes after introducing a suspension of Pu(IV) hydroxide. Subsequent measurements showed a relatively quick additional conversion of the remaining Mn(VII) to Mn(VI) in the hot sample with a solution color change to purely green in the first 60 to 70 minutes. In the case of a hypothetical conversion of Pu(IV) to Pu(VI), one equivalent of Pu should reduce 2 equivalents of Mn(VII) or, in other words, the consumption of Mn(VII)

should stop when all Pu(IV) gets dissolved. On the other hand, if the final oxidation state of Pu in solution is Pu(V), then 1:1 reaction stoichiometry is expected. In reality, however, more than 2 equivalents of Mn(VII) were consumed at the moment of the last spectral scan [red trace #12 shows not less than 95% of Mn(VII) converted to Mn(VI), which is the equivalent of $0.95 \times 3.38 = 3.2$ molar equivalents of Mn(VII) spent per one equivalent of Pu(IV) added]. The possibility of Pu(IV) oxidation to Pu(VII) can be excluded at such low alkalinity. Therefore, the experimentally observed superstoichiometric consumption of permanganate indicated another possible pathway of its decomposition via catalytic reduction by water in the presence of unreacted Pu(OH)₄ solid. This possibility was confirmed by LSC analysis, which showed only 53% of total Pu dissolved in 2.3 hr since Pu introduction.

Both samples were stirred for several more days with only occasional spectrophotometric monitoring. Two more samples were taken for determination of dissolved Pu in solution 1 day and 4 days after the beginning of this experiment. According to LSC data, the fraction of the dissolved Pu dropped down from 53% to 49% for the “1-day-after” sample and further to 38% for the “4-day-after” sample. This decreasing trend in concentration of leachable Pu qualitatively correlated with a progressive accumulation of dark brown precipitate of MnO₂ in the hot sample, which likely acted as a precipitating agent for initially soluble Pu(V) or Pu(VI) under these conditions.

In summary, this experiment did not provide sufficient data to establish the stoichiometry of permanganate consumption to distinguish between Pu(V) (expected 1:1 Pu:Mn(VII) molar ratio) and Pu(VI) (expected 1:2 Pu:Mn(VII) ratio) as the final oxidation state of Pu in the leachate.

For the second experiment, it was decided to generate Pu(OH)₄ directly in the oxidizer-containing solution by adding a small amount of acidic Pu(IV) solution to an excess of the alkaline solution of NaMnO₄. The idea of this experiment was to minimize catalytic decomposition effects of permanganate by solid Pu^{IV}(OH)₄ particles to calculate the stoichiometry of permanganate consumption in the process of Pu(IV) oxidation. The approach was to prepare freshly hydrolyzed Pu(IV) hydroxide in the same solution where permanganate was already present. This was achieved by spiking a tiny volume of relatively concentrated acidic Pu(IV) solution in 1 M DNO₃ into a much larger volume of 0.2 mM of NaMnO₄ in 0.25 M of NaOD/D₂O. The estimated perturbation of the alkalinity level of the initial 0.25 M NaOD solution was less than 4%. The calculated concentration of Pu in solution in the case of 100% solubilization was 18.9 μM (three times less than in the previous experiment). In terms of other experimental details (application of cold solution as control, solution stirring mode, frequency of spectral data acquisition), this experiment was identical to the first one described above. The spectral data from this run are shown in Figure 3.30. Again, as in the previously observed case, adding Pu results in a much more noticeable in-growth of Mn(VI) compared with the control (see spectral traces 00 and 01 in both series). Further spectral changes in the hot sample indicate a practically complete conversion of Mn(VII) to Mn(VI) in the time frame of spectral monitoring (2.3 hr). This fact indicates that the effect of catalytic decomposition of Mn(VII) by Pu(IV) or its oxidation products could not be completely eliminated even with freshly formed Pu(IV) hydroxide.

LSC analysis indicated that 81% (15.3 μM) of total Pu spiked into solution was found in dissolved form after spectral scan #6 (~ 1 hour of contact time), and 76% was found after spectral scan #12 (2 hr of agitation). By comparing the peak intensities of manganate at 603 nm for spectral scans #00 and #06, the concentration of permanganate consumed in contact with Pu(VI) can be estimated as 45 μM.

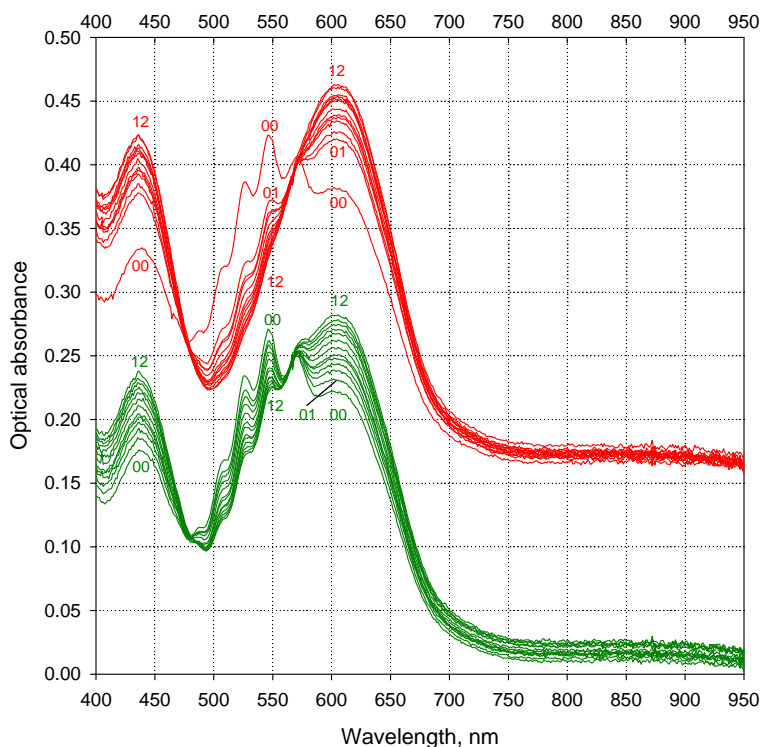


Figure 3.30. Spectral Monitoring over Mn(VII) Conversion to Mn(VI) in the Presence of *in situ* Generated Pu(OH)₄ in Alkaline Solution of Mn(VII). Green series: control experiment without Pu(OH)₄; red series: identical solution and volume of 0.2 mM of Mn(VII) after adding 12.6 µg of Pu in the form of Pu(IV) nitrate in 4 M of DNO₃. The red series is upshifted by 0.15 absorbance units for clarity. The molar ratio of permanganate to the total plutonium added is set to 10.5:1. Time intervals between consecutive spectral scans within each series are 7.5 ± 0.5 minutes.

Thus, the calculated molar ratio of Mn(VII) consumption to soluble Pu generation is found to be 45:15.3 = 3:1. This ratio is 50% higher than the expected 2:1 ratio in the case of Pu(IV) oxidation to Pu(VI) and 3 times higher than the anticipated 1:1 ratio for the hypothetical case of Pu(IV) oxidation to Pu(V). Excessive consumption of permanganate might be related to its catalytical decomposition by the remaining 19% of undissolved Pu present in solution (most likely in the form of Pu(OH)₄).

At this stage, it can be concluded that the data obtained provide more support for Pu(VI) as the final oxidation state of leachable Pu in the presence of excess manganate and residual permanganate in solution. A detailed discussion of the possibility of Pu(V) coexistence with manganate in the same solution will be given later in Section 3.9.

After the stoichiometry of the Pu(IV) reaction with Mn(VII) was established, one more experiment with Pu(OH)₄ solid was performed. In this experiment, oxidative leaching of Pu(OH)₄ was studied as a function of the oxidizer concentration at three different levels of permanganate. For each level of Mn(VII), the kinetics of Pu solubilization was measured in a more systematic way with a sampling

frequency of 15 minutes. The amount of $\text{Pu}(\text{OH})_4$ taken for dissolution was sufficient to create Pu concentration in solution at $31\ \mu\text{M}$ in the case of complete dissolution of the starting compound. No spectral measurements were conducted in this series. The results are shown in Figure 3.31.

The data presented show that **a)** the kinetics of this process is relatively fast with no statistically significant changes in the concentration of leached Pu observed after the fourth kinetic point (60 minutes after $\text{Pu}(\text{IV})$ addition; **b)** the extent of Pu solubilization is a sensitive and non-linear function of the initial concentration of permanganate in solution.

The lowest level of $\text{Mn}(\text{VII})$ used in this experiment ($0.19\ \text{mM}$) was tested earlier for leaching $\text{Pu}(\text{OH})_4$ at the same alkalinity. Earlier data revealed a progressively higher leaching efficiency of Pu from its hydroxide (53% in the very first experiment, and then 39% in the next experiment 8 days after). This data scattering for the same initial concentration of the oxidant becomes more understandable after taking into account the age of the $\text{Pu}(\text{OH})_4$ at the day of run of each experiment. In the very first test with 53% dissolution, the extent of $\text{Pu}(\text{OH})_4$ suspension was 3 days old; in the second test, it was 11 days old, and in the last test with 16% of Pu leached, the age of the suspension increased to 17 days. Apparently, the $\text{Pu}(\text{OH})_4$, which was stored under mother liquid, underwent slow transformation from a completely amorphous material to a substance with a higher degree of microcrystallinity, and this process determined the progressively increased resistance of the $\text{Pu}(\text{IV})$ phase in each subsequent oxidative-leaching experiment. For future studies, it would be desirable to prepare $\text{Pu}(\text{OH})_4$ well in advance of oxidative-leaching testing and accelerate its aging process by digesting the precipitate at a elevated temperature for several weeks. This treatment should minimize time drift in its degree of aggregation and microcrystallinity for different experiments.

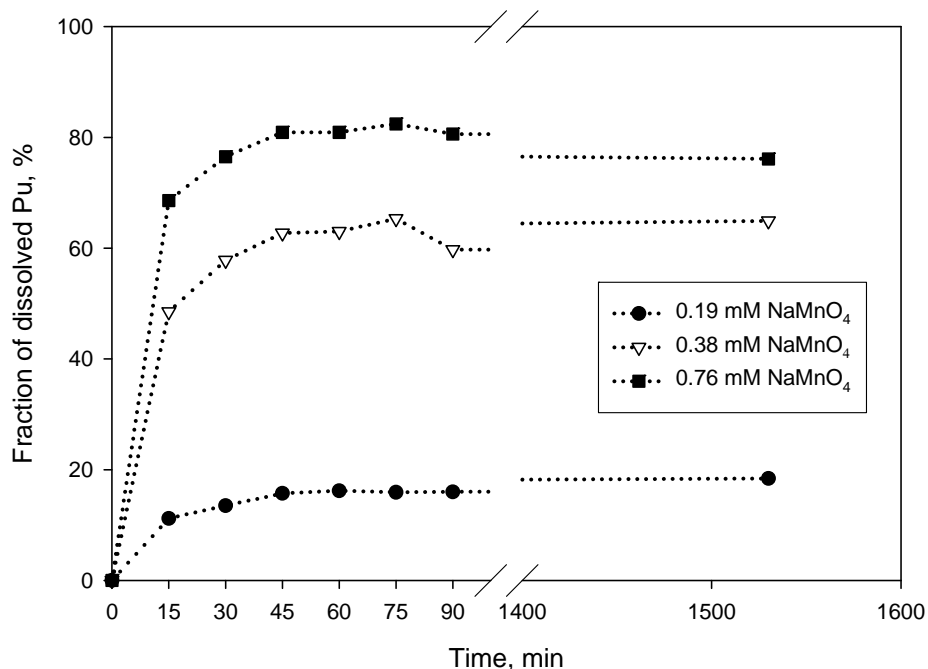


Figure 3.31. The Kinetics of Oxidative Dissolution of $\text{Pu}^{\text{IV}}(\text{OH})_4$ Suspension in a Series of NaMnO_4 Solutions in $0.25\ \text{M}$ of $\text{NaOD}/\text{D}_2\text{O}$ at Three Levels of Permanganate. The $\text{Mn}(\text{VII})$ to

Pu(IV) molar ratio is 6:1, 12:1, and 24:1 for 0.19-mM, 0.38-mM, and 0.76-mM concentrations of Mn(VII), respectively.

In the very first leaching experiment (with 53% dissolution efficiency of Pu(OH)₄ achieved in 2 hr), it was found that the level of soluble Pu decreased with time from 32 μM to 29 μM and further to 23 μM in 1 day and 4 days, respectively. Two alternative possibilities were considered to explain this negative drift. First, the 32 μM concentration of leached Pu might be close enough to the solubility of Pu^{VI}O₂(OH)₂ under these conditions of moderate alkalinity and with time that the level of Pu(VI) concentration decreased because of a decrease in the solubility product of Pu(VI) hydroxide. Second, the increasing amount of MnO₂ might be slowly formed in the Pu(VI)-containing leachate with time as a result of manganate decomposition at this alkalinity. The MnO₂ is known to be an efficient adsorbent for Pu(VI) in a weakly alkaline medium at pH <10 (Reilly et al. 2003). It is possible that this compound can co-precipitate Pu(VI) in solution at a 0.25 M NaOD concentration used in this study.

To test the first possibility, an additional experiment was performed in which sodium carbonate was added to the leaching solution of 0.2 mM NaMnO₄ in 0.25 M NaOD. Carbonate is known as a strong complexing agent for Pu(VI) in alkaline medium, which should significantly enhance the solubility of Pu(VI) hydroxide and eliminate possible oversaturation conditions for this compound. Three different levels of carbonate addition were tested for the same Mn(VII) concentration: 0 M, 0.125 M, and 0.25 M. The Pu concentration (if fully dissolved) was set at 31 μM, and the permanganate concentration (initial) at 0.750 mM with a Mn(VII)-to-Pu(IV) molar ratio at 25 to 1. The results of this experiment are shown in Figure 3.32. No effect of the presence of carbonate on kinetics and the extent of dissolution of Pu(OH)₄ was observed. In all three cases, 65 to 75% of the Pu was dissolved after a 1-hr contact time with stirring. Overnight exposure of the remaining Pu(OH)₄ under the same solutions (no stirring) resulted in complete conversion of permanganate to manganate (solutions turned green), but the extent of dissolution of plutonium hydroxide did not increase. After 3 days of observation, all three solutions remained equally green and homogeneous with no colloidal MnO₂ visibly formed. After approximately 1 week of observation, it was qualitatively noted that the presence of carbonate had no effect on manganate stability (green color of manganate faded away to the same extent in all three samples).

Therefore, this experiment led to the conclusion that the drop in Pu(VI) concentration with time is not related to the limited solubility of Pu(VI) hydroxide in the 20- to 30-μM range of Pu(VI) concentration.

3.7.2 Oxidative Dissolution of Pu^{IV}(OH)₄ Suspension by Sodium Manganate in 0.25 M NaOD

It was of interest to examine the dissolution behavior of Pu(OH)₄ in an alkaline solution of sodium manganate. The reduction potential for Mn(VI)/Mn(IV) in 1 M NaOH is +0.62 V (Nash et al. 2005); hence, thermodynamically, it is as powerful an oxidizer as permanganate.

A sodium manganate solution was produced by the spontaneous conversion of Mn(VII) to Mn(VI) while storing permanganate solution in a plastic cell overnight. Approximately 10% of the manganate anion was found reduced to colloidal MnO₂. Therefore, the solution was not perfectly homogeneous at the moment of Pu(OH)₄ addition to it. The amount of Pu(OH)₄ added (30.1 μg as elemental Pu) was sufficient to achieve a concentration of dissolved Pu in solution at 59 μM in the case of complete dissolution. The manganate to Pu molar ratio was set at 3:1 for this experiment. Spectral data are presented in Figure 3.33.

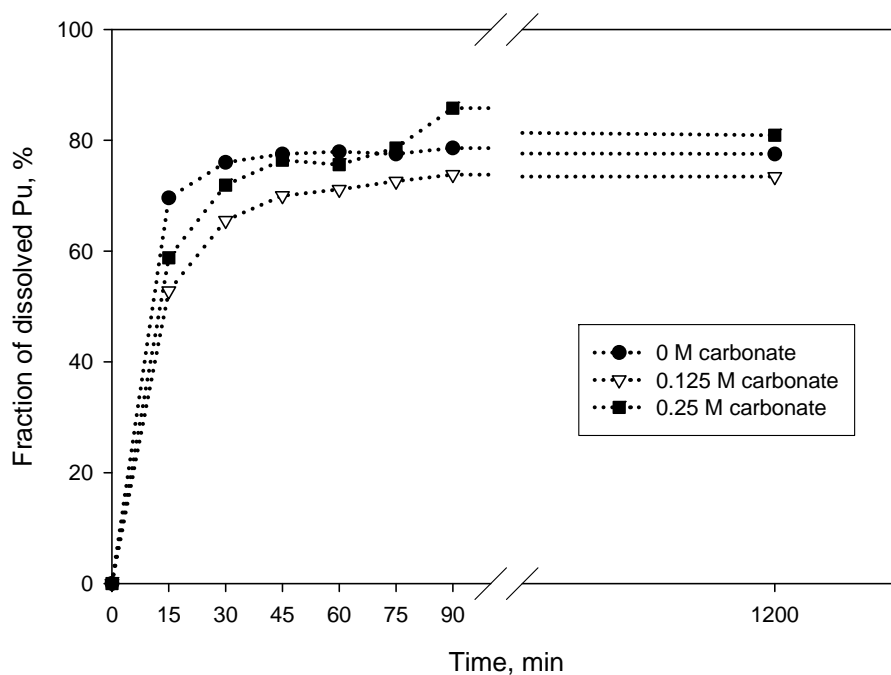


Figure 3.32. The Effect of Carbonate Concentration on the Kinetics of Oxidative Dissolution of $\text{Pu}^{\text{IV}}(\text{OH})_4$ Suspension in a Series of NaMnO_4 Solutions in 0.25 M $\text{NaOD}/\text{D}_2\text{O}$ at 0.75 mM of Permanganate. The $\text{Mn}(\text{VII})$ to $\text{Pu}(\text{IV})$ molar ratio is 25:1.

A significant baseline shift of the $\text{Mn}(\text{VI})$ spectrum after adding $\text{Pu}(\text{OH})_4$ (spectral traces 00 and 01 in the red series) is an indication of increased turbidity as a result of the light-scattering from fine solid plutonium hydroxide particles. Both series showed a gradual decomposition of manganate, but in the presence of $\text{Pu}(\text{OH})_4$, this process occurred with a significantly faster rate (compare residual magnitude of manganate peak for spectral traces #12 in both series). Assuming that the oxidation of $\text{Pu}(\text{IV})$ proceeds to $\text{Pu}(\text{VI})$ and the $\text{Mn}(\text{VI})$ reduction proceeds to $\text{Mn}(\text{IV})$, the 1:1 stoichiometry of the oxidative dissolution reaction is expected, which should leave 2 equivalents of $\text{Mn}(\text{VI})$ in solution in case of complete dissolution of $\text{Pu}(\text{VI})$. A tentative estimate of $\text{Mn}(\text{VI})$ consumption in the presence of $\text{Pu}(\text{OH})_4$ based on the $\text{Mn}(\text{VI})$ peak magnitude analysis (red trace #12) indicates that ~ 0.85 equivalents of manganate were consumed 1.75 hr after $\text{Pu}(\text{IV})$ hydroxide introduction. However, LSC analysis of the solution sample taken shortly after spectral scan #12 showed that only 7% of the total $\text{Pu}(\text{IV})$ added was found in dissolved form. The dissolved Pu fraction increased to 11% and further to 16% after 2 hr and 22 hr of additional agitation. The next-day observation showed that the green color of $\text{Mn}(\text{VI})$ almost faded away in the hot sample and to a much lesser extent in the cold-reference sample with partial formation of brown precipitate of MnO_2 in both samples. A partial decomposition of $\text{Mn}(\text{VI})$ to $\text{Mn}(\text{IV})$, even in the absence of oxidizable components other than water, proves that the 0.25 M hydroxide concentration is too low to maintain long-term stability of $\text{Mn}(\text{VI})$, even at submillimolar concentrations of this oxidant.

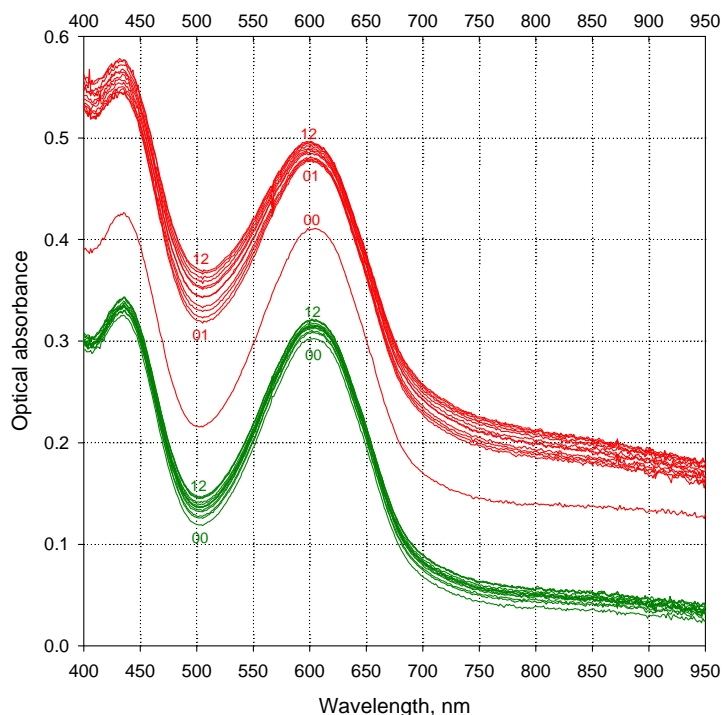


Figure 3.33. Spectral Monitoring over Mn(VI) Consumption in the Presence of Oxidative Alkaline Leaching of $\text{Pu}(\text{OH})_4$ in 0.25 M NaOD. Green series: control experiment without $\text{Pu}(\text{OH})_4$; red series: identical solution and volume of 0.18 mM Mn(VI) after adding of $\text{Pu}(\text{OH})_4$ (with a Pu metal content of 30.1 μg). The red series is upshifted by 0.1 absorbance units for clarity. The molar ratio of permanganate to plutonium is set to 3:1. Time intervals between consecutive spectral scans are 7.5 ± 0.5 minutes.

In summary, the data obtained demonstrate that manganate is a much less efficient Pu solubilizer from $\text{Pu}(\text{OH})_4$ compared with permanganate under similar conditions of 0.25 M alkalinity and an ~ 3 -fold molar excess of Mn(VI/VII) to Pu(IV).

3.8 Oxidation of Pu(IV) by Permanganate in Acidic Solution

3.8.1 Oxidative Dissolution of Pu(IV) Hydroxide Suspension by Permanganate in 1 M DNO_3

After accumulating data on oxidative dissolution of $\text{Pu}(\text{OH})_4$ with permanganate in 0.25 M NaOD, it was of interest to compare these findings with the oxidative action of Mn(VII) on $\text{Pu}(\text{OH})_4$ in an acidic medium (DNO_3). Such a comparison is not only of purely scientific interest, but was potentially practically important in terms of determining the rate of oxidation of poorly soluble $\text{Pu}(\text{OH})_4$ present as fine suspensions in an initially alkaline solution after acidic strike. The dissolution behavior of Pu(IV) hydroxide was studied at three different levels of permanganate in 1 M of DNO_3 . Spectrophotometric measurement was applied to determine the extent of dissolution of the Pu(IV) phase by detecting the absorbance band intensity of Pu(VI) at 831 nm. Data obtained are plotted in Figure 3.34.

All three kinetic curves show a negative curvature for the first 30 to 45 minutes of reaction time. This kinetic feature was observed earlier (Koltunov 1974, pp. 208-212) in the process of oxidation of monomeric Pu(IV) by permanganate and was attributed by the author to the autocatalytic action of Mn(II) as the reduction product of Mn(VII). The extent of Pu(IV) conversion to soluble Pu(VI) is approximately a linear function of the initial permanganate concentration for each given kinetic point during the first 90 minutes of observation.

Comparing the oxidation kinetics of Pu(OH)₄ by permanganate in an alkaline and acidic medium shows that, for comparable concentrations of Mn(VII) and molar ratios of Mn(VII)/Pu(IV), oxidative leaching in an alkaline medium starts more quickly with more than 60% of the Pu solubilized in the first 15 minutes of contact time as opposed to less than 20% in nitric acid for the same time interval. On the other hand, while the rate of oxidation of Pu(IV) in alkali slows down at longer contact times, and the system reaches equilibrium with ~75% of Pu dissolved after 90 minutes (and no additional dissolution after an overnight exposure), in an acidic medium, this process first accelerates and then slows down a little bit within the 90-min time interval. After that, it slowly goes to completion with practically all of the Pu oxidized and dissolved after an overnight contact time. One of the factors that might be responsible for reaction-rate retardation in alkaline medium is the relatively fast catalytic conversion of permanganate to manganate in the presence of undissolved Pu(OH)₄ (and possibly other particulates, including freshly formed colloidal MnO₂).

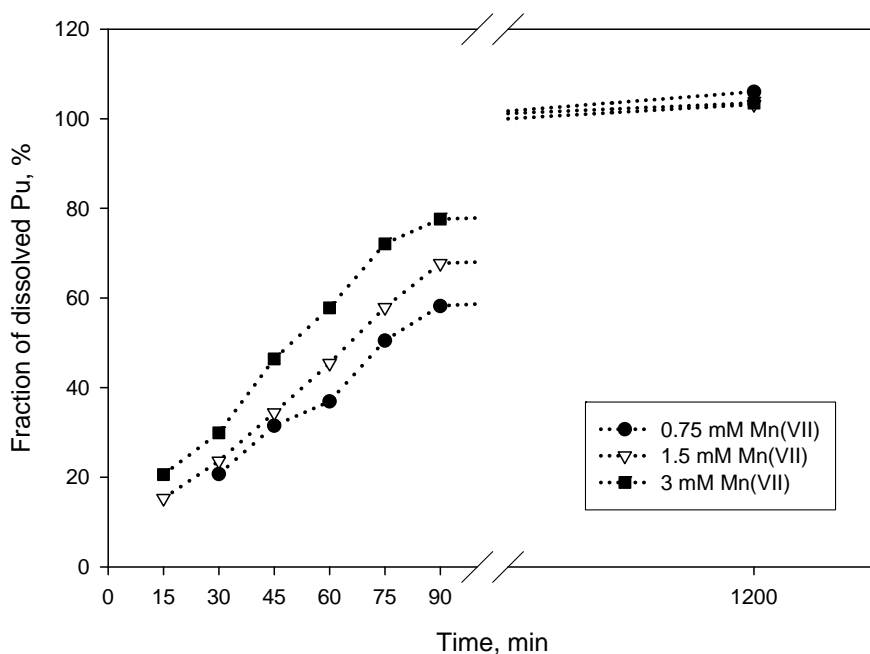


Figure 3.34. The Kinetics of Dissolution of Pu(OH)₄ by Mn(VII) in 1 M DNO₃. The starting Pu(IV) concentration in these tests is 100 μM [based on the amount of Pu(OH)₄ taken for oxidation]. The Mn(VII) to Pu(IV) molar ratio is 7.5:1, 15:1, and 30:1 for series 1, 2, and 3, respectively.

3.8.2 Oxidation of Ionic Pu(IV) by Permanganate in 1 M DNO₃ and the Effect of Dichromate on the Kinetics of this Process

As has been previously discussed in Section 3.6, the spectral identification of Pu(IV) in an alkaline medium is extremely difficult, even with the application of highly sensitive LWCC detection due to the low solubility of tetravalent Pu and the lack of characteristic absorbance bands suitable for direct speciation of Pu(IV). In a real oxidative sludge leach process, if any soluble Pu(IV) survives the oxidative action of permanganate, it would be present in an alkaline solution together with chromate and possibly with unreacted permanganate if the latter were added in excess with respect to Cr(III) phases in the sludge. The detection of Pu(IV) is demonstrated to be much more sensitive on the acid side with a detection limit of less than 30 nM. Therefore, an attempt was made to examine the stability and redox behavior of Pu(IV) in the presence of chromate, permanganate, and their mixture after acidification of an initially alkaline solution containing these components. This series of experiments was conducted by spiking an acidic solution of Pu(IV) into Cr(VI) and/or a Mn(VII) solution in 1 M DNO₃ and using conventional spectrophotometry to monitor the extent of oxidation of Pu(IV) to Pu(VI) by measuring the absorbance band of Pu(VI) at 831 nm. The starting concentration of Pu(IV) was set at 200 μ M and 190 μ M for Mn(VII) and Mn(VII) + Cr(VI) tests, respectively. The concentration of Cr(VI) was set to 7.5 mM of dichromate (equivalent of 15 mM of chromate from alkaline side), and the concentration of permanganate was fixed at 1.5 mM. Two tests were performed with single component oxidizers [Cr(VI) only and Mn(VII) only], and one test was done with the mixture of Cr(VI) and Mn(VII). The results are shown in Figure 3.35. It can be seen that dichromate reacts very slowly with Pu(IV), resulting in less than 10% oxidation efficiency in 1.5 hr. Permanganate acts more quickly with 50% of Pu(IV) oxidized in 30 minutes despite a 5-times-lower concentration compared with dichromate. Again, as was observed in the Pu(OH)₄ + Mn(VII) experiment (Section 3.8.1), the rate of Pu(IV) oxidation initially is slow with subsequent acceleration of the oxidation process. Most interestingly, the oxidation rate of Pu(IV) increases drastically when two oxidizers are mixed together with about 50% of the Pu(IV) converted to Pu(VI) within 3 minutes after mixing the reagents and quantitative conversion in less than 10 minutes. This effect was not previously reported in the technical literature to the best of our knowledge, and its nature cannot be fully explained at this time. One possibility is the formation of a complex reaction between Pu(IV) and dichromate, which makes this new species kinetically less stable toward the oxidative action of permanganate.

In summary, the data obtained indicate that the technique of acidic strike on an initially alkaline Pu-containing solution in the presence of Cr(VI) and Mn(VII) causes significant perturbations of lower oxidation states of Pu with very fast oxidation of Pu(V) by Cr(VI) alone (see Section 3.5.4) and rapid oxidation of Pu(IV) by mixing Cr(VI) and Mn(VII). Consequently, the acidification of an initially alkaline Pu(IV+V+VI) solution with chromate can possibly distinguish between soluble Pu(IV) and Pu(V+VI) only in the absence of Mn(VII).

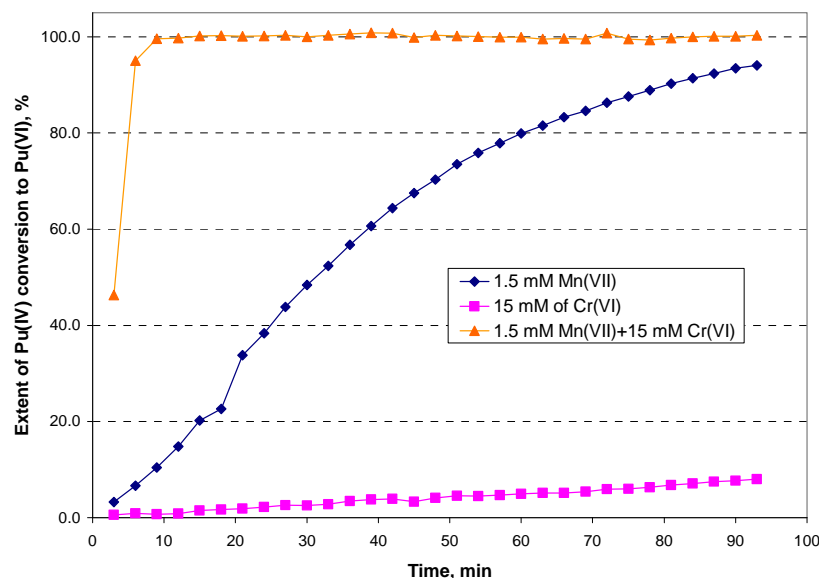


Figure 3.35. The Kinetics of the Oxidation of Monomeric Pu(IV) by Mn(VII), Cr(VI), and Their Mixture in 1 M HNO₃. The initial Pu(IV) concentration was set at 200 μ M for Mn(VII) and 190 μ M for both Cr(VI) only and Cr(VI) + Mn(VII) tests, respectively.

3.9 Interaction of Pu(V) with Low Levels of Manganese in 0.25 M NaOD

3.9.1 ORP Measurements in Manganate-Containing Solutions and Manganate-Permanganate Mixtures in NaOD Solutions

A 2 mM stock solution of manganate was prepared via spontaneous reduction of 2 mM permanganate solution in 2.5 M NaOD. The reaction mixture was stored in a glass container to prevent contact of the solution with any plastic materials. The solution color was observed to change gradually from purple to green. The complete conversion of Mn(VII) to Mn(VI) was achieved in 3 months as confirmed by the absence of absorbance bands of Mn(VII) in the spectrum of the resulting solution. A series of six solutions of 0.2 mM of manganate in 0.25 M, 0.4 M, 0.55 M, 0.70 M, 0.85 M, and 1.0 M of NaOD was prepared by 10-fold dilution of the Mn(VI) stock in NaOD solutions of appropriate concentrations. Oxidation reduction potentials of these solutions were measured according to the procedure described in Section 2.7. After an initial ORP measurement in pure manganate solution was complete, a series of stepwise additions of a 7.5 mM solution of permanganate in D₂O was made to the starting solution to achieve 0.5, 1, 2, and 5 molar ratios of Mn(VII) to Mn(VI). Each addition was followed by ORP measurement of the modified solution before adding the next portion of Mn(VII) to the mixture. The results of these measurements are summarized in Table 3.6.

Table 3.6. Oxidation Reduction Potentials of Manganate Solutions and Permanganate-Manganate Mixtures in NaOD. The Mn(VI) concentration is fixed at 0.2 mM in all solutions.

Mn(VII)/Mn(VI) Molar Ratio	Oxidation Potential, V					
	0.25 M NaOD	0.4 M NaOD	0.55 M NaOD	0.70 M NaOD	0.85 M NaOD	1.0 M NaOD
0 (pure manganate)	0.39	0.39	0.40	0.39	0.38	0.38
0.5	0.50→0.46	0.54→0.51	0.55→0.53	0.55→0.52	0.55→0.53	0.55→0.52
1	0.52→0.50	0.55→0.54	0.56→0.55	0.56→0.54	0.56→0.55	0.56→0.54
2	0.54→0.52	0.57→0.56	0.58→0.56	0.58→0.56	0.58→0.56	0.58→0.56
5	0.57→0.56	0.59→0.58	0.60→0.59	0.60→0.59	0.60→0.59	0.60→0.59

Pure manganate solutions showed stable readings of oxidation potential while permanganate-manganate mixtures exhibited a downward drift of the potential with up to 30 to 40 mV of negative difference between the initial reading (within the first 1 to 1.5 minutes after electrode immersion) and final reading (~10 minutes after). This drift correlated with a gradual color change from gray-purple to green, suggesting a relatively fast reduction of permanganate to manganate by water and walls of a plastic vial used for ORP measurements. We believe that the initial readings represent more accurately the oxidation potentials of permanganate-manganate mixtures due to less significant perturbation of the targeted Mn(VII)/Mn(VI) ratio.

Comparing the measured potentials of permanganate-manganate solutions with the formal redox potential of the Pu(VI)/Pu(V) couple (Section 3.5.5) makes it possible to conclude that thermodynamically, Pu(V) is expected to undergo complete oxidation to Pu(VI) regardless of the Mn(VII)/Mn(VI) ratio in solution.

3.9.2 Instability of Permanganate and Manganate in 0.25 M NaOD at Low Micromolar Concentration of Initially Added Mn(VII) by Spectral Measurements with LWCC

In preliminary experiments on the redox stability of millimolar permanganate solutions in 0.25 M NaOH, it was shown that permanganate is not stable in alkaline solution. It slowly (within hours) gets partially reduced to Mn(VI) followed by precipitation of MnO₂. The nature of the reductant was not identified, but the positive value of the Mn(VII)/Mn(VI) electrochemical potential is so high that it might be hydroxide itself, which undergoes oxidative decomposition ($4\text{OH}^- - 4e^- = \text{O}_2 + 2\text{H}_2\text{O}$). Introduction of K₂S₂O₈ as a holding oxidant did not prevent or slow down the unwanted reduction of permanganate in this medium.

At the next stage of studying Mn(VII) behavior, it was of interest to examine permanganate speciation at a low micromolar concentration range of initially added Mn(VII). Using the Ocean Optics instrument with a scanning range from 550 nm, it was not possible to monitor the major peak of Mn(VII) at 528 nm, but the presence of permanganate could be detected and quantified by its descending slope from 550 to 700 nm and by its characteristic shoulders at 563 nm and ~630 nm. A series of four solutions of

permanganate in 0.25 M of NaOD was prepared in the concentration range from 1 μM to 4 μM of initially added Mn(VII). The spectral acquisition started ~ 1 minute after solution injection into the LWCC and continued for another 15 to 20 minutes to monitor possible changes in Mn(VII) redox speciation with time. All solutions were so dilute that it was not possible to distinguish any color after spiking already diluted Mn(VII) stock into ~ 1000 excess of the colorless diluent. The results of these experiments are presented in Figure 3.36. Quite surprisingly, all spectra show a complete absence of permanganate in the solution at the moment of the very first spectral scan (absolutely no shoulder at the 563- to 567-nm region, major peak maximum position is at 603 nm, and no decreasing absorbance in the 550- to 603-nm range, which is characteristic for the predominance of Mn(VII) over Mn(VI). Even more interesting is the relatively quick disappearance of Mn(VI) itself from the solutions (see a steady decrease of the 603-nm peak intensity with time within each series). It is not possible to conclude why Mn(VII) reduction under these conditions is so fast compared with a relatively slow kinetics of Mn(VII) conversion to Mn(VI)) at ~ 1000 times higher concentrations of Mn(VII). In addition to a very low level of reductive admixtures already present in D_2O and NaOD, the membrane filter attached to the inlet fluidic port of LWCC might be a very significant contributor to this process.

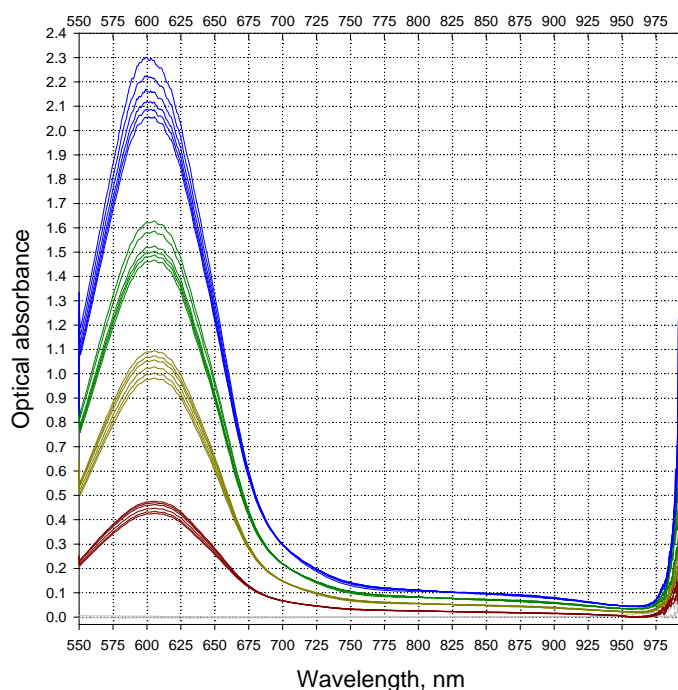


Figure 3.36. Evidence of Mn(VII) and Mn(VI) Reduction in 0.25 M NaOD Using LWCC Detection. Initial concentrations of Mn(VII) are as follows: 1 μM , 2 μM , 3 μM , and 4 μM for the red, dark yellow, green, and blue series, respectively. Within each series, the intensity of the 603-nm peak of manganate decreases with time. Time intervals between consecutive spectral scans are 2.5 ± 0.3 minutes.

Comparing the manganate spectra in a relatively flat range of low absorbances from 750 to 960 nm shows that the manganate ion still has significant molar absorptivities there (in the order of 150 to 50 $\text{M}^{-1}\text{cm}^{-1}$), which makes it difficult to study Pu(V) and Pu(VI) speciation with molar absorptivities in the order of 1 to 15 $\text{M}^{-1}\text{cm}^{-1}$ in the presence of even such low levels of Mn(VI).

In a separate series of experiments, more concentrated solutions of permanganate [25 to 100 μM of initial Mn(VII)] were used to determine the spectral range still accessible for measurements with a 500-cm LWCC. It was found that the optical range from 550 to ~ 750 nm is completely out of scale as no or very little light reaches a spectrophotometric detector. The absorbance measurements would be possible to perform in the ~ 780 - to 920-nm range if a strong positive drift of optical absorbance reading in time [due to conversion of Mn(VII) to Mn(VI)] could be eliminated.

It can also be concluded that plutonium speciation cannot be studied in this region in $\text{H}_2\text{O}/\text{NaOH}$ solutions because of the very intense and steeply changing absorbance of Mn(VI) in the 550- to 700-nm spectral range.

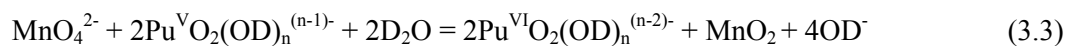
3.9.3 Oxidation of Pu(V) by Manganate in 0.25 M NaOD Monitored by LWCC Spectroscopy

Preparation and Characterization of Homogeneous Stock Solution of Mn(VI) in 0.25 M NaOD/D₂O

It has been shown that approximately one week is required to obtain a stable homogeneous Mn(VI) solution in 0.25 M NaOD/D₂O. The initial preparation is based on spiking permanganate solution into 0.25 M NaOD to achieve 0.2 mM total Mn concentration. The slow kinetics of Mn(VII) to Mn(VI) conversion (in the absence of any artificially added reductants) gradually ends with a complete disappearance of permanganate from the solution. The solution color becomes purely green with no precipitate or colloidal matter visually present in the sample. The Mn(VI) concentration in the final solution (calculated from a 603-nm peak intensity of manganate) is $\sim 15\%$ less than the initial concentration of Mn(VII). The spectrum of the final solution scanned in a broader range confirms the absence of permanganate and shows some deviations from a classical manganate spectrum in the 300- to 500-nm range. This difference is most likely associated with the partial conversion of Mn(VI) to lower oxidation states of Mn, which is consistent with 15% deficiency in Mn(VI) concentration with respect to initial Mn(VII) concentration.

Interaction of Pu(V) with Mn(VI)

The above prepared stock solution of Mn(VI) was diluted down to 15 μM in 0.25 M NaOD and spiked with Pu(V) stock solution in 14 M NaOD to achieve an approximately 1.2:1 manganate-to-Pu(V) molar ratio. The spectra measured immediately after mixing the reagents (Figure 2.2, blue and red traces) show a drastic drop in manganate signal intensity, presumably due to its consumption via redox reaction with Pu(V):



The formation of MnO_2 as a possible reduction product is qualitatively confirmed by the appearance of brown coloration on the membrane filter used to protect the liquid waveguide tubing from dust and colloidal matter. No Pu(VI) spectral signature centered at 625 nm could be identified in the spectrum because of the significant presence of residual manganate in solution, which has a 160-times higher molar absorptivity. The spectral signature of Pu(V) at 809 nm is completely absent, which confirms a full conversion of Pu(V) to a higher oxidation state by manganate.

As follows from reaction (3.3) above, the oxidation of Pu(V) by Mn(VI) should be 2:1 in stoichiometry [one equivalent of Mn(VI)], which oxidizes two equivalents of Pu(V). But in reality, the spectrophotometric analysis of the Mn(VI) absorbance intensity at 700 nm ($\epsilon = 205 \text{ M}^{-1}\text{cm}^{-1}$) before and after Pu(V) addition indicates the consumption of 9.64 μM of Mn(VI) in the process of converting 12.5 μM of Pu(V) to a higher oxidation state, or in other words, a 1:1.3 stoichiometry. The possibility of a partial conversion of Pu(V) oxidation to Pu(VII) (which should have the 1:1 stoichiometry) can be ruled out based on the inability of Mn(VII) and Mn(VI) to produce Pu(VII) from Pu(VI), even at much higher alkalinity than the 0.25 M used in this experiment. Another possibility is that the product of Mn(VI) reduction by Pu(V) is not only Mn(IV) (as insoluble MnO_2), but to some extent, Mn(V) as well. The latter is known to be unstable at a millimolar range of concentrations and higher, but might be more stable for a limited time in the low micromolar range of Mn concentrations used in this study.

Direct proof of the presence of Pu(VI) in blue and red spectra is difficult to obtain because of the steeply changing optical absorbance of residual Mn(VI) in the region of the major absorbance band of Pu(VI) at 625 nm. The second major peak of Pu(VI) is located in the 890- to 940-nm range with a peak maximum at ca. 920 nm (see calibration plots in Section 3.4.). However, the spectra in Figure 2.2 are significantly burdened by a waveform-shaped interference of unknown origin. To eliminate this interference, an approach described in Section 2.10 was applied, and the processed spectrum is shown in Figure 3.37. The peak at 920 nm is seen much more clearly now, and calculating the Pu(VI) concentration based on its net intensity of 0.012 absorbance units and net molar absorptivity of $1.9 \text{ M}^{-1}\text{cm}^{-1}$ results in a Pu(VI) concentration in solution of 12.6 μM . This number is in close correspondence with an initial Pu(V) concentration of 12.5 μM . This observation proves that Pu(V) is not stable in the presence of even very low concentrations of Mn(VI) and undergoes quantitative oxidation to Pu(VI) at a 0.25 M concentration of sodium hydroxide.

3.10 Oxidative Leaching of $\text{Fe}(\text{OH})_3/\text{Cr}(\text{OH})_3/\text{Pu}(\text{OH})_4$ Sludge Simulant with Permanganate

A relatively large portion of the $\text{Fe}(\text{OH})_3/\text{Cr}(\text{OH})_3/\text{Pu}(\text{OH})_4$ sludge stimulant was prepared as described in detail in Section 2.6 and aged for 2.5 weeks before subsampling small portions (5% of the total amount prepared) for oxidative-leaching experiments described in this section. In all experiments, the ratio of oxidizer-containing solution volume to the compacted sludge volume was approximately 3:1. The tests were performed under conditions of very intense magnetic stirring with a highly efficient Spin-Plus stir bar occupying approximately 20% of the compacted sludge volume.

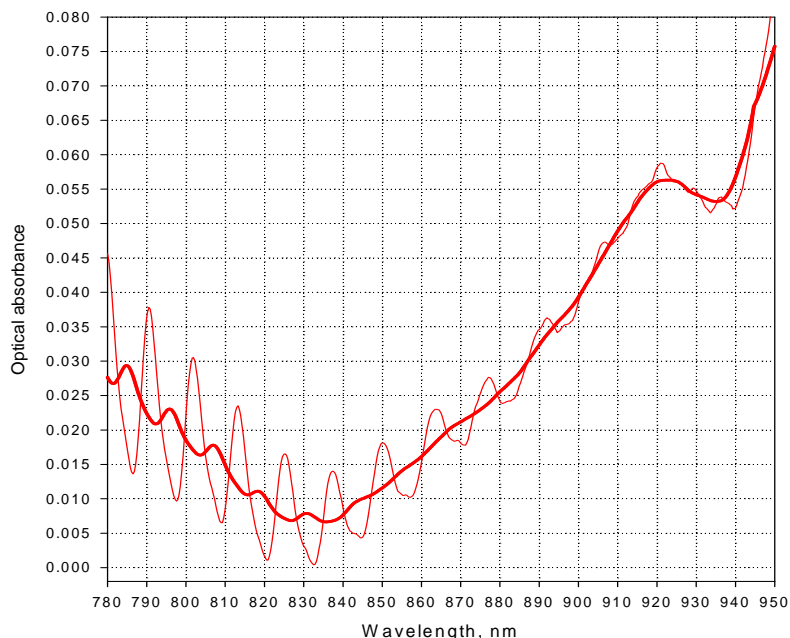


Figure 3.37. Red Trace Spectrum from Figure 2.2 After Application of the Waveform Suppression Treatment and Spectral Smoothing. Thin red line: processed spectrum before smoothing; bold red line: the same spectrum after a 41 points smoothing. The peak at 920 nm corresponds to 12.6 μM of Pu(VI) in solution.

3.10.1 Leaching in 0.25 M NaOD Solution

Substoichiometric to Stoichiometric Amount of Permanganate

The initial amount of Mn(VII) added to the sludge sample was calculated so as to achieve a 0.983:1 Mn(VII)/Cr(III) molar ratio. No visual evidence for any unreacted permanganate was observed in the filtered sample withdrawn after 3 to 4 minutes of contact time under stirring as judged by the absence of purplish tint in the lemon yellow color of the filtrate. A 250-fold dilution of the filtrate in 0.25 M of NaOH was applied to measure the intensity of the chromate spectrum. The spectrum of this diluted solution along with subsequent spectral analysis data are shown in Figure 3.38. The Cr(VI) concentration estimated from the spectrum of diluted sample (spectral trace s02) was approximately 85% of the theoretically expected value. However, the exact expected concentration of Cr(VI) could not be calculated with high certainty because of the unknown volume of interstitial liquid in the compacted sludge sample. The second sample, withdrawn 30 minutes after additional stirring, did not show any increase in the magnitude of the Cr(VI) peak at 372 nm (spectral trace s03). Both spectra indicated the complete absence of any absorbance bands in the 500- to 700-nm range, proving that there was no excessive Mn(VII) and/or Mn(VI) left in the mixture. Complete consumption of permanganate in merely 3 to 4 minutes after its addition to the sludge simulant indicated that the reaction between $\text{Cr}(\text{OH})_3$ and the oxidizer was too fast to be studied kinetically, even with a 3-min sampling frequency.

The leaching test was then continued by adding several more portions of permanganate to the reaction mixture to see if any more soluble chromate could be leached out from the sludge and to find conditions for the appearance of excessive Mn(VII) and/or Mn(VI) in the spectra. The amount of permanganate in

the reaction mixture was increased by 17% in 9 increments (spectral traces s04 to s12) with still no indication of permanganate or manganate in the spectra. The Cr(VI) signal at the same time increased by approximately 7%. Finally, a further increase of permanganate by 1.7% indicated a filtrate color change from lemon yellow to reddish-yellow. Diluting this sample resulted in the detection of a weak absorbance band at ~605 nm, which could be attributed to manganate. Two more additions of permanganate were made, and spectral analysis showed progressive intensification of the 605-nm peak with no additional accumulation of chromate in solution (spectral traces s14 and s15). The spontaneous conversion of excessive permanganate to manganate after dilution was not understandable at first, but later, it was discovered that the 0.24 M of NaOH used to dilute the filtrates contained some reductive constituents (accumulated as result of its storage in a polycarbonate container), and those admixtures were present at a sufficiently high level to convert excessive Mn(VII) to Mn(VI) in the diluted solution.

In total, 15 leachate samples were collected, and samples #2, 5, 10, 12, 13, 14, and 15 were acidified and analyzed by liquid scintillation counting. In all samples, no statistically significant difference between the observed counting rate and the background counting rate was found. The estimated percentage of Pu dissolution in the samples is less than 2.1%, which corresponds to less than $0.021 \times 5.6 = 0.117 \mu\text{M}$ of soluble Pu in the leachate ($5.6 \mu\text{M}$ is the estimated level of Pu concentration in the leachate in a hypothetical case of its complete solubilization).

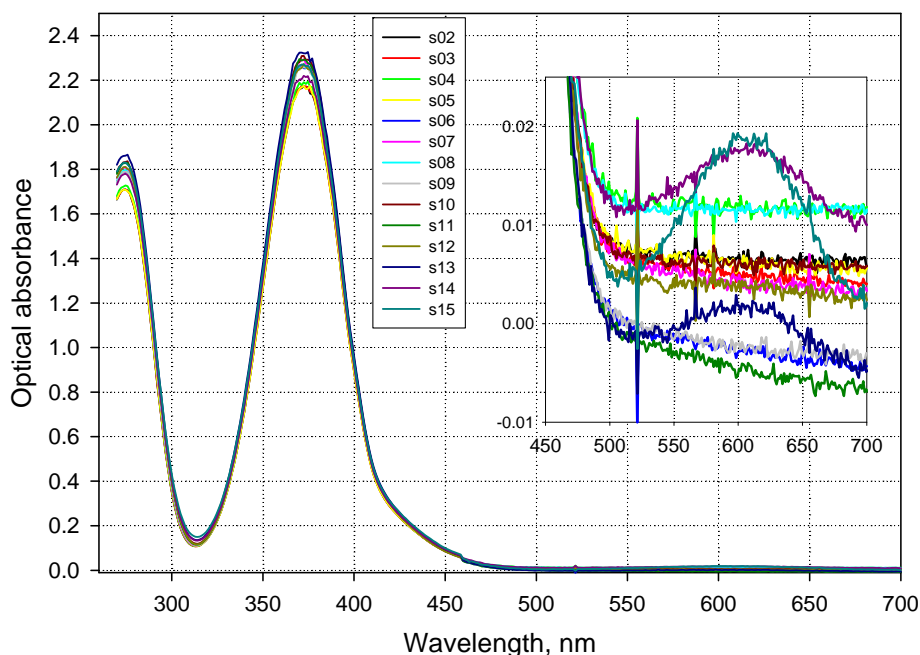


Figure 3.38. Oxidative Leaching of $\text{Fe}(\text{OH})_3/\text{Cr}(\text{OH})_3/\text{Pu}(\text{OH})_4$ Sludge Simulant with a Substoichiometric to Stoichiometric Amount of Permanganate in 0.25 M NaOH. The major peak at 372 nm belongs to chromate. The inset shows a 500- to 700-nm region in more detail where Mn(VII) and Mn(VI) peaks resulting from an excessive amount of added permanganate become visible for the last three additions of permanganate.

12% Molar Excess of Mn(VII)

In the second experiment, the initial portion of Mn(VII) solution added at the very beginning was equivalent to the condition represented by spectral trace s12 in the previous experiment when the theoretically calculated amount of Mn(VII) had to be increased by 17% in 10 small increments to achieve the real 1:1 Mn(VII)-to-Cr(III) ratio. The spectral analysis data are shown in Figure 3.39. In agreement with the previous experiment, spectral analysis of the diluted sample (s01) did not show any excessive Mn(VII) or Mn(VI) (spectral trace s01). After that, the amount of permanganate in the reaction mixture was increased in five increments (spectral traces s02 to s06) to achieve the 1.12:1 Mn(VII) to Cr(III) molar ratio. Time intervals between adding Mn(VII) and withdrawing the respective sample were 30 minutes. After adding the last portion of permanganate, the reaction mixture was stirred for another 120 minutes with four more samples taken out with 30-min intervals (s07 to s10). The spectral data that show that no statistically significant increase in the level of Cr(VI) concentration in leachate can be found with time compared with the very first sample taken 3 minutes after Mn(VII) addition to the sludge and the s07 to s10 samples. A small increase in the chromate peak intensity for the s02 to s06 group of samples is related to the contribution of manganate absorbance in this region of the spectrum. This observation confirms that all Cr(III) present in the sludge stimulant was converted to Cr(VI) by reaction with one molar equivalent of Mn(VII). Also, there is no variation on manganate peak intensity in the s06- to s10-group of samples, which indicates that there is no detectable consumption of the excess oxidizer via its potential catalytic decomposition by water in the presence of $\text{Fe}(\text{OH})_3$ and newly formed MnO_2 .

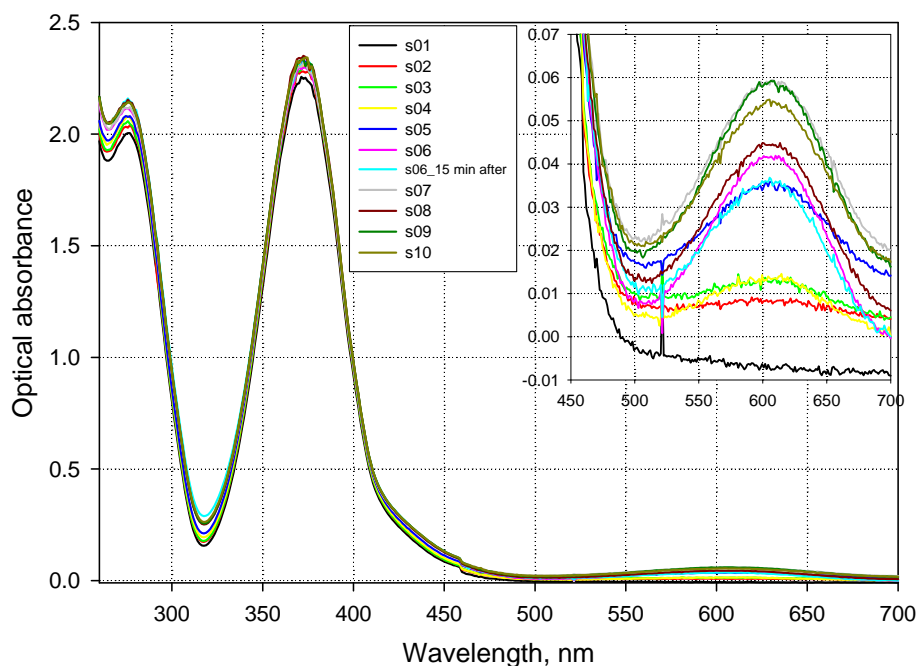


Figure 3.39. Oxidative Leaching of $\text{Fe}(\text{OH})_3/\text{Cr}(\text{OH})_3/\text{Pu}(\text{OH})_4$ Sludge Simulant with Excessive Amount of Permanganate. The permanganate to Cr(III) molar ratio is as follows: 1:1, 1.033:1; 1.05:1; 1.066:1; 1.083:1, and 1.117:1 for samples s01, s02, s03, s04, s05, and s06, respectively. Samples s07 to s10 represent the kinetics of oxidative leaching at the 1.117:1 molar ratio with a 30-min sampling frequency.

In total, 10 leachate samples were collected, acidified, and analyzed by liquid scintillation counting. In all samples, no statistically significant difference between the observed counting rate and the background counting rate was found. The calculated percentage of Pu dissolution is less than 1.8%, which corresponds to less than $0.018 \times 5.6 = 0.10 \mu\text{M}$ of soluble Pu in the leachate.

In summary, oxidative-leaching tests at 0.25 M NaOD resulted in very low concentrations of solubilized Pu in the leachates (less than $0.1 \mu\text{M}$), which are below the detection limit of Pu(VI) in this medium by OAS. Therefore, no attempt to apply LWCC detection for identifying the oxidation state of soluble Pu was made. No evidence of additional solubilization of Pu with longer contact times of the sludge stimulant with an excess of the oxidizer was found. The results obtained in this study are consistent with prior results of Pacific Northwest National Laboratory (PNNL) oxidative-alkaline leaching with washed Hanford tank sludges using permanganate in 0.1 M NaOH medium (Rapko et al. 2004). In those tests, the average fraction of Pu removed from the sludges was found to be $0.44 \pm 0.40\%$ (based on results of eight tests). The average fraction of Cr removed for the same tests was determined to be $70 \pm 30\%$, which is about $\frac{1}{3}$ lower than the practically quantitative leaching of Cr observed in this project for 1:1 and higher Mn(VII)-to-Cr(III) molar ratios.

3.10.2 Leaching in 3 M NaOD Solution

PNNL oxidative-alkaline leaching tests performed with permanganate at a 3 M NaOH concentration with washed Hanford tank sludges (Rapko et al. 2004) showed much higher levels of dissolved Pu (from 2 to 69% of Pu removed; with an average value of $24 \pm 25\%$) and a higher efficiency of Cr removal (from 45% to 99.6% with an average value of $88 \pm 18\%$). Therefore, in this project, it was decided to run several oxidative-leaching experiments at this higher level of alkalinity to see to what extent the enhanced leaching of Pu could be reproduced with simplified sludge simulant and to examine the kinetic features of this process.

Experimental conditions used for this group of tests (amount of sludge, liquid to solid ratio, stirring speed, etc.) were essentially the same as with leaching tests at 0.25 M NaOD.

Superstoichiometric Amount of Permanganate

Three superstoichiometric ratios of Mn(VII) to Cr(III) in the sludge were studied. The 1.15:1 ratio was tested initially (using the 3-week-old simulant) followed by two more experiments with a higher excess of oxidant run in parallel 7 days later (4-week-old simulant from the same main batch). The results of these tests are shown in Figure 3.40. All three tests demonstrate the very unexpected trend of decreasing the yield of solubilized Pu with time for the first 4.5 hr of contact time. The same tendency is observed in the 1.15:1 curve for much longer contact times (up to 6 days). The highest concentration of dissolved Pu in all three tests was achieved just 3 minutes after simulant agitation in the presence of permanganate-containing solution and was found to be $1.8 \mu\text{M}$, $2.0 \mu\text{M}$, and $2.0 \mu\text{M}$ for the tests with a 15%, 28%, and 45% excess of permanganate, respectively. In 2 to 2.5 hours, it drops down to $1.0 \mu\text{M}$, $1.2 \mu\text{M}$, and $1.3 \mu\text{M}$ of dissolved Pu, respectively. An analysis of the technical literature indicates that the decrease in concentration of dissolved plutonium was observed before in some tests with oxidative-alkaline leaching of real Hanford tank sludges using washed SX-101 sludge solids (see Figure 3.13 in Rapko et al. [2004]).

The Cr(III)-dissolution efficiency curve (data not shown) indicates practically complete dissolution of $\text{Cr}(\text{OH})_3$ from the simulant for the very first kinetic point (3 minutes after contact) regardless of the

Mn(VII)-to-Cr(III) molar ratio followed by the same level of chromate concentration in leachate solutions in subsequent measurements. The leachate color in these tests after filtration was always green-yellow as opposed to the tests at a 0.25 M NaOH concentration where it was purple-yellow for Mn(VII)/Cr(III) ratios greater than 1:1. The greenish color at 3 M of NaOD corresponds to the conversion of unreacted permanganate to manganate under these conditions. The manganate absorbance peak intensity was found to decrease with time for all three series, indicating partial reduction of Mn(VI) to insoluble Mn(IV). It is likely that additional removal of soluble Pu from the solution with time is related to the formation of additional MnO₂ in the process of oxidative leaching and co-precipitation of Pu(VI) with manganese dioxide. More experiments are needed to verify this hypothesis.

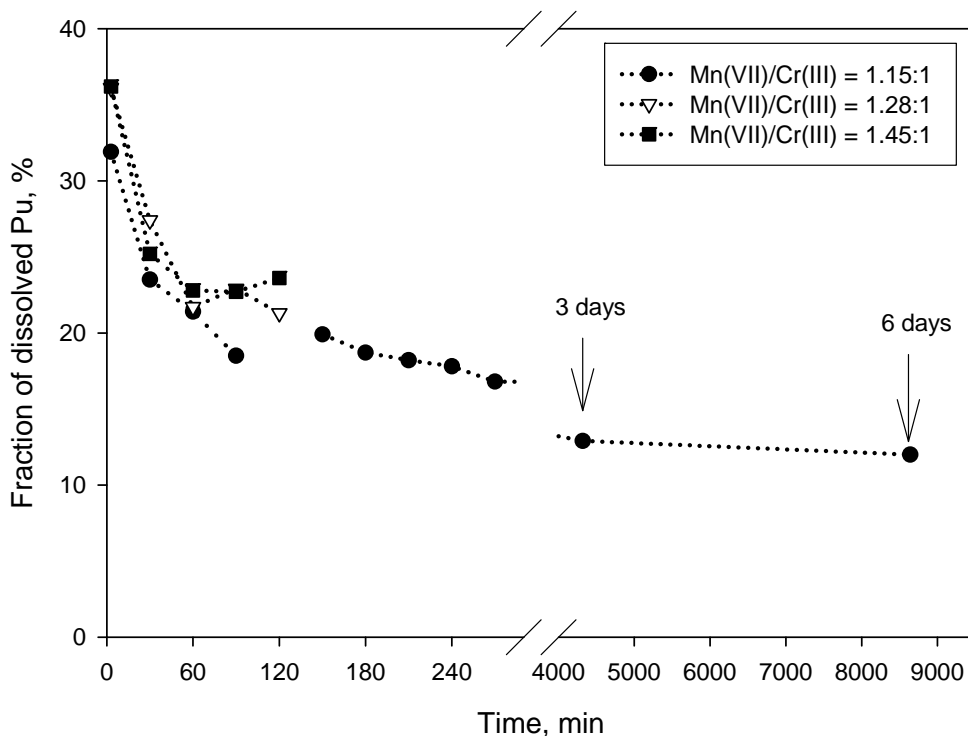


Figure 3.40. The Kinetics of Oxidative Leaching of Fe(OH)₃/Cr(OH)₃/Pu(OH)₄ Sludge Simulant with Excessive Amount of Permanganate. The 120-min point for the 1.15:1 curve showed an abnormally high leaching percentage both for Cr(III) and Pu(VI) (most likely associated with a pipetting error) and is not included in the plot.

Substoichiometric to Stoichiometric Amount of Permanganate

Three series of oxidative alkaline leaching were performed with molar ratios of Mn(VII) to Cr(III) set at 0.66:1, 0.83:1, and 1:1. Only two kinetic points were measured in these experiments: 3 minutes after mixing and 30 minutes after mixing. No additional increase in the level of Cr(VI) concentration in leachate was found between these two points within each series. In all three cases, the filtrate color was yellow, indicating complete consumption of Mn(VII) [and Mn(VI)] in the process of Cr(III) conversion to Cr(VI). Liquid scintillation counting (LSC) data showed no signs of Pu solubilization for all three ratios studied (<1.8% of potentially soluble plutonium present in the leachates). Table 3.7 summarizes the results of these tests.

Table 3.7. Concentrations of Cr(VI) and Soluble Pu in the 3 M NaOD Leachates with Substoichiometric to Stoichiometric Addition of Mn(VII)

Mn(VII)/Cr(III) Molar Ratio	$C_{Cr(VI)}$ Expected, $M^{(a)}$	$C_{Cr(VI)}$ Actually Measured, $M^{(b)}$	Calculated Volume of Interstitial Liquid in the Sludge, mL	C_{Pu} in leachate, μM		Fraction of Pu Removed from the Sludge, %	
				3 min	30 min	3 min	30 min
0.66:1	0.100	0.085	0.62	<0.102	<0.102	<1.8	<1.8
0.83:1	0.123	0.104	0.64	<0.102	<0.102	<1.8	<1.8
1.00:1	0.144	0.124	0.57	<0.102	<0.102	<1.8	<1.8

(a) Assuming zero volume of interstitial liquid.
(b) Assuming that the product of molar absorptivity of chromate by optical pathlength is equal to $5000 M^{-1}$.

3.10.3 Quenching of Excessive Manganate in the Leachates with Weakly Acidic Solution of Cr(III)

As follows from the results of oxidative alkaline leaching tests of the sludge simulant in 3 M NaOD, appreciable solubilization of Pu from the sludge (in the 1.5- to 2- μM range) can be achieved only with an excessive amount of oxidizer in terms of the Mn(VII)/Cr(III) molar ratio. The leachate produced in these tests always had a green color of varied intensity due to the presence of unreacted oxidant as manganate. Manganate absorbs strongly in the red region of the spectrum and (see Section 3.9.1) obscures weak spectral features of Pu(V) and Pu(VI) by its own absorbance in the 550- to 770-nm range when both Pu and Mn(VI) are present in comparable concentrations. In the solutions produced by the oxidative leaching of the $Fe(OH)_3/Cr(OH)_3/Pu(OH)_4$ sludge simulant with 15% molar excess of permanganate, the residual manganate was found to be present approximately at the 0.018 M level of concentration, which represents $0.018:2 \times 10^{-6} = 9000$ -fold excess with respect to the concentration of soluble Pu. This enormous ratio makes the application of LWCC for detecting Pu spectra in undiluted solution impossible, simply due to a huge attenuation of light, not only in the region of the major absorbance band of Mn(VII) at 603 nm, but in all of the usable range of solvent transparency (550 to 960 nm). One possible way to decrease the level of manganate in the leachate solution is to add a reducing agent to convert soluble Mn(VI) to insoluble MnO_2 . Several reductants were considered, but it was concluded that the solution of Cr(III) nitrate would be the best choice for practical application because the Cr(III) in the process of Mn(VI) reduction gets oxidized to Cr(VI), which is already present in the leachate solution and (as was shown earlier) does not interfere with Pu(V) and Pu(VI) spectra in the 550- to 960-nm range. Before applying the Cr(III) to the Pu-containing solution, it was tested in a cold experiment with manganate to establish reaction stoichiometry between these species.

Verification of the Reaction Stoichiometry in the Process of Manganate Reduction with $Cr(OH)_4^-$

A solution of sodium manganate was prepared by the spontaneous reduction of permanganate by water in 2.5 M of NaOD. This reaction was performed in a glass vial and was observed to proceed slowly as it did not go to completion even after 9 weeks, as shown in Figure 3.41 (black trace [s00] showing several finely structured peaks of residual permanganate with the most prominent ones at 528 and 546 nm).

Therefore, Cr(III) addition was performed in several increments with the first addition made to convert all residual permanganate to manganate (this step is not shown as a separate spectral trace in the figure).

Each subsequent time after adding Cr(III), the solution became less greenish and turbid because of Mn(VI) conversion to Mn(IV). The turbidity was eliminated by centrifuging the sample before spectral measurement to remove colloidal MnO₂ from the beam propagation zone and to measure the manganate peak intensity more precisely. Three more additions of Cr(III) resulted in significant discoloration of the reaction mixture (dark red, green, and pink spectral traces). A decrease in the 603-nm peak intensity between the second and the third addition of Cr(III) ($\Delta A_{603} = 1.95 - 1.41 = 0.54$) corresponded to a reduction of 0.3375 mM of manganate with 0.222 mM of Cr(III). The ratio between these two numbers is 1.52:1, which is very close to the theoretically expected ratio of 3:2. Therefore, the process of Mn(VI) quenching with Cr(III) can be described by the following chemical reaction:

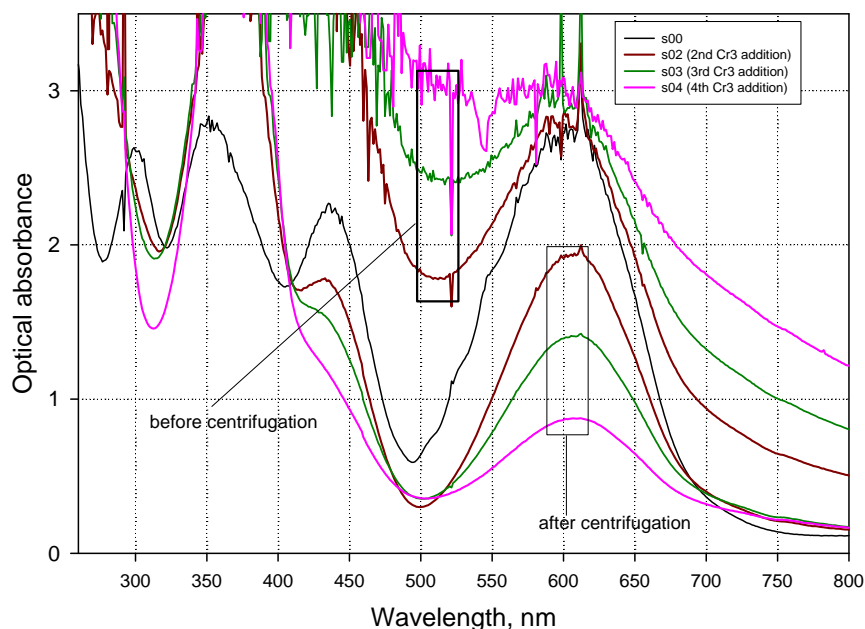


Figure 3.41. Cold Experiment on Stepwise Reduction of Manganate by $\text{Cr}(\text{OH})_4^-$ in 2.5 M NaOD. The spectral trace s00 represents the starting solution of manganate with a small admixture of remaining permanganate.

Application of Soluble Cr(III) Treatment to Leachate from Oxidative-Leaching Test with 15% Molar Excess of Permanganate in 3M NaOD

After the reaction stoichiometry between Cr(III) and Mn(VI) was established, an attempt was made to treat the Pu-containing leachate solution from the experiment on sludge simulant leaching with a 15% excess of permanganate in 3 M NaOD. All 6 days before this experiment was conducted, the leachate had been stored in the original oxidative-leaching container without separation from the undissolved fraction of the sludge simulant and newly formed MnO₂. As follows from Figure 3.41 (11 points curve with filled circles), during this storage period, the percentage of leached Pu decreased from 32% to 12%, which

corresponds to the remaining concentration of soluble plutonium at $1.8 \times 12/32 = 0.68 \mu\text{M}$. At the same time, the manganate peak intensity at 603 nm dropped down from 0.071 to 0.058 absorbance units (data not shown) because of the partial conversion of Mn(VI) to insoluble MnO_2 . This indicates that the spontaneous decomposition of manganate in the leachate with time was accompanied by an additional removal of soluble Pu from the solution, presumably due to the co-precipitation of Pu(VI) with newly formed MnO_2 .

To eliminate manganate completely from solution, five additions of near-neutral $\text{Cr}(\text{NO}_3)_3$ solution were made with 30-min intervals between consecutive additions. The spectral data corresponding to separate steps of Cr(III) addition are shown in Figure 3.42, plot a). After each addition of Cr(III) a small portion of the solution was sampled and acidified for determination of the remaining concentration of soluble Pu. Plot b) in the same Figure shows the concentration profile of soluble plutonium at various stages of elimination of Mn(VI). One can see that complete removal of manganate from solution is accompanied by a decrease in Pu concentration to less than $0.04 \mu\text{M}$. This level of Pu concentration can not be probed by LWCC. The effect of significant drop of Pu concentration at the very last Cr(III) addition stage can be partially related to coprecipitation of soluble Pu with $\text{Cr}(\text{OH})_3$ formed when excess of Cr^{3+} was added to the solution

3.10.4 Comparison of Oxidative Alkaline Leaching of Pu from Sludge Simulant with Other Studies

Enhanced solubilization of Pu after oxidative alkaline leaching of Hanford tank waste sludge simulants by permanganate at 3.0 M NaOH concentration were recently reported by Nash and colleagues (Nash et al. 2005). The leaching efficiency of Pu was found to be a non-linear function of the initial level of MnO_4^- concentration in contact with simulants. Fractions of Pu leached at the highest tested concentration of MnO_4^- of 0.1 M amounted to 35%, 72%, and 80% for the BiPO_4 , plutonium-uranium extraction (PUREX), and REDOX sludge simulants, respectively. The way these simulants were prepared [adding Pu(IV) or Pu(VI) hydroxycarbonato complex to the bulk of non-radioactive sludge simulant matrix], in our opinion, did not result in homogeneous distribution of Pu traces within the simulant matrix and does not simulate the creation of sludge in Hanford waste neutralization processes. For this reason, we believe that leaching results obtain by Nash and colleagues (2005) significantly overestimate the dissolution efficiency of Pu compared with homogeneously distributed samples studied in this project.

A drastic difference observed in this work between the extent of Pu solubilization from the sludge simulant by an excess of permanganate at 0.25 M and 3 M concentrations of NaOD is consistent with results of a study on the co-precipitation of Pu(VI, V) from alkaline solution with manganese dioxide produced by reduction of permanganate by the method of appearing reagents (Krot et al. 1998). These researchers found that “coefficients of decontamination” (K_d) of NaOH solutions from Pu(VI) by precipitation of MnO_2 obtained by MnO_4^- reduction with hydrogen peroxide are a sensitive function of NaOH concentration. There is practically no difference between K_d values in the 0.5- to 1-M concentration range of NaOH and a very significant loss of Pu(VI) affinity to MnO_2 between a 1- and 2-M concentration of NaOH.

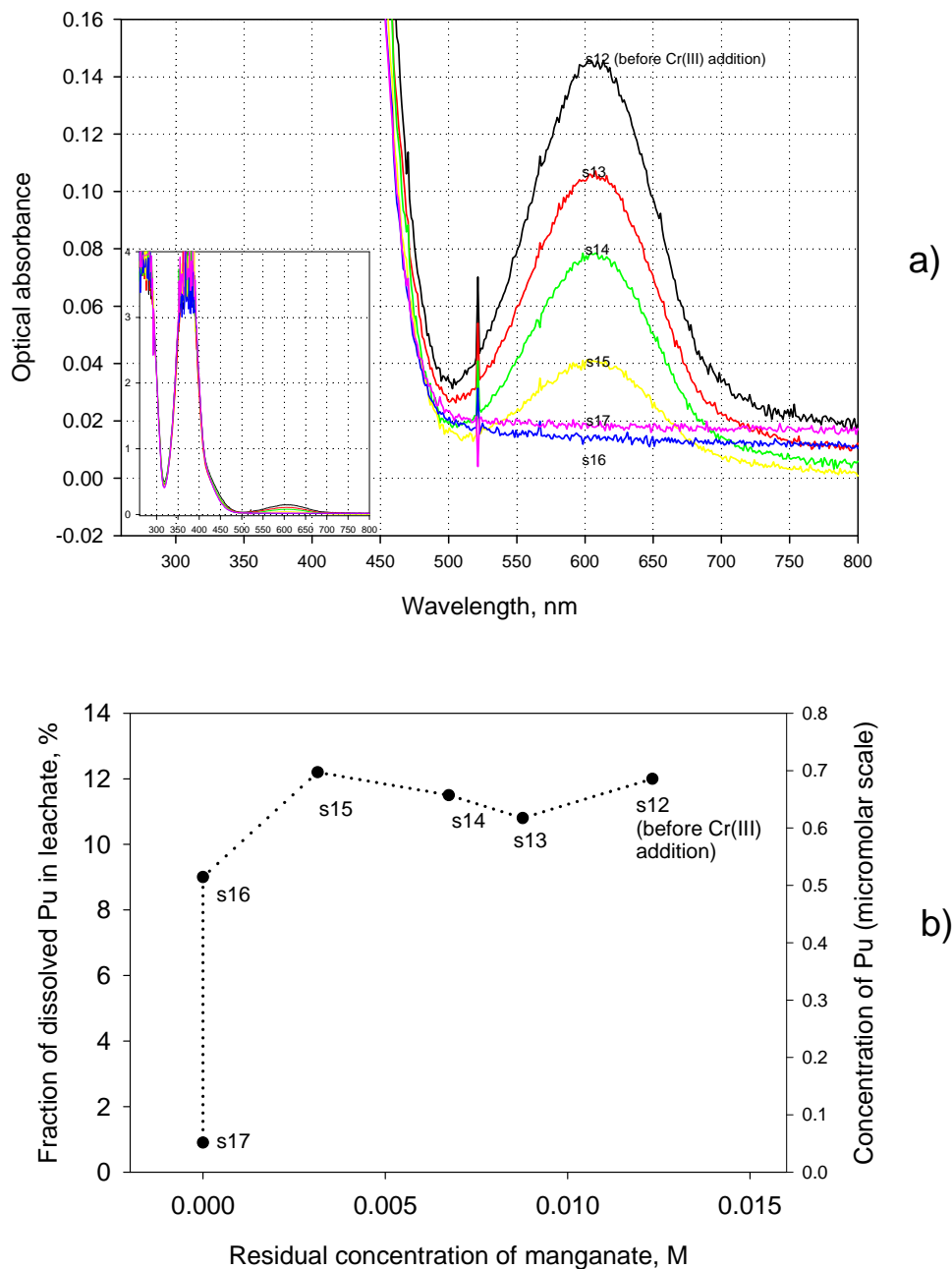


Figure 3.42. Quenching of Excessive Mn(VI) with Soluble Cr(III) Nitrate in 3 M NaOD Leachate 6 Days After Oxidative Treatment of $\text{Fe}(\text{OH})_3/\text{Cr}(\text{OH})_3/\text{Pu}(\text{OH})_4$ Sludge Simulant with 15% Molar Excess of Mn(VI): a) Mn(VI) peak intensity decrease with increasing amount of Cr(III) added; b) concentration profile of soluble plutonium at various stages of elimination of Mn(VI) from solution.

4.0 Conclusions

This section describes findings of the project tests, including spectral ranges and signatures, redox stability, detection limits, and oxidation and redox potentials. There is also a summary of the dissolution of $\text{Pu}(\text{OH})_4(\text{solid})$ in alkaline permanganate and manganate solutions as well as a summary of the oxidative leaching of $\text{Fe}(\text{OH})_3 + \text{Cr}(\text{OH})_3 + \text{Pu}(\text{OH})_4$ sludge simulant.

- A spectral range of 500-cm long LWCC in alkaline chromate containing solutions is found to be 560 to 700 nm and 560 to 960 nm in H_2O and D_2O solvents, respectively.
- Spectral signatures and the redox stability of $\text{Pu}(\text{V})$ and $\text{Pu}(\text{VI})$ in the 0.1- to 1-M $\text{NaOD}/\text{D}_2\text{O}$ solutions at low micromolar Pu concentrations are established:
 - A detection limit of $\text{Pu}(\text{VI})$ at 625 nm is found to be $0.5 \pm 0.04 \mu\text{M}$ both for 0.1- and 1-M NaOD solutions.
 - At 1 M alkalinity, an initially pure $\text{Pu}(\text{VI})$ solution shows partial conversion to $\text{Pu}(\text{V})$ with time (up to 12% in 3 days).
 - Detection limits of $\text{Pu}(\text{V})$ at 653 nm and 809 nm are found to be $0.24 \mu\text{M}$ and $0.38 \mu\text{M}$, respectively, in a 1 M NaOD solution in the concentration range of $\text{Pu}(\text{V})$ up to $23 \mu\text{M}$.
 - $\text{Pu}(\text{V})$ in 0.25 M of NaOD is not stable and undergoes disproportionation to $\text{Pu}(\text{IV})$ and $\text{Pu}(\text{VI})$. A limited linearity of the calibration curve is established up to $1.6 \mu\text{M}$ concentration of $\text{Pu}(\text{V})$.
- $\text{Pu}(\text{IV})$ in 0.25 M NaOD solution does not show any clearly identifiable spectral signatures because of the low solubility of $\text{Pu}(\text{IV})$ ($0.022 \pm 0.005 \mu\text{M}$).
- The redox behavior of $\text{Pu}(\text{V})$ in NaOD does not change in the presence of chromate.
- The effect of carbonate on the spectral characteristics of $\text{Pu}(\text{VI})$, V , and IV is determined:
 - A $\text{Pu}(\text{VI})$ mixed hydroxy-carbonate complex formation manifests itself in the 860- to 870-nm spectral range with an exact peak position being a function of the NaOD concentration and the $\text{CO}_3^{2-}/\text{OD}^-$ ratio.
 - The effect of carbonate on the $\text{Pu}(\text{V})$ spectra is the most clearly seen in the 725- to 775-nm range in addition to the red shift of the major peak of $\text{Pu}(\text{V})$ from 809 nm to 825 nm.
 - Solubility enhancement for $\text{Pu}(\text{IV})$ solutions in 0.25 M of NaOD in the presence of carbonate is related to the partial oxidation of $\text{Pu}(\text{IV})$ to $\text{Pu}(\text{V})$ (weak spectral signatures at 653 nm and 825 nm).
- Formal oxidation potentials of $\text{Pu}(\text{VI})/\text{Pu}(\text{V})$ were measured in a series of NaOD solutions from 0.25- to 1-M hydroxide concentration.

- Redox potentials of the Mn(VII)/Mn(VI) couple were measured in 0.25- to 1-M NaOD solutions with a wide variation of permanganate-to-manganate ratios, including pure manganate solutions.
- Ionic forms of Pu(IV) and Pu(V) in a 0.25 M NaOD solution undergo rapid oxidation to Pu(VI) in the presence of Mn(VII) and Mn(VI).
- Pu(OH)₄(solid) interacts with an alkaline solution of Mn(VII), not only as a catalyst of Mn(VII) to Mn(VI) reduction by water, but also as a reducing agent itself with significant solubilization of Pu via oxidation of Pu(IV) to Pu(VI), even at a low molar excess of Mn(VII).
- The technique of acidic strike of initially alkaline plutonium-containing solution in the presence of Cr(VI) and Mn(VII) causes significant perturbation of lower oxidation states of Pu with very fast oxidation of Pu(V) by Cr(VI) alone and rapid oxidation of Pu(IV) by mixture of Cr(VI) and Mn(VII).

4.1 Summary of Dissolution of Pu(OH)₄ (solid) in Alkaline Permanganate and Manganate Solutions

- Evidence of significant dissolution of Pu(OH)₄ by alkaline solution of Mn(VII) was obtained [up to 53% at 3.4:1 molar ratio of Mn(VII) to Pu(IV) in 0.25 M NaOH].
- Mn(VI) is a much less efficient dissolving agent (6 to 15% of Pu(OH)₄ dissolved under identical conditions) than is Mn(VII).
- The consumption of permanganate in experiments with aged Pu(OH)₄ exceeds the expected 2:1 stoichiometry for the Pu(IV)+ 2Mn(VII) = Pu(VI)+ 2Mn(VI) reaction. This gives evidence of catalytic reduction of Mn(VII) by water in the presence of undissolved Pu(IV) hydroxide.
- A 3:1 oxidative reaction stoichiometry is found with *in situ* formed Pu(OH)₄ in an alkaline solution of Mn(VII).

4.2 Summary of Oxidative Leaching of Fe(OH)₃+Cr(OH)₃+Pu(OH)₄ Sludge Simulant

Note: This work appears to be the first reported study in which plutonium-containing sludge simulant for the REDOX Process Hanford tank sludge was prepared by neutralizing an initially homogeneous solution of Fe(NO₃)₃ + Cr(NO₃)₃ + Pu(NO₃)₄ from an acidic medium as opposed to spiking a Pu(IV) solution into a heterogenous mixture of Fe(OH)₃ + Cr(OH)₃ in an alkaline medium.

- Oxidative leaching of sludge simulant in 0.25 M of NaOH
 - The quantitative dissolution of Cr(OH)₃ by NaMnO₄ occurs in the first 3 minutes after Mn(VII) addition with stirring, starting from a 1:1 Mn(VII)/Cr(III) molar ratio.
 - No detectable Pu concentration was found in the leachate at 0.25 M of NaOH regardless of contact time (up to 3 days) and a molar excess of Mn(VII) with respect to Cr(III) (the dissolved fraction of Pu is less than 1.8%; the estimated soluble Pu concentration is less than 0.1 μM). Excess oxidant remains in the leachate solution as permanganate.

- Oxidative leaching of sludge simulant in 3.0 M of NaOH
 - The dissolution of $\text{Cr}(\text{OH})_3$ is very fast and quantitative if a sufficient amount of permanganate is added.
 - 32% of Pu is present in the leachate in the first 3 minutes after oxidant addition at a 1.15:1 Mn(VII)/Cr(III) molar ratio ($C_{\text{Pu}} = 1.5 \mu\text{M}$).
 - A higher excess of oxidant (up to 1.45:1) does not increase the percentage of dissolved Pu.
 - The dissolved fraction of Pu in the leachate in contact with metathesized sludge and an excess of manganate decreases with time ($32\%_{3 \text{ min}} \rightarrow 21\%_{1 \text{ hr}} \rightarrow 18\%_{4.5 \text{ hr}} \rightarrow 13\%_{3 \text{ days}} \rightarrow 12\%_{6 \text{ days}}$).
 - There is no detectable Pu in the leachate at a substoichiometric Mn(VII)/Cr(III) molar ratio.
 - Excess oxidant in the leachate solution is present as manganate.
 - The quenching of excess oxidant with Cr(III) nitrate ($3\text{MnO}_4^{2-} + 2\text{Cr}^{3+} + 4\text{OH}^- \rightarrow 3 \text{MnO}_2 + 2\text{CrO}_4^{2-} + 2\text{H}_2\text{O}$) results in additional 95% removal of Pu from the leachate. As result of this treatment, the dissolved Pu concentration decreases from $0.67 \mu\text{M}$ to $0.032 \mu\text{M}$.

Distribution

**No. of
Copies**

**No. of
Copies**

OFFSITE

ONSITE

1 Savannah River National Laboratory
Richard Edwards
Savannah River National Laboratory
Westinghouse SA
Aiken, SC 29808-0001

7 Pacific Northwest National Laboratory
C.H. Delegard P7-25
D. E. Kurath P7-28
G.J. Lumetta P7-22
B.M. Rapko P7-25
S. I. Sinkov P7-25
Project Office (2) P7-28

2 Bechtel National, Inc.
D. Alford (2) H4-02